FABRICATION AND CHARACTERIZATION OF NOVEL POLYMER/ORGANO-MMT (ORGANO-SILICA)/ BIOPOLYMER NANOCOMPOSITE BLENDS BY REACTIVE EXTRUSION

YENİ POLİMER/ORGANİK MMT (ORGANİK SİLİKA)/ BİYOPOLİMER NANOKOMPOZİT KARIŞIMLARININ REAKTİF EKSTRÜZYON YÖNTEMİYLE ÜRETİMİ VE KARAKTERİZASYONU

BAYRAM ALİ GÖÇMEN

PROF. DR. A. GÜNAY KİBARER

Supervisor

Submitted to Graduate School of Science and Engineering of Hacettepe University as a Partial Fulfillment to the Requirements for the Award of the Degree of Doctor of Philosophy in Nanotechnology and Nanomedicine.

2018

This work named **"Fabrication and Characterization of Novel Polymer/ Organo-MMT (Organo-Silica)/ Biopolymer Nanocomposite Blends by Reactive Extrusion"** by **BAYRAM ALİ GÖÇMEN** has been approved as a thesis for the Degree of **DOCTOR OF PHILOSOPHY IN NANOTECHNOLOGY AND NANOMEDICINE** by the below mentioned Examining Committee members.

Prof. Dr. Nursel DİLSİZ ....

Head

Prof. Dr. A. Günay KİBARER...

Supervisor

Prof. Dr. Mehmet SAÇAK...

Member

Assoc. Prof. Dr. Memed DUMAN ....

Member

Assoc. Prof. Dr. Eylem GÜVEN...

Member

This thesis has been approved as a thesis for the Degree of **DOCTOR OF PHILOSOPHY IN NANOTECHNOLOGY AND NANOMEDICINE** by Board of Directors of the Institute of Graduate School of Science and Engineering.

Prof. Dr. Menemşe GÜMÜŞDERELİOĞLU

Director of the Institute of

Graduate Studies in Science

To my mother…

YAYINLAMA VE FİKRİ MÜLKİYET HAKLARI BEYANI

Enstitü tarafından onaylanan lisansüstü tezimin/raporumun tamamını veya herhangi bir kısmını, basılı (kağıt) ve elektronik formatta arşivleme ve aşağıda verilen koşullarla kullanıma açma iznini Hacettepe üniversitesine verdiğimi bildiririm. Bu izinle Üniversiteye verilen kullanım hakları dışındaki tüm fikri mülkiyet haklarım bende kalacak, tezimin tamamının ya da bir bölümünün gelecekteki çalışmalarda (makale, kitap, lisans ve patent vb.) kullanım hakları bana ait olacaktır.

Tezin kendi orijinal çalışmam olduğunu, başkalarının haklarını ihlal etmediğimi ve tezimin tek yetkili sahibi olduğumu beyan ve taahhüt ederim. Tezimde yer alan telif hakkı bulunan ve sahiplerinden yazılı izin alınarak kullanması zorunlu metinlerin yazılı izin alarak kullandığımı ve istenildiğinde suretlerini Üniversiteye teslim etmeyi taahhüt ederim.

☑ **Tezimin/Raporumun tamamı dünya çapında erişime açılabilir ve bir kısmı veya tamamının fotokopisi alınabilir.**
(Bu seçenekle teziniz arama motorlarında indekslenebilecek, daha sonra tezinizin erişim statüsünün değiştirilmesini talep etseniz ve kütüphane bu talebinizi yerine getirse bile, tezinin arama motorlarının önbelleklerinde kalmaya devam edebilecektir.)

☐ **Tezimin/Raporumun .... tarihine kadar erişime açılmasını ve fotokopi alınmasını (İç Kapak, Özet, İçindekiler ve Kaynakça hariç) istemiyorum.**
(Bu sürenin sonunda uzatma için başvuruda bulunmadığım taktirde, tezimin/raporumun tamamı her yerden erişime açılabilir, kaynak gösterilmek şartıyla bir kısmı ve ya tamamının fotokopisi alınabilir)

☐ **Tezimin/Raporumun .... tarihine kadar erişime açılmasını istemiyorum, ancak kaynak gösterilmek şartıyla bir kısmı veya tamamının fotokopisinin alınmasını onaylıyorum.**

☐ **Serbest Seçenek/Yazarın Seçimi**

23/ 01/ 2018

Bayram Ali GÖÇMEN

ETHICS

In this thesis study, prepared in accordance with the spelling rules of Institute of Graduate Studies in Science of Hacettepe University,

I declare that

- all the information and documents have been obtained in the base of the academic rules
- all audio-visual and written information and results have been presented according to the rules of scientific ethics
- in case of using others Works, related studies have been cited in accordance with the scientific standards
- all cited studies have been fully referenced
- I did not do any distortion in the data set
- and any part of this thesis has not been presented as another thesis study at this or any other university.

12/01/2018

Bayram Ali GÖÇMEN

ABSTRACT

FABRICATION AND CHARACTERIZATION OF NOVEL POLYMER/ORGANO-MMT (ORGANO-SILICA)/BIOPOLYMER NANOCOMPOSITE BLENDS BY REACTIVE EXTRUSION

Bayram Ali GÖÇMEN

Doctor of Philosophy, Department of Nanotechnology and Nanomedicine

Supervisor: Prof. Dr. Günay Kibarer

(Prof. Dr. Z. M. O. Rzayev)

January 2018, 136 pages

Recently, polymer nanocomposites have attracted great attention of industrial and academic society to get different kind of enforced valuable material. Biodegradable nanocomposites of different polymers are also in focus during new product development due to environmental concerns and regulations. Material properties of polymers can be enhanced dramatically by incorporating layered silicates and biodegradation can be suited with lactic acid or caprolactone based polymers together with suitable compatibilizers and fillers. Different kinds of formation of layered nanocomposite type materials frequently exhibits remarkable improvements, such as high storage modulus, tensile, and flexural properties, decrease in gas permeability and flammability or fire retardency and provide an increase in the biodegradability.

In this study, novel isotactic polypropylene (PP) based multi-functional nanocomposites were fabricated in melt by a one-step reactive extrusion using a Rondol twin-screw extruder at preoptimized processing conditions and investigated in situ chemical and physical processes occurring during the extrusion of multifunctional polymer blend compositions.

The compositions of reactive blends include PP as a matrix polymer, PP-g-MA graft copolymer as a reactive compatibilizer, copolymer covalently encapsulated silica nanoparticles (NPs) as reactive nanofiller-compatibilizer, and intercalated biodegradable poly (D, L-lactide) (PLA) or poly (ε-caprolactone) (PCL) silicate layers nanocomposites using ODA-MMT as a reactive or DMDA-MMT as a non-reactive nanofillers.

The chemical and physical structures, morphology, thermal behaviors and mechanical and rheological properties (shear stress and viscosity) as well as effects of origin organoclay and polyester, and copolymer encapsulated silica NPs on the main properties of nanocomposites were investigated by FTIR, solid state ^{13}C and ^{29}Si NMR, XRD, SEM-TEM, DSC-TGA and DMA (shear stress and viscosity) analysis methods, respectively.

There was demonstrated that the essential improvement of crystallinity, thermal stability, rheological and mechanical parameters, surface and internal morphologies of the nanocomposites as compared with those for a matrix polymer. Better results were observed for nanocomposites containing reactive organoclay and PCL polyester. Colloidal copolymer-silica NPs showed a well dispersion effect on structure of new polypropylene composites due to interactions of molecular bonds between different layers.

Similarly, together with PP based pristine polymer, investigations made on multifunctional polymer blend nanocomposites (NCs) consisting EPDM elastomer as a matrix polymer, bioengineering polyesters (PLA and PCL), PP-g-MA compatibilizer and covalently encapsulated colloidal alternating reactive copolymer-g-APTS (γ-aminopropyl trimethoxysilane)-silica nanoparticles (NPs) as reactive compatibilizer-nanofillers, and organoclays (reactive ODA-MMT and complexable DMDA-MMT) nanofillers that were fabricated in melt by a one-step reactive extrusion nanotechnology.

The chemical and physical structures, morphology, thermal behaviors, mechanical and rheological properties of NCs, as well as effects of origin organically and polyester, and colloidal copolymer-g-silica (NPs) on the main properties of the nanocomposites were confirmed again by FTIR, solid state ^{13}C and ^{29}Si NMR, XRD, SEM-TEM, DSC-TGA and dynamic rotary rheometric analysis methods.

The effects of bioengineering polyesters and their molecular mass, origin of organology, and reactive PP-g-MA compatibilizer were evaluated. Moreover, colloidal copolymer-g-silica NPs as reactive compatibilizer-nanofiller play an important role in the formation fine

dispersed morphology on nanocomposites structure of polymer blends. This structural occurrence is due to affective in situ physical and chemical interactions in multifunctional polymers/nanofillers blends. These interactions occur in the chosen lower temperatures of the five barrier zones at 120 ℃, 130 ℃ and 130 ℃, 145 ℃ and 145 ℃ during a one-step cycle (around 5-10 min) of reactive extrusion processing. Chemistry and physics of in-situ interfacial interactions in multifunctional NCs during extruding process were also estimated. These interactions of bonds due to multifunctional groups of reactive compatibilizers and silica copolymers inside nanocomposite material show behaviour difference on thermal, rheological properties compared to pristine polyesters/polymers.

Keywords: PP, PP-*g*-MA, EPDM rubber, polyesters, silica NPs, organoclays, reactive extrusion, structure-composition-property relationships, morphology, thermal stability, shear stress, rheology, bioengineering polyesters, copolymer-*g*-silica NPs, nanocomposites, reactive extrusion nanotechnology, polymer compatibilizer, nanostructure-composition-properties relationships.

ÖZET

YENİ POLİMER/ORGANİK MMT (ORGANİK SİLİKA)/ BİYOPOLİMER NANOKOMPOZİT KARIŞIMLARININ REAKTİF EKSTÜZYON YÖNTEMİYLE ÜRETİMİ VE KARAKTERİZASYONU

Bayram Ali GÖÇMEN

Doktora, Nanoteknoloji ve Nanotıp Anabilim Dalı

Tez Danışmanı: Prof. Dr. Günay Kibarer

(2. Danışman: Prof. Dr. Z. M. O. Rzayev)

Ocak, 2018, 136 Sayfa

Günümüzde polimer nanokompozitler endüstri ve akademik toplum için güçlendirilmiş farklı tip maddeleri elde etmede dikkat çekicidir. Farklı polimerlerin biyobozunur nanokompozitleri, çevresel sorunlar ve düzenlemeler dolayısıyla yeni ürün geliştirmelerinde ayrıca önem verilen konular arasındadır. Polimerlerin malzeme özellikleri, tabakalı silika eklenmesi, biyobozunurluğun sağlanması için polilaktik asit veya polikaprolakton bazlı polimerlerin uygun uyumlaştırıcıları ve dolgu mazlemeleri ile kullanılmasıyla iyileştirilebilir. Katmanlı nanokompozit malzeme tiplerinin farklı formlarının oluşumu sıklıkla önemli gelişmeler gösterir örneğin yüksek depolama modülüsü, gerilme ve eğilme özellikleri, gaz geçirgenliğinin azalması ve yanıcılık veya yanmaya direnç özellikleri gibi. Ayrıca bu farklı formlar biyobozurnurluk artışı da sağlamaktadır.

Bu çalışmada, yeni izotaktik polipropilen bazlı çok fonksiyonlu nanokompozit malzemeler eriyik bazlı tek aşamalı reaktif ekstruzyon sistemi ile üretilmiştir. Rondol tipi çift vidalı ekipman ve önceden optimize edilmiş proses şartları kullanılmıştır. Çalışmada, eşanlı kimyasal ve fiziksel proseslerin oluşması, çok fonksiyonlu polimer karışım içeriklerinin

extruzyonu ile araştırılmıştır. Reaktif karışımların içeriği şunlardan oluşmaktadır; ana matriks polimer, Polipropilen, uyumlaştırıcı olarak PP-g-MA aşılanmış kopolimer, reaktif dolgu ve ilave uyumlaştırıcı olarak kovalent bağlı sargılanmış silika nanopartiküllü kopolimer ve reaktif ODA-MMT ve reaktif olmayan DMDA-MMT kullanılarak hazırlanmış interkalasyonlu biyobozunur Polilaktik Asit (poli (D,L-lactide, PLA) veya Poli (ε-caprolactone) (PCL) silika katmanlı nanokompozitlerden oluşmaktadır.

Nanokompozitlerin kimyasal ve fiziksel yapıları, morfolojileri, termal davranışları, mekanik/reolojik özellikleri(kesme gerilmesi ve viskozite) ve ayrıca organokil ve polyester yapı etkileri ile silika nanopartiküllerini içeren kopolimerin ana nanokompozite yapı üzerindeki etkileri, FTIR, katı fazlı ^{13}C ve ^{29}Si NMR, XRD, SEM-TEM, DSC-TGA ve DMA (kesme gerilmesi ve viskozite) analiz metotları ile incelenmiştir.

Nanokompozitin kristallenmede, ısıl stabilitede, reolojik ve mekanik parametrelerde, yüzey ve iç morfolojide, ham matriks polimere göre önemli gelişmeler olduğu gösterilmiştir. Reaktif organokil ve PCL polyester içeren kompozitler için daha iyi sonuçlar gözlemlenmiştir. Kolloidal kopolimer-silika Nanopartiküller-NPs, yeni polipropilen kompozit yapılarında faklı katmanlar arasındaki moleküler bağlanmaların etkileşiminden dolayı iyi karışım etkisi göstermiştir.

Benzer şekilde, Polipropilen bazlı ham polimer çalışmanın yanında, martiks polimer olarak EPDM elastomer, biyomühendislik poliesterleri (PLA ve PCL), PP-g-MA uyumlaştırıcı ve reaktif uyumlaştırıcı-dolgu malzemesi olarak kovalent bağlı kolloidal yapıda değişken reaktif kopolimer-g- APTS (γ-aminopropyl trimethoxysilane)-silika nanopartikülleri (NPs) ve organokil (reaktif ODA-MMT ve kompleksleştrici DMDA-MMT) nanodolguları içeren çok fonksiyonlu polimer karışımlı nanokompozitler üzerinde çalışmalar yapılmış ve bu kompozitler eriyik fazda tek aşamalı reaktif ekstruzyon nanoteknolojisi ile üretilmiştir.

EPDM bazlı nanokompozitlerin kimyasal ve fiziksel yapıları, morfolojileri, termal davranışları, nanokompozitlerin mekanik/reolojik özellikleri ve ayrıca organokil ve polyester yapı etkileri ile silika nanopartiküllerini içeren kopolimerin ana nanokompozit yapı üzerindeki etkileri, FTIR, katı fazlı ^{13}C ve ^{29}Si NMR, XRD, SEM-TEM, DSC-TGA ve dinamik döner reolojik analiz metotları ile incelenmiştir.

Reaktif uyumlaştırıcı ve dolgu malzeleri olarak kullanılan nanopartiküller nanokompozitlerde, dağılmış bir morfoloji oluşturulmasında önemli rol oynamaktadırlar. Bu

yapısal oluşum, çok fonksiyonlu yapıdaki polimer ve nanodolgu karışımlarında eşanlı gerçekleşen etkili fiziksel ve kimyasal etkileşimlerden kaynaklanmaktadır. Bu etkileşimler, tek çevrim zamanlı (5-10 dakika) reaktif extruzyon prosesi sırasında, seçilmiş ve optimize edilmiş beş adet düşük bariyer sıcaklığında, 120 °C, 130 °C, 130 °C, 145 °C ve 145 °C, oluşmaktadırlar. Ektruzyon prosesi sırasında oluşan çok fonksiyonlu nanokompozitlerde gerçekleşen yüzeyler arası etkileşimlerinin kimyasal ve fiziksel detayları tahmin edilmiş ve raporlanmıştır. Nanokompozit yapıdaki reaktif uyumlaştırıcılar ve silika kopolimerlerindeki çok fonksiyonlu grupların etkileşimleri yine termal ve reolojik özelliklerinde, ham polimer ve poliesterlere göre büyük davranışsal farklılıklar göstermektedir.

Anahtar Kelimeler: PP, PP-*g*-MA, EPDM kauçuk, poliesterler, silika Nanopartiküller NPs, organokiller, reaktif extruzyon, yapısal-içeriksel-özelliksel ilişkiler, morfoloji, termal stabilite, kayma gerilimi, reoloji, biyomühendislik poliesterleri, kopolimer-g-silika NPs, nanokompozitler, reaktif extruzyon nanoteknolojisi, polimer uyumlaştırıcılar, nanoyapı-içerik-özellik ilişkileri.

ACKNOWLEDGEMENT

Bayram Ali Göçmen

TABLE OF CONTENTS

LIST OF TABLES

LIST OF FIGURES

SYMBOLS and ABREVIATIONS

LA:	L-lactic Acid
PLA:	Poly lactic Acid
NPs:	Nanoparticles
EPDM:	Poly (Ethylene-*co*-Propylene-*co*-Vinylidene norbornene diene Monomer)
RAFT:	Reversible Addition–Fragmentation chain Transfer
SME:	Specific Mechanical Energy
NC:	Nanocomposites
Nm:	Nanometer
Mw/MW:	Molecular Weight
ODA:	Octadecyl Amine
CNF:	Carbon Nanofiber
SiO_2:	Silicium Dioxide
PP-g-MA:	Maleic anhydride grafted Polypropylene
iPP:	Isotactic Polypropylene
TEOS:	Tetraethoxysilane
APTS:	γ-aminopropyltriethoxysilane
MFNCs:	Multi-Functional Nanocomposites
MMT:	Montmorillonit
FTIR:	Fourier Transform Infrared Spectroscopy
NMR:	Nuclear Magnetic Resonance Spectrometer
XRD:	X-ray Diffraction
SAXS:	Small-Angle X-ray Scattering
WAXS:	Wide-Angle X-ray Scattering
TGA/DTG:	Thermogravimetric Analysis
SEM:	Scanning Electron Microscope
TEM:	Transmission Electron Microscopy
T_g:	Glass Transition Temperature
T_m:	Melting Temperature
T_c:	Crystallization Temperature

PET:	Poly Ethylene Terphetalate
PVC:	Poly Vinyl Chloride
PCL:	Poly ε-Caprolactone
DSC:	Differential Scanning Calorimetry
PP:	Polypropylene
PS:	Polystyrene
MA:	Maleic Anydride
DOM:	Dioctyl Maleate
LDPE:	Low Density Poly Ethylene
UV:	Ultra Violet
KPS:	Potassium Persulfate
AFM:	Atomic Force Microscope
SIMS:	Secondary-ion Mass Spectrometry
GPC:	Gel Permeation Chromatography
GPC-MALLS:	GPC Coupled to Multiage Laser Light Scattering
THF:	Tetrahydrofuran
ΔH_{rel}:	Endothermic Enthalpy Relaxation Value
ISBM:	Injection Stretch Blow Molding
OPS:	Oriented Polystyrene
OPP:	Oriented Polypropylene
PEO:	Polyethylene Oxide
VMT:	Vermiculite
TPO:	Thermoplastic Olefins
DMDA:	Dimethyldidodecyl Ammonium Cation
DSR:	Dynamic Shear Rheometer
DR:	Dynamic Rheometer
POSS:	Polyhedral Pligomeric Silsesquioxanes
T:	Tetrahedral
O:	Octahedral
PEG:	Polyethylene Glycol
PBS:	Polybutadiene Styrene
DMA:	Dynamic Mechnaical Analysis
PHA:	Polyhydroxyalkanoates
PMMA:	Polymethyl Metaacrylate

ENB:	Ethylidene Norbernene
FWHM:	Full-Width Half-Maximum
Da:	Dalton
PI:	Polydispersity Index
GPC:	Gel Permeation Chromatography
Mn:	Number of Average Molecular Weight
MU:	Mooney Viscosity
HCl:	Hydrochloric Acid
EVA:	Ethylene Vinyl Acetate
CEC:	Cation Exchange Capacity
MFI:	Melt Flow Index
CAS:	Chemical Abstracts Service

1. INTRODUCTION

Nanoscience and nanotechnology are the study and application of ultra-small electron microscope level things and nanoscale is once in a billion under metric scale. As nanoscience research, polymer nanocomposites includes of matrix polymer, mostly, together with copolymer consisting nanoparticles and nanofillers dispersed within polymer matrix structure. Shapes of nanostructured polymers differ as plates, fibers, etc. that, at least, one dimension shall be 1-50 nm size, are together with different types of phases as viscous blends, composites, crystals, foams. Polymer nanocomposites needs to be controlled by compounding/mixing, dispersion stabilization of the constituents in polymer matrix, phase orientation during dispersion, and compounding/blending conditions/types/methods of them.

Improvements of polymer blends and nanocomposites produced from renewable resources to overcome disadvantages like insufficient mechanical properties of polymers have been developed over the last decade. Behind the poor mechanical improvement, researches deal also with environmental results of conventional polymers and therefore, need to develop new types of material to fulfil expectations and requirements of new environmental regulations. Additionally, fossil derivative products tend to be changed as renewable types not only to get material continuously but also to provide natural partial forms of material to be destroyed easily when it faces with organisms and physical effects like sunlight. Therefore, attention of many researchers as newly topic was focused on fabrication of the biodegradable materials/plastics and layered silicate or silica nanocomposites of them, polymer blends/nanocomposites manufacturing using renewable resources.

In this study, most bulky produced petrochemical derivative polymers, polypropylene (PP) and poly (ethylene-*co*-propylene-*co*-vinylidene norbornenediene monomer) (EPDM), have been chosen in academic researches and these are also very important polymers that are widely used for industrial applications.

Polypropylene composites reinforced with various natural fibrous nanomaterial such as palm fiber, fiber of palm oil waste fruit bunch and their cellulose derivatives [1], sisal/Polypropylene composites with minimum fiber [2] and other polymer composites reinforced with natural fibers.

EPDM terpolymer elastomer is one the most widely used synthetic rubber in many static and dynamic applications [3]. The many industrial polymer composite products such gaskets, bumpers, auto parts, auto brake systems, electrical installation, conveyor belts, standard profile materials for automobiles and etc. were fabricated using EPDM as matrix.

Mostly, reactive extrusion systems have been used to process novel polymers to mix ingredients in melt form. All reactants are added to get well formed structure under mechanical forces. The machinery for this purpose is extruder, which have zones of heat ingress and cooling. Forces on melted form are provided with one or double screw systems. This is one of the typical way of processing polymers in both industries and researches.

Here, novel polymers (PP, EPDM) are used as bed in melt form and continuously all other ingredients are added one by one or in combined form. PP-g-MA (polypropylene copolymer of maleic anhydride) as a reactive compatibilizer and isostructural correlation may provide starting materials for generation of new different types of PP and EPDM based materials synthesis.

Natural polymers are in the center of hot topic area of research for biodegradable polymers. Natural polymers have hydrophilic character. This would contribute to the successfully developed composites that are environmentally friendly. Most natural fibers and nanofillers (clays) have hydrophilic properties naturally. Blends getting by using these types of polymers which supplied from renewable resources—(i) natural polymers, cellulose, protein, and starch; (ii) synthetic polymers produced with natural monomers, like polylactic (PLA) acid; (iii) polymers getting by microbial fermentation, i.e. polyhydroxybutyrate—are defined as an effort on potential researches [4]. Compatibilizers in focus of this search as nanoclays and PLA and reactive extrusion technology is using to advance interfacial adhesion between natural and synthetic polymers.

Biodegradability of newly structured polymer will be provided by PLA and polycaprolactone (PCL). PLA and PCL are biodegradable biopolymers which are mostly used in most of recent studies. Lee et al.[5] prepared PP/poly (ε-caprolactone) (PCL) reinforced with cellulose nanofiber (CNF) hybrid nanocomposite by using a batch-type kneader with six twin-screw elements in being present of PP-g-maleic anhydride (MA) graft copolymer/ compatibilizer to improve the distributions of PCL domain and cellulose nanofiber(CNF) in PP matrix.

2

Organoclays are important and preferred by most of researchers to provide polymer structure an increase with respect to mechanical properties and compatibility. Montmorillonite based organoclays are more attractive due to their availability and effect on polymer interactions. Domenech et al. [45] fabricated PP/PP-g-MA compatibilizer/organoclay nanocomposites by mixing at melt phase with masterbatch process by using twin-screw extruder using specific mechanical energy (SME). Evaluation of the effect of process/operational conditions of extrusion (screw rotation speed, feed rates of each component, and barrel temperatures) on filler (clay) dispersion inside Polypropylene/organoclay nanocomposites.

Copolymer (MA-alt-1-dodecene)-g-SiO$_2$ is another compatibilizer reactant that is prepared and used in this study. In previous publications, synthesis and characterization of the functional copolymers covalently incorporated with in-situ produced silica nanoparticles (NPs) together with γ-aminopropyltriethoxysilane precursor were achieved [6-8]. Silica nanoparticles have been used in some articles like Das et al.[9] who has prepared the silica filled EPDM by hydrolysis of triethoxysilyl-grafted EPDM and tetraethoxysilane (TEOS) in n-butylamine solution (aquous) via in-situ generation of silica nanoparticles. Therefore, the prepared silica nanoparticles will be added to mixture in melt form together with PP-g-MA to see effect on layer for both PP and EPDM cases.

The main purpose/goal of these works is to design new multifunctional polymer blend compositions to fabricate polymers/silicate and silica multi-functional nanocomposites (MFNCs) within melt phase by reactive extrusion (one-step) using EPDM and PP as a matrix polymer, PP-g-MA as a reactive compatibilizer, polylactide (PLA) and/or poly (ε-caprolactone) (PCL) as bioengineering polyesters, poly (MA-alt-1-dodecene)-g-SiO$_2$ nanoparticles (NPs) as reactive compatibilizer-reinforcement, octadecylamine monmorillonite (ODA-MMT) as reactive and dimethyldidodecylammonium monmorillonite (DMDA-MMT) as non-reactive organoclay nanofillers. Another aspect of this work is the investigation physical and chemical interactions/structures, surface and internal morphologies, mechanical, thermal, and rheological properties of multifunctional nanocomposites (MFNCs). Besides, the effects due to bioengineering polyester and origin of organoclays and copolymer (MA-alt-1-dodecene)-g-SiO$_2$ NPs on the in situ interfacial interactions during melt compounding processes have been evaluated. This work also presents the synthetic pathways for copolymer-g-SiO$_2$ NPs by sol-gel method using functional amphiphilic copolymer, γ-aminopropyltriethoxysilane (APTS) and

tetraethoxysilane (TEOS) precursors. Consequently, chemical and physical structures and thermal behaviors of organo-silica NPs and their influence on the main structural, thermal and rheological properties, and SEM-TEM morphology of nanocomposites have been investigate. This work also estimates the chemistry and physics of covalence, complexing and hydrophobic/hydrophilic interfacial interactions as important nanoprocessing through effects of biothermolastic esters, polymer stabilizers, organoclays, and colloidal organic silica NPs during reactive extrusion of multifunctional EPDM based nanocomposite blends.

2. LITERATURE SURVEY /GENERAL INFORMATION

2.1. The Use of Polymers (Plastics) and Impact on Environment

Plastic as a word is coming from "plastikos" and "plastos" which come from Greek and means to suit for molding and molded, respectively. Plastics are mainly polymers (again in Greek means "many parts"), that are simply materials or chemically, molecules consist of repeating molecular parts, called as monomers (Greek word "one part"). Hydrogen and carbon/hydrocarbons come together to build monomers to form long chains with bonds called as polymers/ plastics. Petroleum, coal, natural gas are the main resources for most of synthetic plastics.

Plastics are comparatively cheap, low weight, stable, strong, long duration, corrosion preventive materials, with side benefits of insulation to electricity and thermally effective properties compared to other alternative materials in use like metals. Change in properties provide them broad range of application areas providing technological or medical improvements, saving of energy, and many other benefits to society.

There is an increase in the production of plastics at the last half of century (over 60 years). The amount of gross profit was near 2 million tons in 1950s, now it has reached to over 335 million tons today (see Figure 2.1). There is almost 3% of increase observed from last five years. Total world export profit is around 500 billion dollars [10].
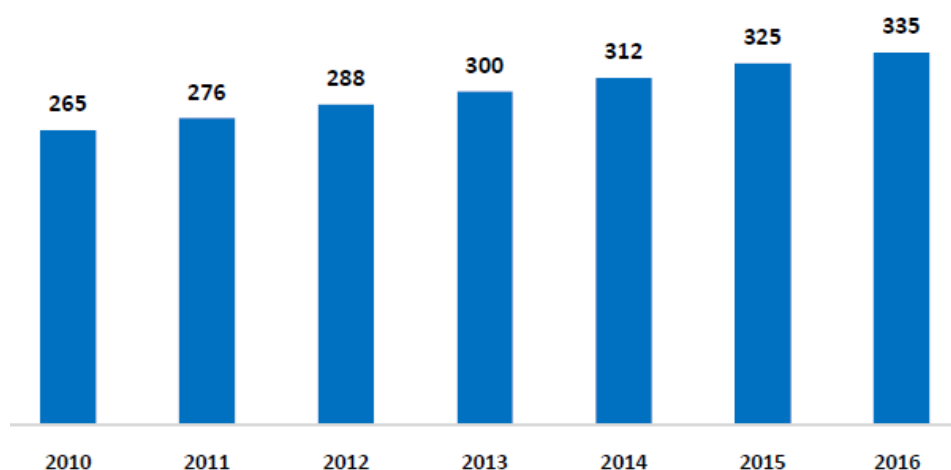
Figure 2.1. World Plastic Production- million tons/year (PAGEV World Plastic Report Reference) [10].

Plastics are involved all in daily life processes like transport, telecommunication, textile, footwear, and used as packaging materials of packaging utilized for transportation of wide range of drinks, foods, and other commodities. New developing applications of plastics are still going on which will provide benefits in near future i.e. medical application, renewable energy, and transportation of goods.

Polymers are mainly divided as thermoplastics, thermosets, and elastomers according to their thermal and physical behaviors. Mostly, all of them are called as plastics in daily life; most popular used plastics are tabulated in Table 2.1;

Table 2.1. Some plastics used in daily life.

Thermosets:	Thermoplastics:	Elastomers:
Polyesters	PET-Polyethylene terephthalate	EPDM- Ethylene Propylene Diene rubber
Epoxy resins	PVC-Polyvinyl chloride	Polybutadiene
Phenol formaldehyde resins	PS- Polystyrene	Polychloroprene
-	PP- polypropylene	-
-	PE-Polyethylene	-

Polypropylene and EPDM are two favorable polymers that are in focus of this study. Propylene is used mainly for food containers (i.e. ketchup, yogurt, etc.), bags, bottles. EPDM is also a material used mainly for covering, corrosion/water resistant material mainly used in conveyor belts, automobiles, etc.

Pristine polymers/plastic are not useful and mostly, resins, raw material of polymer are mixed with many effective additives to enhance performance. Improvement fillers/ingredients consist of inorganic additives like silica and carbon that improve the material to make it stronger; plasticizers to make newly generated material pliable; stabilizers having ultraviolet and thermal properties, as colorings and flame retardant.

Recently, environmental effect of polymers/plastics is getting a problem to soil, aqua life. Especially, plastic packaging materials are main source of landfill waste. Numerous land and marine animals regularly consume them. This is leading to catastrophic consequences to environment cycles. Synthetic plastics are not disappearing in environment long time due

to they are not biodegradable. They just accumulates and grows in landfills and causes pollution of the environment. Plastics is getting waste nightmare for municipality.

Efforts to reduce the use of synthetic polymers/plastics are mainly summarized as usage of biodegradable and degradable plastics, collection of used plastics to recycle, incineration of used plastics, non-usage/reduction in usage of polymers/plastics.

Governments are promoting new regulations that summit all over the world either trying to decrease plastic use or to increase using/selling biodegradable types of polymers/plastics to eliminate any effect on environment due to their long resistance time. The focus of study is about to generate new type of biodegradable polymers from mostly used synthetic pristine polymers providing an environmentally safe research in this area.

2.2. Market Investigation of Pristine Materials: Polypropylene and EPDM

2.2.1. Polypropylene Market

In this study, Polypropylene thermoplastic and EPDM rubber have been selected due to their different types of applications not only in food industry but also in energy saving material researches to get benefit by consuming less. Here, it is better to mention about global/local market share/growth, local production/availability, and prices.

Polypropene/ Polypropylene (PP) is one of mostly consumed material (polymer resin) in the world. PP is a synthetic thermoplastic polymer that have high molecular weight. It has been produced under catalytic polymerization. Due to quality of polymer to use and its wide range of application, its demand will continue to increase, specifically in automobile industry and disposables of goods. This caused countless opportunities for the global polypropylene market. Additionally, the substitution of all wooden and metal materials has been replaced with polypropylene leading to the growth of global PP market.

Polypropylene is the second largest polymer that is produced, consumed, and export in the world after polyethylene. Last 5 year, from 2011 to 2015, total world trade of polypropylene is changed from 51 million tons (91 billion dollar) to 57 million tons (80 billion dollar) with 3 % growth [11].

In Turkey, the only producer of polypropylene is PETKIM that has a plant with a capacity 144000 t/year. Maximum production was about 134000 t/year in 2010. In 2015, Turkey's

polypropylene export was around 40000 tons. The import amount has reached 194300 tons in 2015 (cost 2.6 billion dollars).

2.2.2. Ethylene Propylene Diene Monomer (EPDM) Market

EPDM is one of synthetic rubber, having resistance to heat, whether, corrosive materials, oxygen components and provide good insulation properties to electricity. EPDM has a wide range of application such as roofing insulation, car industries. Automotive industry is good to apply EPDM based materials such as washers, vibrators, belts, electrical insulation parts, tubes, orings, electric wires, internal design parts, doors, seats, etc.

EPDM is used as a substitute of thermoplastic olefins (TPO) in plastic manufacturing industry. Upgrading technology in manufacturing of plastic modification further helps in the growth of EPDM market. Many companies deal with manufacturing of innovative EPDM by including various materials, which reduces their negative impact on environment. Biodegradable innovation is one of them. These environmental friendly innovation leads to increase the world demand for EPDM. Today, the EPDM market globally is expected to be worth near USD 7 Billion by 2020 [12]. However, due to wide range of applications and substitution of other polymers, and innovative products which saves the environment, would increase rapidly the future demand. This is the reason why researchers are strongly willing to search on new materials based on EPDM.

2.2.3. Biodegradable Plastics Market

As seen above, PP and EPDM market is huge and growing steadily. Nowadays, biodegradable new products take some share on this market and PP and EPDM based biodegradable ones are one of these.

The biodegradable plastic market consists of some major applications, like extrusion and molding, packaging, agricultural applications, fibers/fabric, and other. The demand of biodegradable polymers in extrusion and molding applications is projected to have one of the biggest growth among these applications. The biodegradable market is separated into some main divisions, such as cellulose regenerated, PHA, PCL, PLA, PBS, and starch blends.

Largest segment of biodegradable product derivatives has been generated by using PLA. Above 45.1 % of completely biodegradable plastics market has been observed in 2015. Also,

second largest growth rate among biodegradabe product markets has been expected in PLA market. Processability easiness and superior mechanical properties are the main reasons to this market expansion of PLA. In 2020, total amount of biodegradable plastics and elastomer markets is thought to be reached around USD 3.4 billion in world [13].

2.3. Additives for Generation of Biodegradable Stable Polymer Nanocomposites

Polymer additives are used to give superior properties to pristine polymer. These properties are related with their usage areas. Some additives are used to improve mechanical properties such as strength, permeability, optical properties; additionally, nowadays, organic additives to enable degradation with time can decrease catastrophic environmental effects of synthetic polymers.

Thermoplastic nanocomposite preparation can be accomplished by mainly nanoscale fillers and classified as chemical or physical structures. They are mainly divided as inorganic or organic nanomaterials. Some inorganic additives mainly used in latest researches are classified as oxides (SiO_2, Al_2O_3, MgO, ZnO, FeO_x etc.), hydroxides of metals (Al $(OH)_3$, Mg $(OH)_2$), inorganic salts ($BaSO_4$, $CaCO_3$, $CaSO_4$), silicates (kaolin, talk, montmorillonite, and mika) and metal dusts (Ag, Au, Ni, Pt, Cu vs.). Organic fillers/improvers are carbon based materials (carbon nanotubes, carbon black, graphite, fullerene, etc.), natural biopolymers (cellulose, caprolactone, polylactic acid) and synthetic polymers such as polyesters, polyamides, etc. Main classification of recently used fillers can be observed in Figure 2.2.
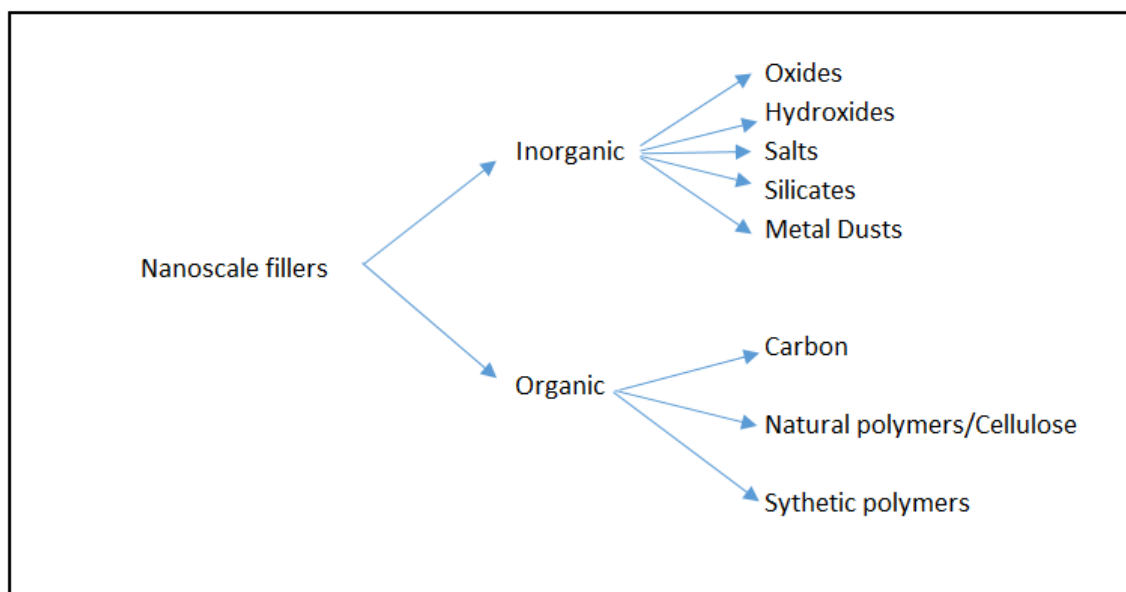
Figure 2.2. Nanoscale Fillers Classification.

Some biodegradable polymers are shown in Figure 2.3 below. Biodegradable polymers are mainly generated from renewable resources or natural polymers.
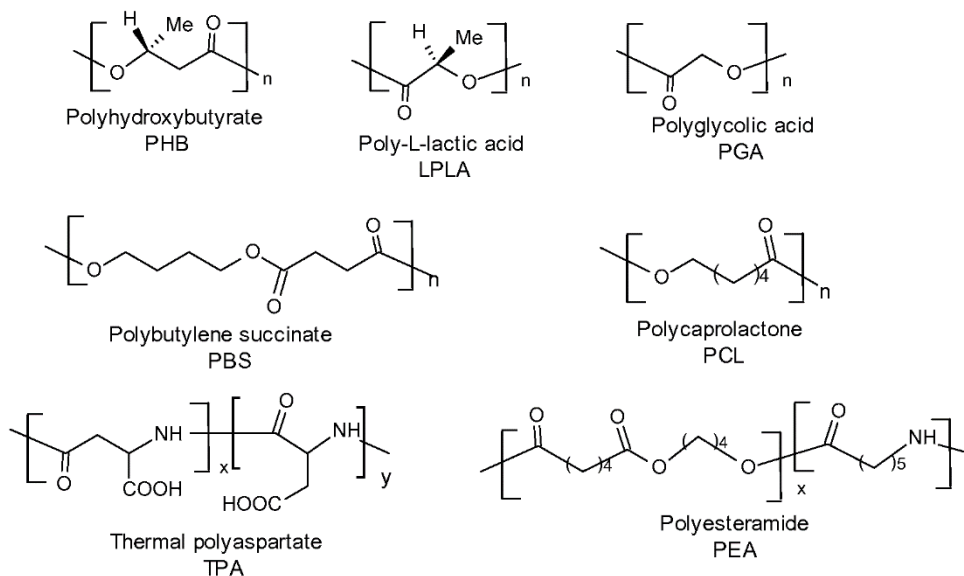
Figure 2.3. Some examples for biodegradable polymers.

Filler properties are mainly related with particle type, size, distribution, porosity, surface area and activity. According to surface activity and behavior inside pristine polymer matrix, fillers are discriminated as inert, semi, mid or high active fillers. Due to the conditions employed in the production of nanocomposite polymer, blending efficiency and properties of nanofillers, settling inside polymer matrix or formation of phase separation /intercalated structure play an important role. Processing conditions during production of nanocomposite is also important to get a desired product. Polymer nanocomposites can be produced by in-situ polymerization, solution mixing, and blending in melt phase. The conditions of each process and properties both have effect on last generated structure and properties of the nanocomposite.

In this study, some organic ingredients, namely, polylactic acid and polycaprolactone, have been used to make biodegradable type of improved nanocomposites. Different types of organoclay (montmorillonites) nanofillers, synthetic copolymer silica nanoparticles as compatibilizer and PP grafted maleic anhydride have been used to improve mechanical properties which will be explained briefly.

2.3.1. Biopolymer Additives

2.3.1.1. Bioengineering polyesters- Poly Lactic Acid

Polylactic acid is one of the main additives in this study to make the main polymer matrix degradable. In the latest century, because of the emerging environmental awareness, renewable resource based and naturally biodegradable/compostable polymers receive more attention. Mainly, starch is a good renewable source to produce biopolymers and its fermentation allows the production of lactic acid (LA) and polylactic acid (PLA) [14]. Industrial production of LA is accomplishing by microbial fermentation due to cheap and on spec manufacturing compared to chemical synthesis.

Typical feedstocks are cornstarch, sugarcane, wheat and tapioca roots to produce polylactic acid that is a thermoplastic polyester. The global PLA market is expected to reach a market size of more than USD 5 billion by 2020 [15]. Oil resources and rising fossil fuel decreases are important factors changing world consumption figures. Increasing environmental issues, environment pollution, and government regulations are key factors helping the preference of PLA by end users of final products as well as manufacturers in industries such as medical, coating, textile, packaging, transportation, electronics, etc.

The homofermentative method is a common industrial practice in production of LA due to higher yields of lactic acid and low by-products. This fermentation process utilize Lactobacillusgenus like Lactobacillus delbruecki, Lactobacillus amylophilus, at certain pH and temperature with insufficient oxygen conditions. Most of the time, L-Lactic acid (pure) is fed for PLA production as raw material [16].

PLA is a polymer, which differs in molecular weights, packaging industry is using high molecular weight PLAs. There are three types of production methods for polymerization of LA; (i) direct condensation polymerization; (ii) direct polycondensation under azeotropic medium (solution) and (iii) polymerization by lactide formation. Figure 2.4 shows mechanism at once for transformation of LA to PLA [17].

PLA, high molecular weight type, generation by polycondensation under catalyst under azeotrope solution is a common way to produce it. The catalyst variety and contents, the volumetric ratio of solvent, and time of reaction on the production of PLA are main parameters to generate high molecular weight PLA, and have seen sophisticated equipment and proper complex catalyst system provides near $M_w = 1.000.000$ Da [18].

11
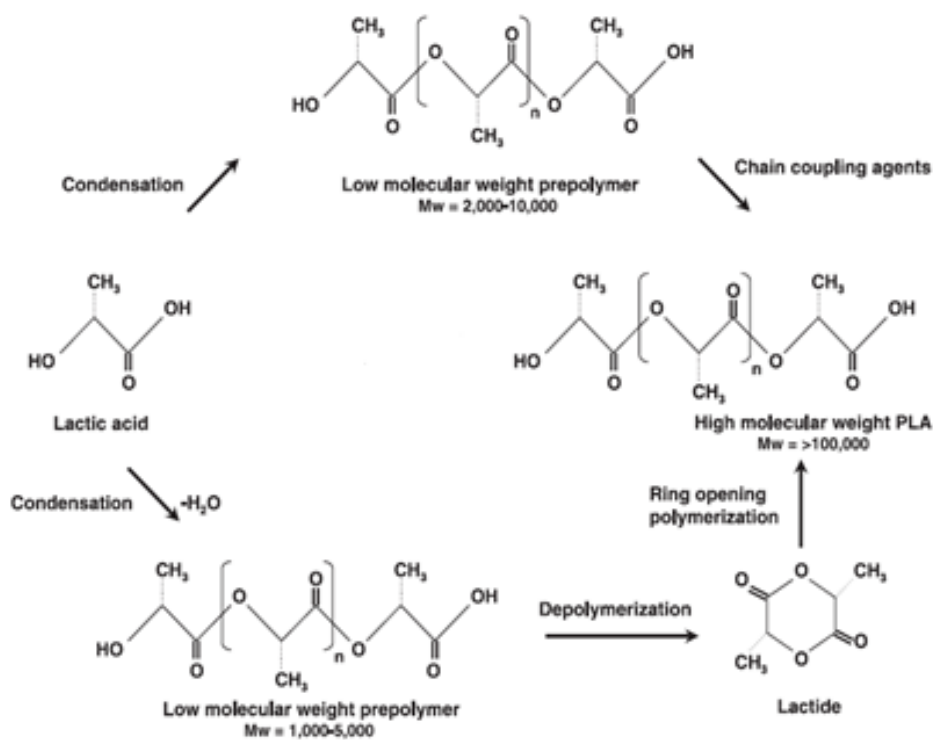
Figure 2.4. PLA Synthesis Methods [21].

Microstructure, morphology, and conformation are the most important properties of PLA. They are determining factors to reflect changes in polymer composition. These factors are interactions, immiscibility, and degradation. M_w is one of the most important property that affects these interactions. M_w changes of PLA is also a focus of this study.

When biodegradability is considered, PLA has been analyzed as degraded naturally in compost or soil. Although, it has found that PLA is one of low rate of degradation natural polymer than other aliphatic biodegradable polymers like poly ε-Caprolactone (PCL) in natural life [19].

PLA nanocomposites/montmorillonites (5 % w/w) loading were generated by blending in melt phase with the help of an inside mixer and then started to degrade in a commercial compost. Nanoclay addition has seen to increase the rate of PLA degradation, especially degradation is much better in highly dispersed clay samples in polymer matrices. Biodegradation has been accomplished by the bacteria named Bacillus licheniformis [20]. This result promises the prospective usage of this biopolymer in polymer blends together with some inorganic fillers to increase the mechanical properties of material and surface area

to end up with a higher degradation by water, sun, physical forces, and microorganisms when it reaches the environment.

2.3.1.2. Bioengineering Polyesters: Poly (ε-Caprolactone)

Poly (ε-Caprolactone) (PCL) is an artificial aliphatic biodegradable polyester that has been considered, in recent years, mostly in medical areas, such as drug delivery, scaffolding for tissue engineering. Additionally, during the researches, this material has been used to produce microspheres, pellet, microcapsule, nanoparticles, implants, and films. Fabric industry is also trying reinforced fibers of many forms of this material by spinning into filaments for repeated fabrication of desired textile structures. According to web of science data, latest publications reached more than five hundred per year in bioapplication and tissue engineering. Figure 2.5 shows cyclic monomer of PCL. Oxygen bonds provide interactions between O-H, H-H bonding which in turn result in strong fiber properties in macroscale. Oxygen bonds and chemical structures of caprolactone and polycaprolactone are shown in Figure 2.5.
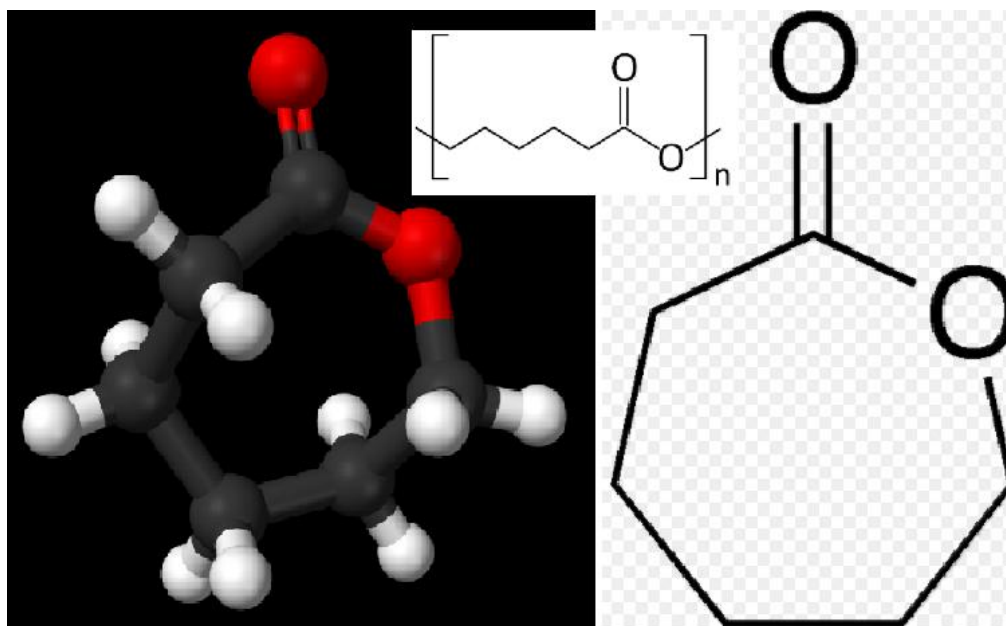
Figure 2.5. ε -Caprolactone chemical structure showing oxygen bonds and Poly (ε – Caprolactone) structure.

PCL can be generated by polymerization as ε -Caprolactone ring opening studying under different types of cationic, anionic, or coordination catalysts or via ring-opening polymerization of 2-methylene-1- 3-dioxepane with the help of free radicals [22]. PCL is a hydrophobic, semi-crystalline biopolymer. Its crystallinity show trend of reverse relationship (decrease) with increasing molecular weight. Polycaprolactone (PCL) polyester has around 60 ^{o}C-low melting point and about – 60 ^{o}C-a glass transition temperature. The production can be provided by ring opening polymerization of ε-Caprolactone with the help of a catalyst like stannous octoate. Alcohols can be utilized to modify the molecular weight of the generated polymer [23]. PCL have different M_w types of usage. In this study, it has been used as M_w=125.000 Da due to some investigations of high miscibility of organic sites to absorb inorganic fillers in polymer blends. Figure 2.6 shows the mechanism of the chemical reaction under heat and catalyst.
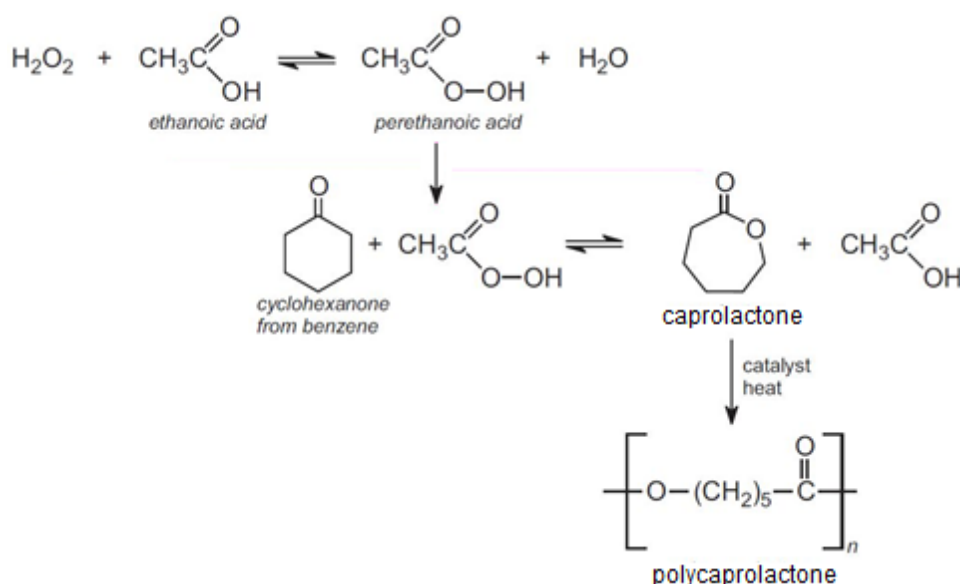
Figure 2.6. Mechanism for poly (ε-Caprolactone) synthesis.

When biodegradability is considered, PCL can be disappeared/biodegraded by living microorganisms like bacteria/fungi in outside environment, but these living organisms are not biodegradable in human or animal bodies due to the lack of suitable enzymes [24]. The biodegradation takes a few years outside depending on the interaction within composite structures. Nowadays, human body materials can be produced by using PCL added materials, which also have ability to own biocompatibility. The biodegradability of PCL is beneficial both for industrial polymer nanocomposites to disappear in environment and it is also

important for drug delivery or tissue engineering due to their ability of being absorbed within the body. This study will use these abilities of PCL to investigate some material improvement mainly for industrial applications.

2.3.2. Compatibilizers and Fillers

2.3.2.1. Copolymer Silica fillers: Reactive/Nonreactive Nanoclays-Montmorillonites and Copolymer (MA-*alt*-1-dodecene) -g-Silica Nanoparticles

Silicates are most abundant and present as different and complicated types/classes of minerals on Earth. Approximately, silicates consist of 30 % of all minerals and almost 90 % of the Earth's crust contains silicates. Oxygen and silicone are the elements found most abundantly, thus, naturally silicates are different forms of these elements.

The main chemical structural unit of silicates is the SiO_4-tetrahedron shaped, anionic group having a negative charge minus four (-4) in this structure. The central silicon ion is positively charged and oxygen has four (4) more electron vacancy to form (-4) in molecular structure. These vacant electrons provides the oxygen with an option to bond to another silicon ion and therefore it links one (SiO_4) tetrahedron one to another, etc. [25]. These formed and linked silicate tetrahedrons forms shows great properties. They will generate single or double units, chains, rings, layers/sheets, and framework structures. These different types of formation of Silicate tetrahedron structures' combination makes Silicate mineral class the largest, most complicated, and having possibility of researches among classes of other minerals.

Silicate based fillers are mainly coming from minerals of silicates which contains also other elements. Eventually, enormous number of minerals are available on earth. Some classification on major mineral examples is shown in Table 2.2.

Table 2.2. Classification of clay minerals-[26] T: Tetrahedral, O: Octahedral.

Structure Type	Group	Mineral Examples	Ideal Composition	Basal Spacing (°A)
2:1(TOT)	Smectite	Montmorillonite	$M_x(Al_{4-x}Mg_x)Si_8O_{20}(OH)_4$	12-17
		Hertorite	$M_x(Mg_{6-x}Li_x)Si_8O_{20}(OH)_4$	
		Saponite	$M_xMg_6(Si_{8-x}Al_x)Si_8O_{20}(OH)_4$	
2:1(TOT)	Illite	Illite	$M_x(Al_{4-x}(Si_{8-x}Al_x)O_{20}(OH)_4$	10
2:1(TOT)	Vermiculite	Vermiculite	$M_x(Al_{4-x}(Si_{8-x}Al_x)SiO_{20}(OH)_4$	9-14
1:1(TOT)	Kaolin	Kaolinite	$Al_4Si_4O_{10}(OH)_8$	7

Each clay mineral contains structure of two sheets, tetrahedral and octahedral [27]. The preparation of nanocomposites have been generated by using mostly Montmorillonite, Hectorite, and Saponite which are mostly preferable types of Smectite layered silicates. Montmorillonite (MMT) is a well known acceptable clay for usage in polymers matrix due to their high surface area and reactivity.

Generally, silicate nanolayers that are organically modified called as 'organonoclays' or 'organosilicates' [28]. Physical mixture of layered silicates and pristine polymer may not generate nanocomposites. In order to provide layered silicates being suitable to mix with polymer matrices, hydrophilic surface property of silicate clay needs to be converted to an organophilic surface one. The surface may be accomplished by ion exchange system reactions via cationic surfactants [29]. Sodium montmorillonite based layered silicate clays can be found as tactoids in micron size that includes several hundreds of individual plate-like structures (1 nm scale) being existed combined by electrostatic forces between layers/plates. Typical structure of clay can be seen in Figure 2.7 together with tetrahedral and octahedral sequences on structure.
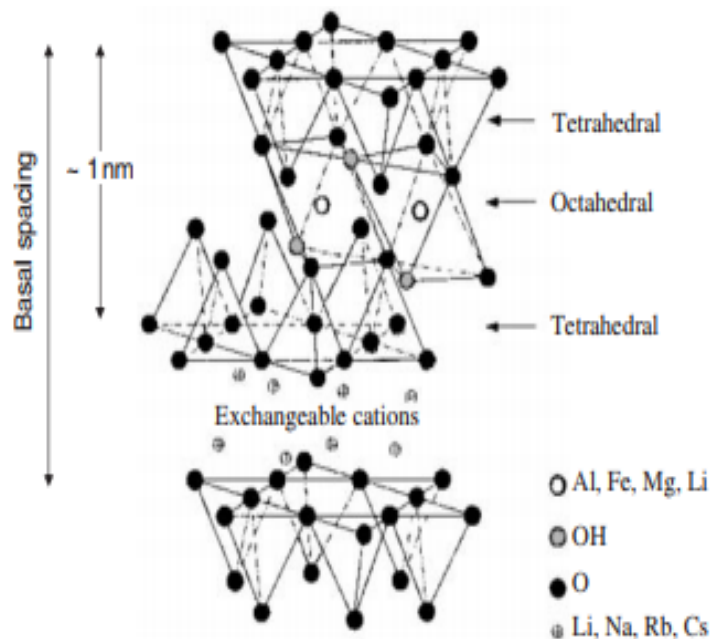
Figure 2.7. Basic structures of 2 : 1 clay minerals-2:1 structure (TOT) [26].

As mentioned before, montmorillonite and hectorite seem to be mostly used smectite-type layered silicates for nanocomposite production. They are hydrophilic in nature in their pristine form making it very difficult for them to be dispersed into biodegradable polymer matrices also. In order to solve this difficulty of interaction/mixing, the most common strategy is to change the interlayer clay cations via quarternized phosphonium/ammonium cations, preferably, to provide organic parts as with long alkyl chains [96]. Consistently, this study consists of octadecyl amine (ODA) and dimethyldidodecyl ammonium cation (DMDA) type reactive and nonreactive montmorillonite organoclay, respectively, which were also used in previous studies for bifunctional reversible addition-fragmentation chain transfer (RAFT) agent system [30].

2.3.2.2. Compatibilizers: MA based Copolymers- PP-g-MA Reactive Compatibilizer and Poly (MA-alt-1-dodecene)-g-SiO$_2$ Compatibilizer

Compatibilizer is a substance to use in mixture of substances to increase interaction between constituents to change morphology and modification between phases in structure by physical or chemical methods. Mostly, they are helping to link between polymer chain and functional groups in additive. The expected properties of these materials are having the same solubility parameter with the polymer, having many functional groups to provide breakage of different bonds and forming new reactions.

17

Maleic anhydride (MA) reactive copolymers, including poly (MA-grafted-olefins) are being widely used to generate engineering, bioengineering and nanoengineering materials that have superior performances [31]. Recently, we have reported the preparation of polypropylene and EPDM rubber silicate layered nanocomposites in melt phase by reactive extrusion system using poly (MA-alt-1-dodecene) as a reactive compatibilizer [32]. Another research work on PP-g-MA/organo MMT nanocomposites involved the determination of gas permeability, heat resistance, and TGA/FTIR analysis. These properties seem to be different according to pristine matrix. Composite with PP-g-MA shows a decrease in heat release peak [33].

Production with melt extrusion system with PP-g-MA based material has been studied in another article [34] and XRD/TEM analyses were used to observe the effect of PP-g-MA in polymer system structures. Intercalation has been observed in macromolecular segments where XRD shows PP crystal sizes have been decreased by PP-g-MA.

High density polyethylene based study has been observed in lots of thesis research like Köksal S. [35]. This study proves maleic anhydride improvements on mixing of the polymer and other additive (clay). All mechanical, barrier, thermal and flow properties have been improved compared to pristine polymer. This has been achieved by exfoliated structure of layers inside polymer nanocomposite with the help of MA based compatibilizer.

These studies show that PP-g-MA has a good compatibility property not only with polypropylene (PP) but also with EPDM based structures. In this study, PP-g-MA will be used to get good mixing during reactive extrusion system under melt inhibition of silica based copolymers as additives to pristine polyester, (EPDM) or polypropylene. Additionally, in previous studies, MA-alt-1-dodecene has been used for nanocomposite studies in previous work of our group [36]. Here, MA based silica copolymer has been generated by sol-gel method and used in the study. The same material has been employed also, in this study, to see the effect on both EPDM and PP based structures. MA-g-Silica has been used as compatibilizer and filler. PP-g-MA is observed to increase the compatibility between layers. Figure 2.8 shows chemical form details of these two materials. The study is also unique in this respect due to the usage of two different forms of MA and two different forms of silica particles to maximize the nanostructural effect on pristine polymers with different functional groups.

18
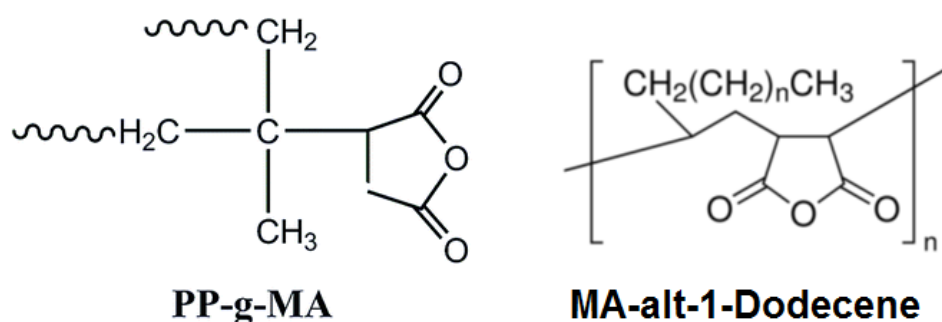
Figure 2.8. PP-g-MA and MA-alt-1-dodecene.

2.4. Polymer Nanocomposites Production Methods

2.4.1. Polymer Intercalation in Solution

Solution based systems have been generated by mixing additives with polymer in solution environment. Organoclay type additive is dissolved in a solution such as ethanol, toluene, water, etc. and dispersed to be absorbed. Polymer is also dissolved and dispersed in same type of solution and the reaction is initiated by mixing the solutions. Chemically, polymer chains start to fill spaces between crystal layers. Finally, solution is dried and solvent is evaporated. The remained part is the nanocomposite portion that contains well-dispersed filler in polymer matrix. Figure 2.9 shows polymer addition in solution and mixing by fillers.
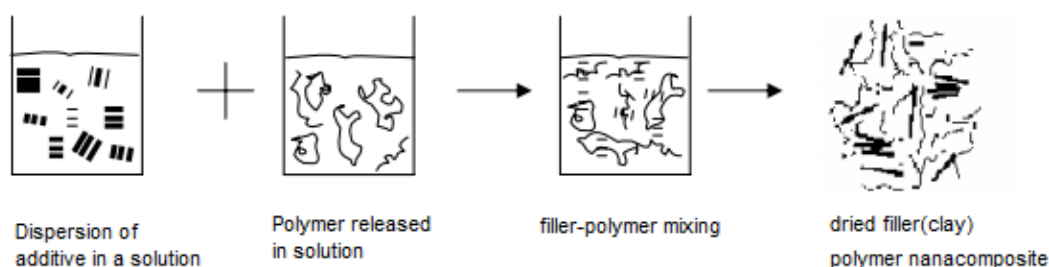
Figure 2.9. Illustration of production of nanocomposite in solution.

Generation of nanocomposite via this method is highly selective due to the polymer and fillers since they have different physical and chemical properties. Additionally, the solvent is also an important factor in this method required to dissolve the polymer and fillers. The usage of a solvent needs high capital expenditures and may not be environmentally friendly in most cases of large scale of production. At the same time, each nanocomposite to be produced is also desired to own specific properties. Therefore, the method is applicable if

parameters both on materials and on final product are in agreement with experimental conditions.

2.4.2. In Situ Intercalative Polymerization

Monomers will be placed in a solution and dispersed with an absorbing solvent. Fillers are also added into solution and dispersed well. Polymerization is started at a given temperature and with the help of a radical agent to get the best dispersed system matrix due to the fillers embedded into chains of the polymer. This is the best method to get high intermolecular distance between filler layers. After termination of polymerization, solvent is evaporated and the nanocomposite is now ready for further modification and usage. Illustration of synthesis is seen in Figure 2.10. Final product is expected to be well dispersed, however, this method contains same difficulties like solution based method due to solvent requirement, large scale economic difficulties, and environmental considerations.
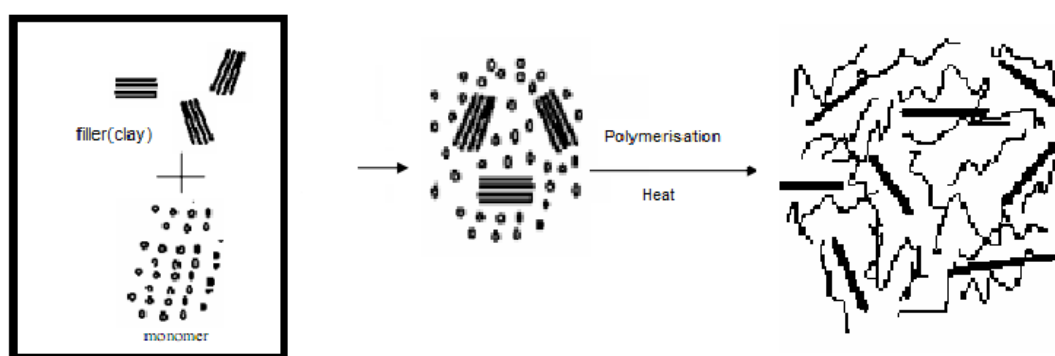
Figure 2.10. In situ polymerization to produce nanocomposite.

2.4.3. Melt Intercalation Technique/ Reactive Extrusion System

This method is based on polymer mixing with additives (filler, compatibilizer, reactive agents) under melt conditions. Melting is suitable above softening point of polymer. This commonly used process is beneficial, mainly, for insoluble polymers and for those of which polymerization is impossible. Recently, solid filler (clay) or masterbatch and polymer haves been mixed under melt conditions in many researches. The method is suitable since solution problems are avoided, but still there may arise some difficulties in getting a well exfoliated nanostructure. In order to provide the most efficient performance of the method, two factors should be considered such as selecting an optimum layered, active surface chain agent and

a polymer-additive/filler (clay) system with high polar interaction between them. Mostly, these disadvantages are eliminated by compatibilizers or pre-modified copolymer nanoparticles, which are produced with this method, or the method mentioned before.

Exfoliation is used to describe mixing of polymer-clay systems. During the development of polymer/clay nanocomposite, initially, the polymer surrounds the organic clay agglomerates by the formation of a tactoid. The next step involves the intercalation that is penetration of the polymer into space between layers of organic clay separations around 2-3 nm. The final step consists of all layers being mixed with polymer called exfoliation/partial exfoliation. All processes are achieved at one step extrusion to provide easy melting of the polymer. Consequently, temperature and mechanical forces can be altered easily to have the best exfoliated structure. This study will utilize this equipment to implement one step extrusion of all ingredients with optimum conditions of temperature and residence time. Experimental part will show details of the equipment and conditions. All simple illustrations of generation of polymer nanocomposite in melt system can be seen in Figure 2.11.
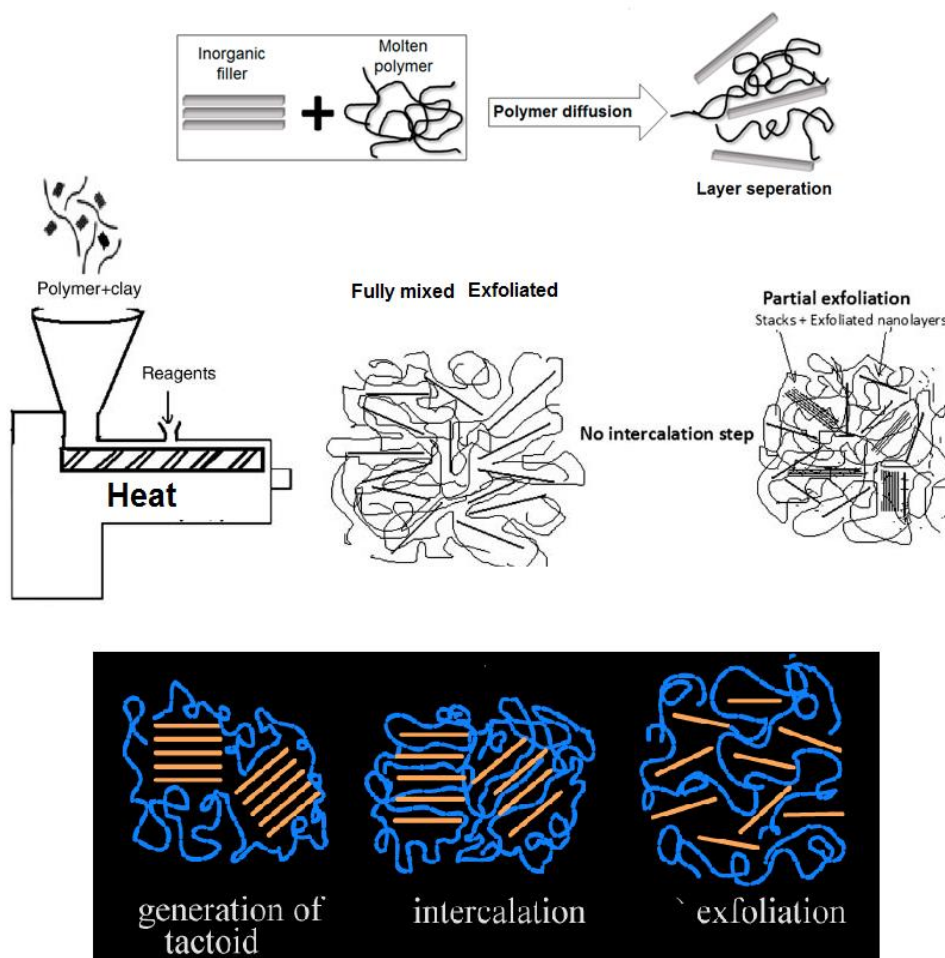
Figure 2.11. Melt Blending of Polymer And Filler/ Illustration of Reactive Extrusion.

2.5. Main Characterization Methods of Nanocomposites

In order to understand all changes inside nanocomposite structure, instrumental analysis is required. Mostly used analytical methods have been searched in literature. Some of them are available to be used in this study too. The selection is based on similar materials used in the study such as silica/polymer blend nanocomposite material characterization. In this section, a brief information is given about the selected methods, followed by conventional methods to analyze new materials. Other information about equipment and methods of characterization can be found in experimental part.

2.5.1. Fourier Transform Infrared Spectroscopy (FTIR)

FT-IR means Fourier Transform infrared spectroscopy to detect molecular bonds in complex structure help to find interactions. In FTIR spectroscopy, Infrared radiation (IR) is sent to sample. Part of the infrared light is taken by the analyzed sample and some of the radiation is transmitted. The final spectrum of radiation/light represents the molecular absorption or transmission that is specific and creation of a molecular fingerprint of the analyzed sample. This specific property of radiation fingerprints of molecules provides infrared spectroscopy useful for analysis to identify unknown materials, determine the consistency of a material, and component amount details in a mixture. This technique is applied on particles, wastes, multilayer materials, esters, and silicones.

Clay based nanocomposites can be analyzed with this method to understand functional group interactions. Experimental and calculated spectrum will provide type of species and the interaction between functional groups in nanostructure [37]. Additionally, internal morphology behavior of clay-polymer composites can be analyzed with this method to see thermal degradation of structures [38].

2.5.2. NMR: Nuclear Magnetic Resonance, Solid State ^{29}Si, ^{13}C

Solid-state NMR spectroscopy is one of the most common techniques for the characterization of solid nanoparticles and polymer-filler based nanocomposites. The technique is good to explore the structure and dynamics of molecules especially in organic chemistry and biochemistry. When a magnetic nucleus is placed in an external magnetic field, the nuclei become aligned in a certain number of orientations due to all nuclei having odd number isotopes (protons and neutrons). They shows an intrinsic magnetic moment and angular momentum properties. These can be seen in spectra to understand molecular bonding. The generally measured nuclei are hydrogen-1 and carbon-13 isotopes. Some other isotopes of elements i.e. ^{15}N, ^{17}O, ^{29}Si, ^{19}F, ^{31}P, ^{11}B, ^{23}Na, ^{35}Cl can also be analyzed in NMR systems.

In literature, clay/polymer or copolymer blend analysis has been observed. Structural characterization of copolymer (3-Aminopropyl) triethoxysilane-modified silica has been made by Silicon-29 and Carbon-13 NMR to see surface interaction and bonding between functional groups [132]. This typical type of example can be enlarged especially when reactive functional group based copolymer or nanoparticle addition like Si to blends needs

to be observed. So, in this study, C or Si based NMR is a good choice to understand nano world under macrostructures.

2.5.3. XRD: X-RAY Diffraction Characterization

X-Ray method uses X-ray beams that have energy between IR and gamma light. Characterization with this equipment depends on the type of sample, detector, and light property. Working principle is mainly sending a beam to a sample and collecting data from the scattered light from the sample. Crystal structure of nanocomposite may give a good light scattering at different angles, which provides better information about details of composite structure. XRD is a powerful technique to determine phase characteristics of crystalline material and give values on unit cell crystalline dimensions.

X-ray diffractometers have some basic parts: a sample holder, an X-ray light generation tube, and an X-ray detector. X-ray light are generated by the cathode through heating of a filament to generate electrons, which in turn these electrons go through a target/sample. Electrons get sufficient energy to release inner shell electrons. As a consequence, X-ray spectra will be produced to characterize the sample components.

XRD is used for analysis of intercalation and exfoliation in composites consisting polymer and layered materials [39]. XRD can show interlayer/d-spacing. Polymer nanocomposite is frozen after melt; some fractions are; polymer chains (0.5 nm diameter); small crystallites (10 nm), and whereas some fractions remain amorphous. The typical size comparison has been shown for a typical nanocomposite fiber in Figure 2.12. XRD will show structural information details of polymer chain and layers at three length scales 1, 10 and 100 nm using scattering at wide-, small- and ultra-small-angles, respectively [40].
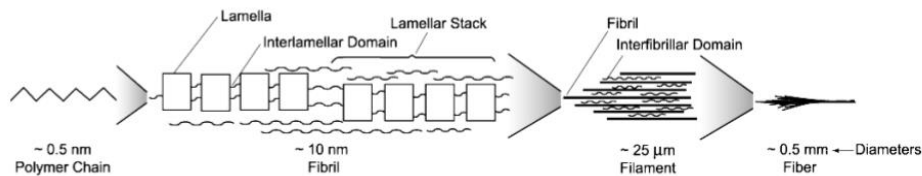
Figure 2.12. Size of polymer nanocomposite from macro to nanoscale [40].

Due to wide application of polymer systems, XRD is also a good method for clay/polymer nanocomposite performance analysis by showing interfiling and crystallization efficiency. This study will show details of structures of generated nanocomposites. Equipment and method details can be seen in experimental part.

2.5.4. SEM/TEM: Scanning/Transmission Electron Microscopy

SEM, Scanning Electron Microscope, is an equipment using beams of high-energy electrons to send signals to the surface of sample that is solid. The signals come from electron-sample interaction emissions and data is obtained about the sample such as morphology, composition, crystallinity, and orientation of materials constituting the nanocomposite. In literature, information is present on a determined area of analyzed sample surface. A 2-dimensional picture is generated as areas change between 1 cm- 5 microns in width with SEM technique by having magnifications varying from 20X to 40000X, at a resolution changing from 50 to 100 nm. Typical illustration of SEM is shown in Figure 2.13.
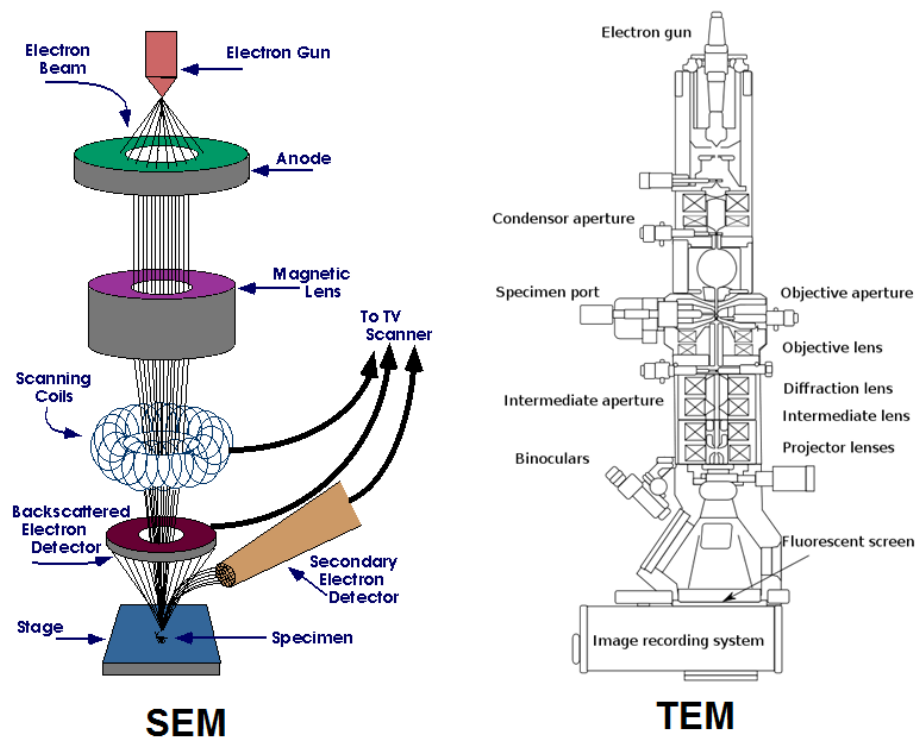
Figure 2.13. SEM and TEM working elements during analysis [41].

Transmission electron microscope (TEM) works with same basic principles as SEM, which important elements of both systems are shown in Figure 2.13. The main difference is that

electron passes through the sample in TEM and detector is below the sample to record transmitted waves whereas in SEM electrons are reflected from the surface of the sample. In TEM, small details of different materials can be observed almost near to atomic levels.

SEM and TEM are two main characterization techniques for polymer nanocomposites and useful for organosilica/polymer blends for investigating the surface morphology-structure-internal orientation. They will give clear evidence of internal polymer chains and intercalation/dispersions of fillers. SEM will also give specific information about surface morphology of organoclay/polymer based composites. Examples for organoclay characterizations are present in literature. Additionally, transmission electron microscopy (TEM) of organo-monmorillonite clay has been used to analyze and understand the arrangements of patterns of plates before, as pristine, and after modifications of clay composites. SEM pictures/images show raw polymer block and clay nanocomposites loading, surface morphology as uniform and SEM is good method to illustrate the dispersion of clays within the pristine polymer matrix represents to their chemical or physical properties [42]. These characterization benefits of SEM and TEM on polymer nanocomposites are beneficial for this study also.

2.5.5. DSC/TGA: Differential Scanning Calorimetry/Thermal Gravimetric Analysis

Differential Scanning Calorimetry (DSC) is commonly referred to characterize thermal and physical properties of polymer nanocomposites. DSC can analyze some important properties such as heat of melting, melting temperature, percent crystallinity, and glass transition temperature (T_g). DSC works by evaluating the difference of heat required for the increase in temperature of a sample and reference sample (witness) when temperature is changed gradually. Both the analyzed sample and reference sample are kept nearly at the same conditions such as temperature, humidity, etc. throughout the experiment. Reference and sample cabin temperatures are recorded. Temperature gradually increases as a function time. Samples absorb heat during phase change and the sensor determines the change in temperature. The point of heat absorption gives peak point in DSC curve.

Similarly, TGA provides supplementary characterization information to DSC which another commonly used method. TGA data gives information about the change change in amount & rate for the sample mass as a function of temperature or time. Thermal stability of materials is measured under oxidation together with their compositional properties. The technique is mostly useful for the research of all types of polymers like thermoplastics, thermosets,

elastomers, composites of them, and their film/fiber derivatives. Another major application of TGA is to determine filler amount inside polymer nanocomposites. Figure 2.14 shows commercial equipment of DSC and TGA.

DSC and TGA are valuable techniques to detect the difference between a newly generated polymer nanocomposite and pristine polymers. Recently, PLA/PEG/montmorillonite blend study has been analyzed [43] with DSC and TGA; providing important results like melting point, thermal stability of the new material.
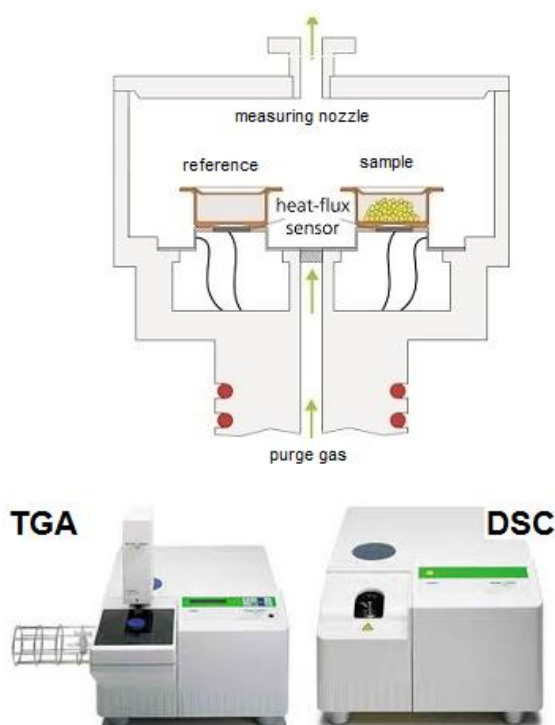
Figure 2.14. Equipment of TGA, DSC, and DSC internal.

2.5.6. Rheology Analysis with Dynamic Rheometer

Rheometer measures flow, forces, and shear associated with substance that is flowing. Solid polymer systems including polymer nanocomposites can be analyzed under heat and pressure to see flow changes at different pressures and flow characteristics like shear or the flow behavior of a substance under certain points of stress/force. The output of a rheometer characterization gives typically sets of curves showing viscosity with time and stress with time under certain material specific process conditions.

Dynamic shear rheometer, DSR is used for research and development as well as for quality control in the manufacturing of a wide range of materials including cement or asphalt. It is is mostly used for studying liquids, gels, and, polymer blends, soft rubbers. In DSR, a sample is placed between two plates, small displacement is applied to the upper plate, and the torque needed for this is measured. Shear stress and strain oscillatory gives the calculation of the viscoelastic response, characterized by the storage shear modulus, loss shear modulus and the loss angle. DSR analysis is a very sensitive technique for studying rheological changes due to polymerization reactions, changing physical interactions.

In polymer characterization systems, literature gives report on the usage of dynamic rheometer i.e. linear oscillatory rheology on composites of polystyrene-grafted silica NPs has been studied and found that there is certainly an analogy between the viscosity of polymer-grafted NP and star polymers [44]. There are considerable amount of examples in literature and so in this study; it has been decided to use the method to see effect of fillers and its structure inside polymer matrix. In industry, PETKIM is using this equipment for polymer characterization. All our samples have also been sent to PETKİM for analysis and results have been tabulated mainly due to viscosity and shear rate as in literature. Equipment details and analysis parameter details can be seen in the experimental part.

2.6. Polymer Nanocomposite Structures Recent Development

2.6.1. PP: Polypropylene Based Structures

In recent days, attention of many researchers was focused on fabrication of the biodegradable polymers and their layered silicate or silica nanocomposites [96, 97], polymer blends and nanocomposites from sustainable renewable resources [4]. They have also research on Polypropylene (PP) composites reinforced with various natural fibrous nanomaterial such as palm fiber [98], bunch fiber of empty fruit of oil palm tree and derived cellulose from oil palm tree [1], short flax fiber bundle [99], rice-husk flour [100], sisal/PP composites with minimum fiber [2], and other polymer composites reinforced with natural fibers [101].

Lee et al. [5] prepared PP/poly (ε-Caprolactone) (PCL) reinforced with cellulose nanofiber (CNF) hybrid nanocomposite by using a batch-type kneader with six twin-screw elements with the addition of PP-*g*-maleic anhydride (MA) graft copolymer as a compatibilizer to improve the distributions of PCL domain and CNF in PP matrix. The anhydride groups on PP easily react with the polyester in situ to form graft compatibilizer in melt phase.

Domenech et al. [45] fabricated PP/PP-g-MA compatibilizer/organoclay nanomaterials by masterbatch mixing in melt phase process via twin-screw extrusion. It has been used the specific mechanical energy (SME) to evaluate the effects of operational parameters of extrusion process which are feed rate, barrel temperatures, and speed of screw) on clay dispersion in PP/organoclay nanocomposites. Chung and Rhubrigh [102] reported synthesis of Polycaprolactone grafted Polypropylene (PCL-g-PP) as an effective compatibilizer for PP based polymer blends with many engineering plastics, such as polycarbonate (PC) and Polyvinylchloride (PVC).

Kaneko et al. [103] prepared the PP/poly (lactide) (PLA) and the PP/PLA/PP-g-poly (methyl methacrylate) (PMMA) binary, ternary blends respectively by reactive extrusion system in melt blending and molding. The authors also observed that the strength, modulus, elongation, and Izod impact strength. The PP/PLA blends showed significant improvement by the addition of the PP-g-PMMA.

Mike Chung [104] reported the importance and future perspectives of new class of functional polyolefin (predominantly PE and PP) with well-controlled molecular structures and high molecular mass with reactive functional groups that are located at ends of chains, side/tail branches, and block/segment. Author also described three energy-related application areas for the functional polyolefin materials, such as polymer film capacitors, mebranes, and absorbents for the industries of energy (electricity) storage, hydrogen systems, and for oil spill cleaning.

PLA is known as highly process able, limited degradable and biocompatible polymer. The extra methyl group in PLA results the polymer to be much more hydrophobic and stable against hydrolysis [105]. PCL is a semi-crystalline polyester with solubility in polar organic solvents having T_g= 54 °C and T_m = 55-57 °C temperatures [106]. PCL is very good process able elastic biomaterial [107] and used to fabricate tissue engineering scaffolds [108] and electrospun fibers [109, 110]. PCL based nanocomposites have been widely used as matrix polymers for bone regeneration [111, 112], nerve [113] and vascular tissues [114]. To improve the thermal stability and usability, a biodegradable PLA was incorporated with hydrophilic fumed silica or MMT clay by twin-screw extrusion [115-117].

Zhang et al. [133] reported the fabrication of an ethylene–propylene terpolymer/i-PP blend via a co-continuous microlayer structure by the injection molding method. Authors found

that the blends showed a low coefficient of linear thermal expansion in both directions (length and width). Additionally, the morphology of microlayers and the behavior of the expansion changing by the sampling position on the injection-molded sheets have been investigated. Orientation of the microlayers strongly depends on the shear rate. Moreover, by the increasing of the shear rate, the orientation state increased and the linear thermal expansion coefficient decreased.

Gomez et al. [134] synthesized silica nanoparticles (NPs) with the spherical shape and 20 and 100 nm diameter sizes through sol-gel technique. The authors evaluated the effect of the silica NPs and PP matrix melt blend on the properties of nanocomposites such as oxygen and vapor (water) permeability and thermal/mechanical behavior. According to the authors, barrier properties of nanocomposites dramatically increased at low loading (<5 mass %) of silica NPs. The nanoparticles also improved thermal degradation of polypropylene with the absorption of volatile compounds on the outer part of the smaller spherical NPs because of the smaller NPs and the greatest stabilization.

Sari et al. [135] prepared hyperbranched-modified PP blends using two type of polyester amide-based amphiphilic and hydrophilic polymers and PP–g-MA as a reactive agent to disperse and improve the structure by grafting the polymer with the PP chains. Authors observed that by the addition of the hyperbranched polymer, the thermal (T_g) and rheological (complex viscosity) properties decrease, and SAXS data exhibit improvement in the cross-hatched morphology of crystalline parts of layers of PP for modified samples by reaction compared with nonreactive-modified samples. Authors prosed that the cross-linked structure formed via the graft reaction between the hyper branched polymer and PP–g-MA compatibilizer.

PP/nanoclay composites were prepared by mixing a nanoclay masterbatch with PP and conventional and shear-controlled orientation– injection molding methods [136]. According to the authors, nano clay behaved as driving force of polymer morphology together with applied processing conditions. The decrease in the core region, the differences between core, skin and the PP γ-phase has been detected. It is responsible for the enhancement in the thermal and fracture properties of shear-controlled orientation PP/nanoscale moldings compared to conventional injected moldings.

Compos-Requena et al. [137] reported the effect of the process parameters for the synthesis of polyolefin (LDPE) /organo-MMT clay nanocomposite films. Authors observed that the clay % parameter is the most important, mixing temperature indicated not any important effect on intercalation in situ processing ($p < 0.05$). A strong interaction between clay and compatibilizer (Polybond 3149) loaded has been shown. The response surface methodology analysis provides for determining the best processing conditions. These conditions results to formulations with the highest intercalations by considering the main factors and their interactions.

Song et al. [118] prepared the PP fabric composites incorporated with polyhedral oligomeric silsesquioxanes (POSS) and SiO_2 NPs using a convenient blending method via melt-blown process with corona charging. According to the authors, both NPs can behave as nucleating agent and cause acceleration of the crystallization process during non-isothermal cooling. The shear storage modulus, loss modulus and complex viscosity, as well as thermal stability of PP/POSS (1 mass %) composite increase compared with pure PP. Barczevski et al. [119] reported a study of thermal stability of i-PP/tetrasilanolphenyl POSS nanofiller (2, 3 and 10 mass %) nanocomposites. They observed that the addition of nanofiller into the matrix polymer increases the thermal stability and significant changes in flammability of the nanocomposites compared with pristine isotactic PP.

Silica-reinforced PP nanocomposites were generated by different methods and investigated their supermolecular structure and mechanical properties [120-122]. Sun et al. [123] prepared the PP/silica nanocomposites by two steps; one is the impregnation of tetraethyl orthosilicate (TEOS) into PP matrix under supercritical medium of carbon dioxide as a swelling agent. The other is hydrolysis/condensation reactions of TEOS that is confined inside polymer network. There was demonstrated that in situ generated nano-sized silica networks distributed uniformly in PP matrix and essentially improved the morphology and mechanical properties of PP/silica composites. Bracho et al. [124] reported synthetic pathways to functionalize silica NPs for PP nanocomposite application. They produced synthetic silica nanospheres that sizes are changing from 20 to 100 nm diameter through sol-gel method and modified the silica surface with organic chlorosilanes to improve the particle interaction with the hydrophobic PP matrix. PP/silica composites were also produced by γ-irradiation method via ultrafine blends with adding PP-g-MA compatibilizer as an effective method for improving physical dispersion nanosilica [125].

Recently, it has been developed a one-step method to fabricate the nanocomposites which includes powdered isotactic polypropylene (i-PP) as a matrix polymer (melt-flow index (MFI) = 7.2 g 10 min^{-1}), oligo (i-PP-g-MA) (MFI = 35-70 g 10 min^{-1}) as a reactive compatibilizer and dimethyldodecylamine-surface-modified montmorillonite clay (organo-MMT) as a 'nano-reactor'. This method involves grafting maleic anhydride (MA) onto i-PP chains in the melt state under controlled thermal degradation conditions and intercalative compounding of the obtained oligo (PP-g-MA) with PP and organo-MMT in melt by reactive extrusion. The effect of extrusion parameters on MFI, composition and properties of the grafted i-PPs, and the mechanism of formation and detailed property investigation of PP/oligo (PP-g-MA)/ organo-MMT NCs were investigated [126]. Synthesis of poly (PP-g-MA) s with different compositions as compatibizers for the preparation of nanocomposites by radical grafting reaction of powder and granular isotactic PP (i-PP) with maleic and citraconic anhydrides in melt by reactive extrusion have been also reported [127, 128].

One of the aim of this work is to fabricate novel multifunctional PP/PP-g-MA compatibilizer/bioengineering polymer (PLA and/or PCL) blend nanocomposites (NCs) chemically and physically incorporated with a new reactive amphiphilic copolymer-g-SiO$_2$ NPs and organoclays in melt by a one-step reactive extrusion processing. Present work also described the synthetic pathways and structural characterizations for copolymer-g-silica NPs in detail, as well as all fabricated multifunctional NCs with various compositions by use of copolymer-g-silica NPs and organoclay nanofillers. Another point of this study is to evaluate the effects of colloidal copolymer-g-silica NPs, origin biopolymer and organoclay (reactive and non-reactive) on the chemical and physical structures, surface and internal morphologies, thermal, mechanical (shear stress) and rheological (viscosity) properties of NCs. Evaluation of the structural factors and their important role in the formation of self-assembled multifunctional NCs through the various chemical and physical in situ interfacial interactions in applied melt extrusion conditions is an important subject of these investigations.

2.6.2. EPDM: Poly (Ethylene-*Co*-Propylene-*Co*-Vinylidene Norbornene Diene Monomer) Based Structures

Poly (ethylene-*co*-propylene-*co*-vinylidene norbornene diene monomer) (EPDM) terpolymer elastomer is one the most widely used synthetic rubber in many static and dynamic applications [3]. The many industrial polymer composite products such gaskets,

bumpers, auto parts, auto brake systems, electrical installation, conveyor belts, standard profile materials for automobiles, etc. were fabricated using EPDM as matrix.

Synthesis of several applicable organic-inorganic nanohybrids by sol-gel method have been already reported [129-131]. In previous publications, it has been synthesized and characterized of the functional copolymers covalently incorporated with in situ produced silica nanoparticles (NPs) with γ-aminopropyltriethoxysilane precursor [6-8].

Messori [46] described the preparation and characterization of rubbers (EPDM, polydimethylsiloxane, styrene-butadiene, acrylonitrile-butadiene, acrylic and polyisoprene natural rubber) based NCs by in-situ production of inorganic oxides, especially silica NPs, using the hydrolytic sol-gel process. Das et al. [9] prepared the silica filled EPDM by hydrolysis of triethoxysilyl-grafted EPDM and tetraethoxysilane (TEOS) in n-butyl amine aqueous media via in-situ generation of silica nanoparticles. According to the authors, EPDM enhanced with in-situ modified silica resulted extra reinforcing efficiency compared with materials generated by means of mechanical blending of precipitated silica inside the rubber matrix. Additionally, According to Karder-Kocsis and Wu [47], the dispersion state of the silicate strongly determines the chemical, physical, and thermal properties of the nanoreinforced rubber. Dispersion state can be influenced by various methods such as silicate origin, production way (latex, in solution or melt compounding), surface alternation of silicate, type of used curatives, activators and compatibilizer and compounding conditions (shear rate, temperature, time, etc.).

Wu and Chu [48] prepared PP/EPDM/SiO$_2$ nanocomposites produced by dynamically vulcanized EPDM and PP blends. The treated SiO$_2$ was melt mixed with PP/EPDM blend with impregnation of PP-g-MA, which acted like a functionalized compatibilizer. Authors found that the strong interaction due to the graft reaction increased the dispersion of silica particles inside the matrix polymers.

Polymer blends generating by polyolefin and ethylene-propylene and dienemonomer terpolymer rubber (EPDM) attract great attention in recent days. These engineering materials have a wide range of applications due to their specific chemical, mechanical, and thermal properties. Elastomeric thermoplastic composite materials generated by mixing of EPDM and polyolefin provide the combination of the technical thermophysical advantages in processing of thermoplastics with the excellent physical properties of elastomers. Therefore,

the material is gained significant importance in different types of usage applications, like, in the packing materials, automotive industries, electrical cables, extruded blocks for windows, and wires.

EPDM rubber layered clay nanocomposites have great interest of significant research attraction due to their improved strength and modulus, better thermal and chemical stabilities [49-51]. Melt compounding is most commonly utilized for the fabrication of PP/EPDM/silica nanocomposites [52, 53]. Synthesis, properties and applications of various EPDM based nanocomposites incorporated with organoclays [54-56] and EPDM/EPDM-g-MA/organoclay nanocomposites [57-61] have been a curious topic for the work of many researches.

To improve physical, chemical properties and compatibility of EPDM rubber blends, Kole et al. [57] used maleic anhydride modified EPDM (EPDM-g-MA). Usuki et al. [58] prepared the hybrid nanocomposites by using organophilic MMT and EPDM rubber via a melt extrusion processing. They found that the organoclay layers were dispersed uniformly as plates of 50-80 nm thickness inside EPDM matrix. Highly filled EPDM rubber/ Al_2O_3 NPs composites and their in-situ modified via ethoxysilane coupling agent (bis-(3-ethoxysilylpropyl)-tetra sulfide) derivatives show great performance in mechanical properties and thermal conductivity [59]. Authors also studied the Payne effect to analyze the structure of the filler networks indirect way and the states of dispersion of nanoparticles (NPs) in EPDM matrix. The particular characteristics of rubber can be analyzed by the Payne effect, specifically rubber composites including nano-sized fillers that is correlated with the filler network structure. Therefore, the structure is dependent mainly on filler amount, interactions between the filler–rubber or the filler–filler, and the dispersion state of filler [60].

Mousa reported cure characterizations and details of thermal behavior of sulfur-cured EPDM matrix nanocomposites by extrusion with layered nano-organoclay [61]. The chemical, thermal and oxidative degradation of EPDM rubber and its cross-linked networks and reactive blends of poly (phenol hydroxyl EPDM) with fluoroelastomer were subject of another several publications [62-65]. EPDM/surface modified fibrillary silicates (FS) rubber composites with enhanced mechanical and thermal properties and good ageing resistance were prepared by melt-blending method [66]. Stelescu et al. [67] reported the structural

characteristics of some polyolefin and elastomer i.e. High density polyethylene (HDPE)/EPDM blends.

Synthesis, characterization and important medical and engineering applications of biodegradable PLA and PCL layered silicate nanocomposites and nanomaterials (nanofibers, tissue scaffolds, nanofilms, coatings, etc.) were subjects of investigations of the many researchers [107, 108, 115]. Krishnamachari et al. [71] reported fabrication PLA/inorganic and organic clays nanocomposites in melt compounding using a Brabender tween-screw extruder. The evaluation of the effects of clay origin/loading on the structure, thermal and mechanical behaviors of intercalated NCs have been studied. PLA-based ternary blends (PLA/cellulolytic enzyme lignin/PP-g-MA with component mass ratio of 80/20/20) were fabricated by extrusion blending [72]. Authors investigated the mechanical properties and the morphology of these new materials. The impact strength together with the elongation at break were doubled compare to pristine PLA.

Recently, the preparation of EPDM based nanocomposites has been reported, including the PP-g-MA compatibilizer, poly (MA-alt-1-octadecene)-g-PEO reactive compatibilizer-internal plasticizer and organoclays, by an extrusion method. It was observed that the thermal and crystallization behaviors of nanocomposites strongly depend on the origin and content of organoclay and Polyethylene oxide (PEO) grafted copolymer-compatibilizer, respectively, and significantly improving the main properties and morphology of nanocomposites compared with EPDM polymer [39, 73, 74]. The maleic anhydride (MA) functional monomer and its isostructural analogs (itaconic and citaconic acids/anhydrides, fumaric acid, etc.) are successively utilized for the grafting onto various polymers (polyolefins, synthetic and natural rubbers, biodegradable polymers, polysaccharides, biopolymers, etc.). It is due to prepare polymer-g-MA graft copolymers useful for the application in polymer/MMT clay blends as effective reactive compatibilizer in the melt extrusion processing [74].

In this study, similar with extrusion systems in literature, polypropylene based experiments, synthesis and characterization of multifunctional i-PP based nanocomposites have been accomplished since they consist of reactive PP-g-MA and poly (MA-alt-1-dodecene)-g-organosilica NPs (molecular mass of 9.060 m/z for oligomer matrix alternating copolymer prepared with 2.5 % of benzoyl peroxide as an initiator) compatibilizers, ODA-MMT and DMDA-MMT organoclay nanofillers, PLA and PCL biothermoplastic polyesters by reactive

extrusion which is a powerful nanotechnological method using Rondol twin-screw extruder at temperatures of the five barrier zones 165 °C/165 °C /170 °C /170 °C /170 °C for Propylene based structures, and the rotation speed of the screw is maintained at 40 rpm. The time of one-step cycle of extrusion processing is 10-15 min.

Unlike above conditions of Polypropylene based composites, multifunctional EPDM rubber based nanocomposites consisting of the same raw materials have been prepared using Rondol twin-screw extruder at relatively lower temperatures of the five barrier zones 120 °C, 130 °C and 130 °C, 145 °C and 145 °C. The time of one-step cycle of extrusion processing is 5-10 min. This applied lower temperature and the time of one-step cycle in extrusion processing are important factors (economically low costing energy) in further industrial application of EPDM based multifunctional nanocomposite materials. Moreover, this work presents chemistry and physics of proposed in situ interfacial interactions during selected reactive extrusion conditions in detail.

Behind the goal of PP based nanostructures, the main goal of this work in EPDM side is a design of new multifunctional polymer blend compositions to fabricate polymers/silicate and silica multi-functional nanocomposites (MFNCs) in melt phase by a one-step reactive extrusion process. These MFNCs are prepared by using EPDM elastomer as a matrix polymer, PP-g-MA as a reactive compatibilizer, polylactide (PLA) and/or poly (ε-caprolactone) (PCL) as bioengineering polyesters, poly (MA-alt-1-dodecene)-g-SiO$_2$ nanoparticles (NPs) as reactive compatibilizer-reinforcement, octadecyl amine/MMT and dimethyldidodecyl ammonium/MMT as reactive and non-reactive organoclay nanofillers, respectively.

Another aspect of this work is investigation of the chemical and physical structures, surface and internal morphologies, thermal, mechanical, and rheological properties of MFNCs, as well as evaluating the effects of bioengineering polyester and origin of organoclays and copolymer-g-SiO$_2$ NPs on the in situ interfacial interactions during melt compounding processes. This work also presents the synthetic pathways for copolymer-g-SiO$_2$ NPs by sol-gel method using functional amphiphilic copolymer, γ-aminopropyltriethoxysilane (APTS) and tetraethoxysilane (TEOS) precursors, as well as investigation of chemical and physical structures and thermal behaviors of organo-silica NPs and their influence on the main structural, thermal and rheological properties, and SEM-TEM morphology of nanocomposites. This work is also estimated reveal the chemistry and physics of covalence,

complexing and hydrophobic/hydrophilic interfacial interactions as important nanoprocessing through effects of biothermolastic esters, polymer stabilizers, organoclays and colloidal organic silica NPs during reactive extrusion of multifunctional EPDM based nanocomposite blends.

2.7. Usage Areas of Biodegradable Nanocomposites

Nanotechnology/Nanocomposites have great influence on industries such as Automobiles, Aerospace, Plastics Containers (Molded Products, Packaging Materials- for electronic or other consumables), Coatings, Adhesives, Fire-retardants, Optical Circuits, Drug Delivery, Membrane Applications, Effluent Treatments, Sensors, Medical Devices, Consumer Goods, etc.

The publications on nanocomposites shows clearly the advantages and superior properties of nanomaterial additives provide to base polymer and its conventional fillers. Substantial improvements on properties of new materials include following;

- Mechanical improvements, i.e. strength, modulus
- Permeability change, gas/liquids
- Thermal properties and heat deviation temperature
- Flame retardant materials
- Stable to chemicals
- Surface appearance
- Conductivity
- Optical clarity

The focus of the search on material improvement on polymer& clay nanocomposites that are mostly used in the automotive, aeronautical, and packaging industry. Great interest has been also given to the biodegradable polymers and their nanocomposites of them that present different applications in these sectors additionally medical applications considering biocompatibility.

In detail, car parts, as belts, handles, view mirror, components of gasoline container, engine plastic cover, outside parts, fender, bumper, tires etc. also uses polymeric nanocomposites, especially with nylon (polyamide), produced by some big companies Bayer, Honeywell Polymer, etc.

In packaging/film industry, polymer (nylon or polyolefin) nanocomposites usage to provide Oxygen or CO_2 barrier properties to save organic materials longer and advanced films/packaging applications for the protection of consumables like food and beverages are common examples of new applications of ultra-sophisticated industrial polymeric materials. Biodegradable packaging materials is today's hot topics trying to decrease pollution of synthetic polymer in environment.

In energy industry, the polymer nanocomposites provide cheap material for sustainable energy production areas such as fuel cell membranes, solar panels, and wind turbines.

In biomedical industry, the alternating property flexibilities of the nanocomposites is favorable due to their variable biomedical applications and they provide expected properties in medical components such as biodegradability, biocompatibility, and good mechanical properties. Enabling these properties, considering and understanding of this thesis topic, synthetic polymer is a good choice with clay/biopolymer additives to provide reinforcement and biodegradability by changing/regulating additive contents, so, as an example, it can also be used in tissue engineering, bone replacement, dental applications, and medicine control release. The proposed fabricated materials may be used to generate some materials in film industry or other end use materials later. This study will try to understand better material production parameters based on common commercial polymers considering their lack of performance parts and satisfy these performances like biodegradation, strength, etc. before application of them for the use of next goal as end used material production.

3. EXPERIMENTAL STUDY

3.1. Materials

The chemical structures, compositions and assignments of all materials using in the extrusion processing were summarized below;

3.1.1. Isotactic Polypropylene (i-PP)

Isotactic Polypropylene (PETOPLEN MH 418) is supplied from PETKIM Petrochemical Holding Inc. /SOCAR Turkey Inc. (R & D Department, Aliaga-Izmir/Turkey). Material is isotactic PP (i-PP) in pure granular (pellets) form. The material is used to produce fiber, bags, and ropes in plastic market. The main properties are MFI 4.0-6.0 g/10 min (at 2.16 g, 230 ºC), Mn and Mw: approximately 40000 Da. The commercial properties which can be provided from market is shown in Table 3.1.

Table 3.1. The properties of i-PP commercially available(from PETKIM).

PROPERTIES	PETOPLEN MH 418
Melt Flow Rate (230 ºC 2.16 kg)	4.5
Density (23 ºC)	0.905
Tensile Strength Yield	34
Tensile Strength at Break	42
Color, b-value (10D65)	1.8
Melting Point (DSC)	163
Deflection Temperature, 0.45 Mpa	113
Izod Impact Strength, 23 ºC	21.6
Rockwell Hardness	94
Flexural Modulus, 23 ºC	1450

3.1.2. EPDM Rubber

EPDM rubber (Hydrocarbon Rubber NORDAL IP 4820, Dow Chemicals Co.) is supplied from R & D Department, Profile Standard Co. (Düzce, Turkey). Main properties of the product are following; Mw: 160000 Da, T_{dmax}: 450 ºC, MFI: 1.0 g/10 min (at 190 ºC/ 2.16 kg), density: 0.910 g/cm^3, Mooney viscosity: 20 MU at 125 ºC. EPDM includes contents of

ethylene unit 85 %, propylene unit 10.1%, and ethylidenenorbornene (ENB-diene monomer) unit as 4.9 %. Some extra details of EPDM raw material can be seen Table 3.2.

Table 3.2. The properties of commercially available elastomer EPDM (NORDAL).

PROPERTIES	NORDAL IP 4820
Density	0.910 g/cm^3
Volatiles	Less than 0.40 %
Mooney Viscosity @Temperature 125 ^{o}C	20
Melt index of compound @Load 2.16 kg, at 190 ^{o}C	1.0 g/10 min
Ash	Less than 0.10 %
Melting Point	90.0 °C
ENB	4.9 mass %
Ethylene	85 mass %
Molecular Weight Distribution	Narrow
Product Form	Pellets
Propylene	10.1 mass %
Residual Transition Metal	Max 10 ppm

3.1.3. Compatibilizer, PP-g-MA

PP-g-MA graft oligomer was purcharsed from Sigma-Aldrich (Germany). General properties of the compatibilizer are Mw = 9.100 and Mn = 3.900 Da (by GPC), PI=2.33, T_m = 156 ^{o}C, acid number = 47 mg KOH/g.

3.1.4. Biodegradable Polymers, PLA and PCL

PLA with different molecular mass Mw=160000, 200000, 360000, 700000, 800000, 1000000 Da by GPC supplied from Biomedtek HU-Industry Research Center (Ankara, Turkey).

PCL (Mn = 80.000, Mw = 125.000 (by GPC), PI = 1.56, MFI 1 g/10 min (125 ^{o}C/44 psi), η_{in} (inherent Viscosity) = 1.2 dL/g, T_m = 55.3 ^{o}C (by DSC) and crystallinity 45.4 % was supplied from PURAS Biomaterials Co. (Corinchem, The Netherlands). PLA and PCL samples were drying under vacuum at 80 ^{o}C for 3 h before use in the extrusion process.

3.1.5. Organoclay Fillers, ODA-MMT, DMDA-MMT

Octadecyl amine/MMT (ODA/MMT) (Nanomer 1.30E) and dimethyldidodecyl ammonium/MMT (DMDA/MMT) organoclays (Nanomer 1.44P) were purchased from Sigma-Aldrich (Germany) and dried under vacuum 3 h at 80 °C before used. The average characteristics of the ODA/MMT are content of octadecyl amine, surfactant-intercalant 25-30 %, bulk density 0.41 g/cm^3, cation exchange capacity (CEC) 95 mEq and crystallinity 52.8 % (by XRD). Some other properties shown in Table 3.3.

Table 3.3. Octadecylamine (ODA-MMT) Properties.

Materials	Octadecyl amine–Montmorillonite
Ingredients	25-30 wt. % octadecyl amine
Matrix	Montmorillonite based material
Phase	Solid, Dust
Humidity	≤3.0 %
Density	200 - 500 kg/m^3 (bulk)
Size	≤20 micron

DMDA-MMT as content of dimethyldidodecyl ammonium surfactant-intercalant is 30-35%. The specific surface area is 43.6 m^2. g^{-1} and specific mesoporous volume is 0.14 m^3. g^{-1}. The content of N is 1.12%, C content is 32.56 %, and crystallinity is 58.2% (by XRD). Some extra properties has been shown in Table 3.4.

Table 3.4. Dimethyldidodecylammonium (DMDA-MMT) Properties.

Materials	Dimethyldidodecyl ammonium-Montmorillonite
Ingredients	30-35 wt.% alcali ammonium
Matrix	Montmorillonite based material
Humidity	≤4.0 %
Density	350-400 gr / lt (bulk)
Size	≤5 micron
Surface Area	43.6 m^2.g^{-1}
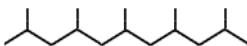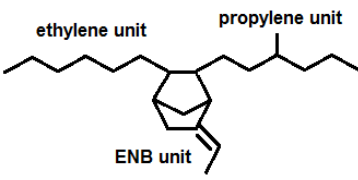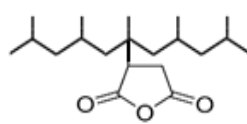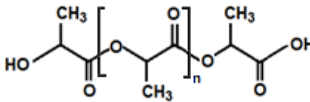
3.1.6. Poly (MA-*alt*-1-dodecene)-APTS-g-(SiO₂) ₙ (Copolymer-*g*-Silica NPs)
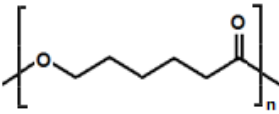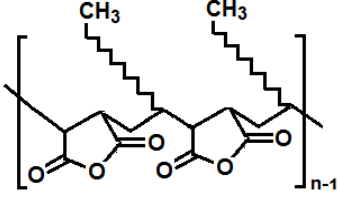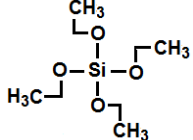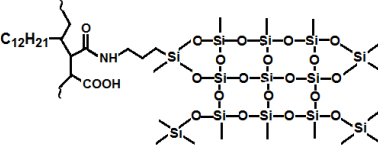
MA monomer was purified by recrystallization in anhydrous benzene. It is further purified by sublimation under vacuum before usage. 1-Dodecene as a α-olefin comonomer (was distilled under moderate vacuum before use. Benzyl peroxide (BP, Fluka) was recrystallized twice from chloroform solution by methanol before use. MA monomer, 1-dodecene were supplied from Sigma Aldrich (Germany), Fluka (Switzerland) respectively.

γ- Aminopropyltrimethoxysilane (APTS, CAS No. 919-30-2, assay = 99 %, boiling point = 217ºC) and tetraethoxysilane (tetraethyl orthosilicate percursor) (TEOS, CAS No. 78-10-4, assay 99.999 %, boiling point =168 ºC) were purchased from Sigma-Aldrich and consumed as received.

All other used materiasl such as solvents, reagents were provide in analytical grade and consumed without purification. The chemical structures, compositions and assignments of intermediate materials using in the extrusion processing were given in Table 3.5.

Table 3.5. The materials and chemical structures of them used in extrusion processing.

Materials (Composition, mass %)	Chemical structure	Assignments
Isotactic Polypropylene (PP)		thermoplastic matrix polymer
EPDM elastomer Poly [(ethylene)$_{0.85}$-*co*-(propylene)$_{0.101}$-*co*-(ENB diene)$_{0.049}$]$_n$ terpolymer M$_w$ 160.000		elastomer matrix polymer
PP-*g*-MA M$_w$ 9.100		reactive compatibilizer
Poly (L,D-lactide) (PLA) Mw : 160, 200, 360, 700, 800, 1000 x 10^3		biodegradable and highly processable bioengineering polymer

Poly (ε-caprolactone) (PCL) M_w = 125.000		biodegradable semi-crystalline and highly processable elastic bioengineering polymer
Alternating amphiphilic copolymer of maleic anhydride with 1-dodecene (α-olefin) Poly(MA-*alt*-1-dodecene) Molecular mass 9060 m/z		high reactive surfactant copolymer with hydrophilic/hydrophobic balance used to prepare silica NPs by sol-gel method
γ-Aminopropyltrimethoxy-silane (APTS)		Reactive/hydrolysable silane precursor used to prepare organosilica NPs
Tetraethoxysilane (TEOS)		hydrolysable and polycondensable monomer precursor
Poly (MA-*alt*-1-dodecene)-APTS-g-$(SiO_2)_n$ (Copolymer-*g*-Silica NPs)		silica NPs covalently encapsulated with functional copolymer as nanofiller/reinforcement agent and reactive compatibilizer
ODA/MMT clay	CH_3-$(CH_2)_{17}$-NH_2/MMT	Chemical reactive low complex able organoclay-nanofiller
DMDA/MMT clay		non-chemical reactive high complex able organoclay-nanofiller

3.2. Synthesis of Poly (Maleic anhydride-alt-1-dodecene)

Amphiphilic alternating copolymer with molecular mass 9060 m/z for PP/EPDM based experiments were synthesized by radical copolymerization of MA and 1-dodecene (molar ratio =1:1) with benzoyl peroxide (2.5 % for 9060 m/z) as an initiator in toluene solution at 80 °C under nitrogen flow up to fully phase separation processing. To prepare copolymer with low molecular mass, higher content of initiator is used in heterogonous solution copolymerization reaction. Self-precipitated copolymer particles from reaction medium

(reaction time 3 h; unlike monomers, copolymer is not dissolved in toluene) were isolated from reaction mixture by filtration and centrifugation and then was purified by dissolving in acetone and precipitation with methanol. White powder product was draying under vacuum at 40 ºC.

3.3. Synthesis of Copolymer-Silica Nanoparticles by Sol-Gel Method

1.4 mL of γ-aminopropyltrimethoxysilane (APTS) (APTS)/THF (1/9 v/v) mixture was added to 5 mL poly (MA-*alt*-1-dodecene)/ THF (0.1 g/mL) solution dropwise under stirring for about 20 min. (at APTS: MA unit mole ratio of 1:1). After that, 14.8 mL of tetraethyl orthosilicate precursor (TEOS)/THF (1:1 v/v) solution and 2.4 mL of 0.14 mol/liter HCl catalyst were added to the reaction mixture obtained above under stirring for about 5 minutes. The transparent P (MA-*alt*-α-olefin)/silica hybrid nanoparticles were obtained upon gelling and drying at room temperature for about 3 weeks. Then, the products were ground into fine powders and sieved. The products were finally dried under vacuum for 6 h at 40 ºC.

3.4. Fabrication of Intercalated Polyester (PLA, PCL) /Organoclay Nanocomposites

Fabrication of intercalated PLA/ODA-MMT, PCL/ODA-MMT and polyester/DMDA-MMT were carried out in melt by reactive extrusion using a Rondol Lab. twin-screw extruder. The extruder has a diameter of 21 mm and 25:1 L/D ratio. The temperatures of the five barrier zones are 160-175 ºC for PP based experiments and 120-145 ºC for EPDM nanocomposites raw materials. The rotation speed of the screw is maintained at 40 rpm. Then extrusion process of the full loading polyester (PLA, PCL)/organoclay (3.5 %) composition was contained in the chosen feeding zones. The time of one-step cycle of extrusion processing is 10-15 min that is the same nanocomposite production parameters of PP and EPDM. The fiber-like extrude is cooled in water bath and then is granulated.

3.5. Equipment Tools and Fabrication of Multifunctional Nanocomposites by Reactive Extrusion System

Reactive extrusion system is recently used method to mix polymer matrix and additives under heat, pressure, and reaction. The system is mainly consisting of feeder, mixing/reactive zones, die, cooling part, cutter, and collector. Some systems have different types of feeder as side or liquid feeder sections. The system is working under preset temperature and pressure levels. Materials to be interacted are fed reaction zones

proportionally. The set temperatures and feeding rates can be changed. The product is mostly cooled enabling the pelletizing or filming. Pelletizing is important to melt new product easily for further reactive extrusion or analysis.

The reaction/mixing barrel length of reactive extrusion machine provides residence time for enough mixing and reaction time. Diameter of screws and pipe on the equipment provides efficient mixing, convective heat transfer, and the rate of production or feeding. The external auto controls electrical heating and cooling system are provided to get flexibility to use the machine in different types of material with different melting & interaction temperatures. Die and cutter under water (pelletizer) is also auxiliaries of equipment to be able to produce pellets.

In this experiment, nanocomposites fabricated in melt by a reactive extrusion which occurs at one-step process using a Rondol Lab. twin-screw extruder C2573 with diameter of twin-screw of 21 mm, 25:1 L/D ratio (Rondol Technology Ltd., England). The temperatures of the five barrier zones are 165 °C-175 °C for PP based nanostructure or 120 °C-145 °C for EPDM based nanostructures. The rotation speed of the screw is maintained at 40 rpm. See Figure 3.1 for the equipment in laboratory.

Figure 3.1. Rondol twin screw equipment in Chemical Engineering department at Hacettepe University.

3.5.1. Experiments with Polypropylene matrix

The i-PP/PP-g-MA/PLA/ODA-MMT/Copolymer-SiO$_2$ nanoparticles (NPs) (NC-1), PP/PP-g-MA/PLA/DMDA-MMT/Copolymer-SiO$_2$ NPs (NC-2) and PP/PP-g-MA/PCL/DMDA-MMT/Copolymer-SiO$_2$ NPs (NC-3, see Table 3.6 for abbreviations) nanocomposites were fabricated in melt by reactive extrusion, a one-step process. The temperatures of the five barrier zones are 165 $^{\circ}$C/170 $^{\circ}$C/170 $^{\circ}$C/175 $^{\circ}$C/175 $^{\circ}$C. The rotation speed of the screw is maintained at 40 rpm. The matrix PP (7.965 g), poly (PP-g-MA) copolymer (0.5 g) and copolymer-g-silica NPs (0.5 g) were incorporated in the first feeding zone. Incorporation of PLA/organoclay (3.5 %) or PCL/organoclay (3.5 %) masterbatches (1.0 g) was carried out in the second feeding zone. Usually the molecular mass of PLA decreased after the extrusion with clay at 190 $^{\circ}$C [27]; because melt blending the PLA/organoclay was performed relatively lower temperatures of 170-175 $^{\circ}$C. Then extrusion process of the full loading polymer/nanofiller composition was contained in the other feeding zones at 170 $^{\circ}$C, 175 $^{\circ}$C and 175 $^{\circ}$C, respectively. The time of one-step cycle of extrusion processing is 10 min. The fiber-like extrudate (diameter ~1.0 mm) is being cooled in water bath and then is granulated.

In order to see effect of molecular weight change in biodegradable ingredients of nanocomposites on physical behaviors under forces, i-PP has been modified again by PP-g-MA/nonreactive filler DMDA/PLA (with different Molecular weights as 200, 360, 700) as NC-4, NC-5, NC-6 or PCL (Mw:125000) as NC-7.

3.5.2. Experiments with EPDM Matrix

Additionally, the EPDM/PP-g-MA/PLA-700/ODA-MMT/Copolymer-SiO$_2$ nanoparticles (NPs) (NC-8), and EPDM/PP-g-MA/PCL-125/DMDA-MMT/Copolymer-SiO$_2$ NPs (NC-9) nanocomposites were generated in melt by a one-step reactive extrusion process using Rondol Lab. twin-screw extruder C2573 (Rondol Technology Ltd., England) maintaining again constant rotation speed at 40 rpm. The matrix EPDM elastomer (79.65 mass %), PP-g-MA copolymer (5 mass %) and copolymer-g-silica NPs (5 mass %) were incorporated in the first feeding zone. Incorporation of PLA/organoclay (3.5 mass %) or PCL/organoclay (3.5 mass %) masterbachs (10 mass %) was carried out in the second feeding zone. Then extrusion process of the full loading polymer/nanofiller composition was contained in the five feeding zones at 120 $^{\circ}$C, 130 $^{\circ}$C and 130 $^{\circ}$C, 145 $^{\circ}$C and 145 $^{\circ}$C, respectively. The time of one-step cycle of extrusion processing is 5-10 min. The PLA/organoclay (ODA-MMT or DMDA-MMT) and PCL/organoclay masterbatchs using in above mention compositions

were prepared using similar operational parameters as mentioned before in extrusion processing. The time of one-step cycle of extrusion processing is 10 min. The fiber-like extruded multifunctional polymer NC (diameter 1.5 mm) is cooled in water bath and then is granulated.

In order to see effect of molecular weight change in biodegradable ingredients of nanocomposites on physical behaviors under forces, EPDM has been modified again by PP-g-MA/nonreactive filler DMDA/PLA (with different Molecular weights as 160, 800, 1000) as NC-10, NC-11, and NC-12 respectively.

The following estimations of predominantly interactions between components of multifunctional polymer blends were proposed: (I and III) covalence (amidization) and (II and IV) complexing interactions, as well as (V) various hydrophobic/hydrophilic physical interactions. Chemistry and physics of proposed in situ interfacial interactions during chosen reactive extrusion conditions were schematically represented in Figure 3.2. The following in-situ covalence and complexing interactions can be estimated: (I) amidization reactive anhydride units with ODA-MMT clay, (II) complexing of MA units of copolymer with ODA-MMT clay, (III) amidization of PP-g-MA with DMDA-MMT clay, (IV) complexing of MA units with DMDA-MMT clay and (V) hydrophobic/hydrophilic interactions of EPDM/PP units with PP-g-MA, PLA and PCL polymers, and reactive and complexable organoclays.
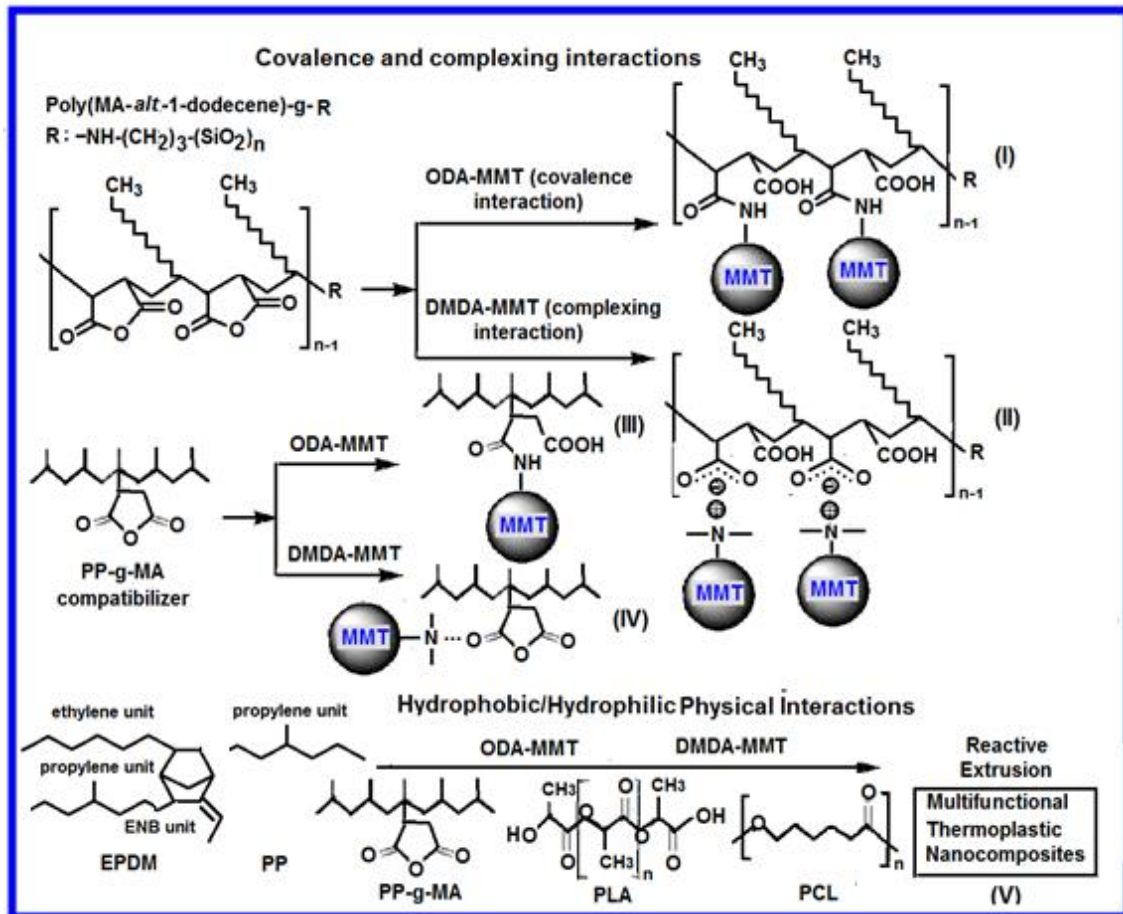
Figure 3.2. Schematically representation of in situ chemical and physical interactions in melt during reactive extruding nanotechnology.

All generated nanocomposites have been tabulated with ingredient in Table 3.6. Some of them has been used in different types of characterization methods to see the results of reaction and interactions. PLA and PCL have been used in small and available quantities due to the lack of availability and so, studied samples have been optimized to use minimum amount of materials. Produced nanocomposites are around below 50 g for further tests. The rondol device minimum effective working amount has been discovered as 20 g sample.

Table 3.6. All nanocomposites that are produced and used in characterization.

#	Experiment& (Report) TAGs	EPDM	PP	PP-g-MA	PLA	PLA Mw_i	PCL (125000)	DMDA-MMT	ODA-MMT	DGZ-22** (Copolymer-g-Silica)	Zero rate viscosity
		wt%***	wt%	wt%	wt%	Da	wt%	wt%	wt%	wt%	Pa.s
PP Matrix Structures											
1*	BAG-PP-6(NC-1)	-	79.65	5	10	mw:700000	-	-	0.35	5	56350
2*	BAG-PP-10(NC-2)	-	79.65	5	10	mw:700000	-	0.35	-	5	3042
3*	BAG-PP-7(NC-3)	-	79.65	5	-	-	10	0.35	-	5	2734
4*	BAG-6-PP (NC-4)	-	80	8.5	6.5	mw:200000	-	5	-	-	624
5*	BAG-3-PP (NC-5)	-	80	8.5	6.5	mw:360000	-	5	-	-	1050
6*	BAG-4-PP (NC-6)	-	80	8.5	6.5	mw:700000	-	5	-	-	29340
7*	BAG-5-PP (NC-7)	-	80	8.5	-	-	6.5	5	-	-	542
EPDM Matrix structures											
8*	BAG-EPDM-8 (NC-8)	79.65	-	5	10	mw:700000	-	-	0.35	5	130000
9*	BAG-EPDM-9 (NC-9)	79.65	-	5	-	-	10	0.35	-	5	26520
10	Az-1-EPDM (NC-10)	80	-	10	5	mw:160000	-	5	-	-	
11	Az-2-EPDM (NC-11)	80	-	10	5	Mw:800000	-	5	-	-	
12	Az-3-EPDM (NC-12)	80	-	10	5	mw:1000000	-	5	-	-	
Masterbatches: Polyester/Clays											
13	BAG-1 (NC-13)	-	-	-	96.5	mw:700000	-	3.5	-	-	
14	BAG-2 (NC-14)	-	-	-	-	-	96.5	3.5	-	-	
15	BAG-7 (NC-15)	-	-	-	96.5	mw:700000	-	-	3.5	-	

Notes: *Samples used in rheology experiment   ** Poly (MA-*alt*-1-dodecene)-APTS-g-$(SiO_2)_n$ *** wt %: weight mass percentage

3.6. Characterization

3.6.1. FTIR and MS

FTIR, the Fourier Transform Infrared spectra of the nanocomposites (KBr pellet) were analyzed with an equipment FTIR Nicolet 6970 spectrometer in the range of 4000–500 cm^{-1} where it is taking 30 scans at 4 cm^{-1} resolutions. The molecular mass of pristine copolymer was studied by laser desorption/ionization mass spectrometry-matrix-assisted (MALDI-TOF MS, Voyager DE PRO model) in THF solution using α-ciyano–4-hidroxycinnamic acid (CHCA) as a matrix and NaTFA as a cationizing agent.

3.6.2. NMR

The solid-state NMR spectra was accomplished at 75.5 MHz for ^{13}C and at 59.6 MHz for ^{29}Si. A Bruker Superconducting FT-NMR Spectrometer AVANCE with high power superconductive paramagnet TM 300 MHz WB in 7 mm MAS with a MAS angle of 54.7° was used for the characterization of nanocomposites.

3.6.3. XRD

The X-ray powder diffraction (XRD) patterns and reflection parameters were performed with a PANANALYTICAL X-ray diffractometer equipped with a CuKα tube and Ni filter (λ = 1.5406 Å). The XRD patterns were measured at 2θ, in the range of 1-50°. The Bragg equation was used to calculate the interlayer spacing (d): $n\lambda = 2d\sin\theta$, where n is the reflection order and 2θ is the angle of reflection. PANANALITICAL High Score Plus program (equipment trademark software) has been used to get data from spectra.

3.6.4. SEM AND TEM

The surface morphology of nanocomposites was examined using a brief description of the ZEISS SUPRA 40 Field Emission Scanning Electron Microscope (FESEM) with image scales: 2 μm x 2000 and 10 μm x10000 magnifications using an acceleration voltage of 20 kV. Specimens were freeze dried. They are coated with a thin layer of platinum before analyzing by using a QUORUM-Q150R ES coating device. The internal morphology of nanocomposites was performed by FEI Tecnai G2 Spirit Biotwin Model High Contrast Transmission Electron Microscopy (CTEM). It has Lantan Hexaboron Electron Gun at 120 kV. Powder polymer sample was suspended in ethanol solution with 0.1 % concentration, then, the solution was sonicated up to the formation of a homogeneously dispersed solution.

Prepared solution (3-5 µL) was dropped on the surface of carbon coated grid and dried up to the formation of full solid phase on grid surface before testing.

3.6.5. TGA and DSC

TGA, Thermogravimetric and DSC, differential scanning calorimetric analyses were performed by SII EXTRAR6000 TG-DTA6300 and Diamond DSC Perkin Elmer Thermal Analyzers. Characterization is accomplished by a linear heating rate of 10 °C/min under nitrogen flow. Samples were measured in alumina pan that is sealed with an amount of about 10 mg. The temperature at onset ($T_{d\ (onset)}$) and the temperature of maximum weight loss ($T_{d\ (max)}$) shows the thermal degradation temperatures.

3.6.6. DYNAMIC RHEOMETER

Some characterization methods include mechanical properties. Most recent studies for mechanical properties are done by rheology devices. Rheology gives the deformation properties of a material under pressure and temperature. Viscosity and shear rates are most common and effective results for materials.

In this study, AR2000 type dynamic rotary rheology device and heating equipment as parallel plates (Commercial name: TA Instrument, MODELAR2000) have been used (see Figure 3.3). It is a double plate device. Plates are providing pressure in an oven that provides temperature regulation (see Figure 3.4). Force applied on plates in regular time intervals is detected and reported.

Figure 3.3. TA instrument, rotary rheometer.

8-10 gr sample is placed in rotary rheometer sample point. Top part of parallel plate (see Figure 3.4) sample holder is moved downwards to squeeze and decrease spaces between composites particles. Oven is closed to heat. A predetermined die temperature of related samples that depend on the main matrix (PP, 175 ℃ & EPDM, 145 ℃) is set. Rotary

rheometer is started to apply forces on the sample that placed between parallel plates while applying heat on it. The rheometer provides analysis about stress and viscosity in a time manner. The data will give specific information with graphs to the makers like viscoelasticity, modulus, time dependence, stress, etc.

Viscosity and shear stress with shear rate has been analyzed. Viscosity graphs has been modelled with famous CARREAU model [87]. Zero shear rate viscosity data are available at the end column of the Table 3.6.
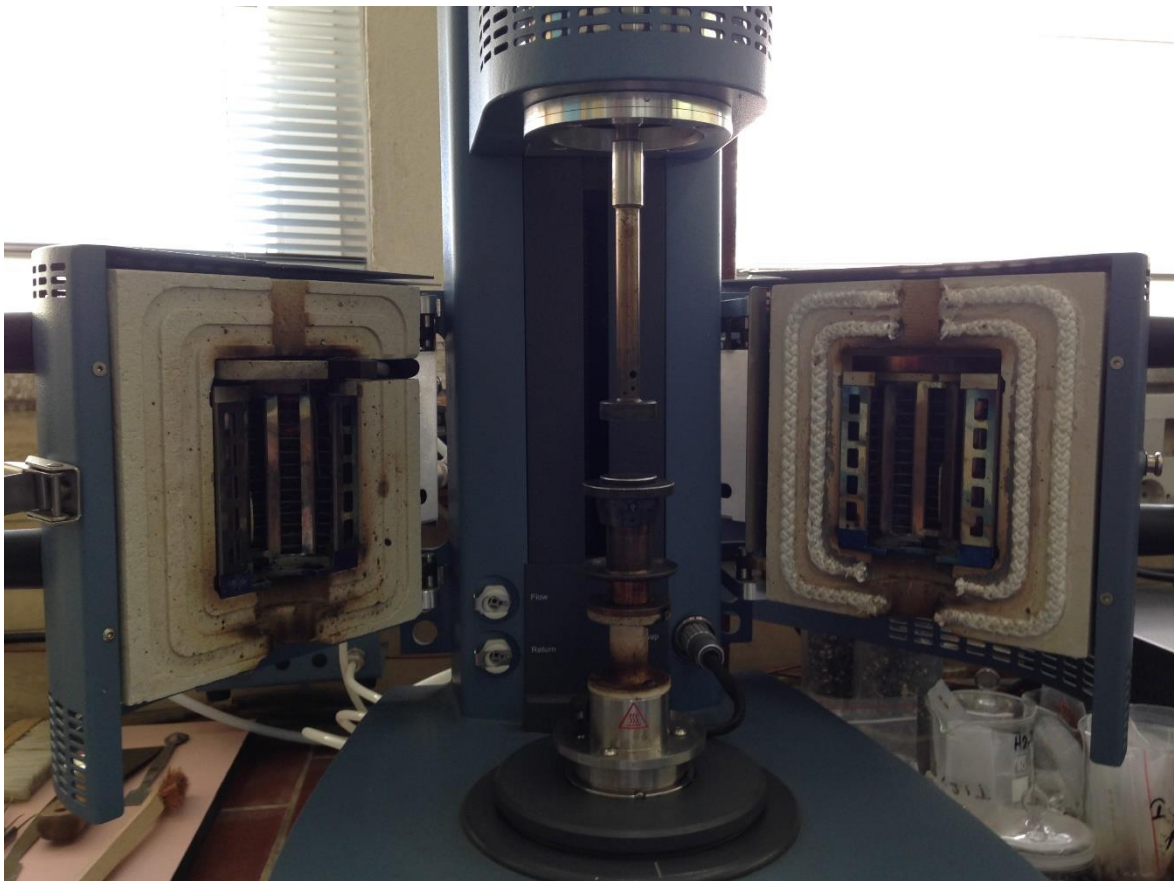
Figure 3.4. Oven and rotary plate details part of rheology device.

4. RESULTS AND DISCUSSION

4.1. Structural Investigation of Copolymer (MA-*alt*-1-dodecene)-g-Silica

4.1.1. Synthetic Pathways of Copolymer (MA-*alt*-1-dodecene)-g-Silica Nanoparticles

Silane-based coupling agents [75] most frequently γ-aminopropyltrimethoxysilane (APTS), vinyltrialkoxysilanes and tetraethoxysilanes, were utilized to improve the surface adhesion in various polymer composites, to surface modify polyolefin films, and to prepare functional polymer/silica nanohybrids through in situ generated silica NPs by sol-gel method [76]. To fabricate the PP/silica nanocomposites and EPDM/PP/silica nanomaterial, twin-screw extrusion and injection molding are the two most commonly used methods [77-79]. The chemistry for the synthetic pathway of the copolymer-*g*-silica NPs through sol-gel processing was proposed by a structural model and was schematically represented in Figure 4.1A, B. The following reactions and in situ interfacial interactions occurring in the generated covalently incorporated silica nanoparticles were proposed: (1) amidation of amphiphilic poly (MA-*alt*-1-dodecene) (copolymer) with APTS, (2) side-chain hydrolysis-condensation of copolymer-*g*-APTS with tetraethoxysilane (TEOS) precursor and (3) the formation of silica NPs encapsulated with copolymer chains via covalent incorporation.

Agreeing with XRD patterns and peak reflection parameters (Figure 4.1D), copolymer-g-SiO_2 nanohybrid predominantly exhibits amorphous structure due to colloidal structure of covalence encapsulated nanoparticles. The famous Scherrer equation has been utilized to estimate the particle size (τsh, mean thickness) [80]. The equation is $\tau = Ksh\lambda / \beta \cos\Theta$. The average size of crystalline domains is τ. These domains can be equal/smaller to the grain size. Whereas, *K* is a Scherrer constant (K_{sh} of 0.89). λ is the X-ray wavelength ($\lambda = 1.5406$ nm). β is the net line broadening, subtracting instrument noise of broadening, at half the maximum intensity (FWHM).

The results for each crystalline peaks are given in the table in Figure 4.1D. Particle size of all nanoparticles is 5.06 nm. Average size of nanoparticles is 0.34 nm and changes around 0.2-0.97 nm that indicates a better distribution of covalence incorporated nanoparticles onto matrix copolymer chains.
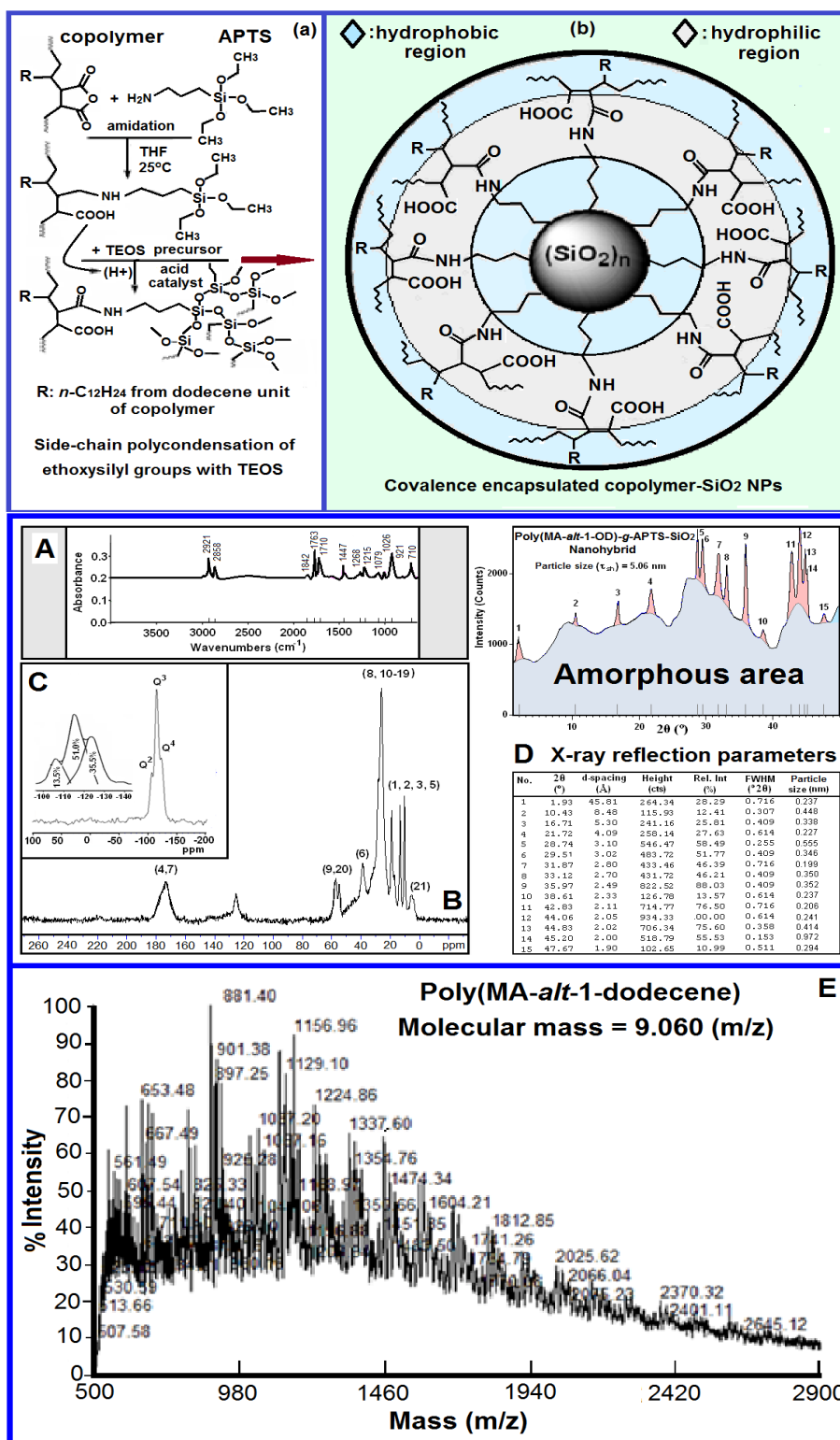
Figure 4.1. Synthetic pathways of (a) copolymer-g-SiO₂ covalence encapsulated NPs by sol-gel method and (b) structural model of copolymer-g-SiO₂ NPs; (A) FTIR, (B) solid state ¹³C-NMR, (C) ²⁹Si NMR spectra, (D) XRD pattern with X-ray reflection parameters of copolymer-g-APTS-(SiO₂)ₙ nanohybrid composite and (E) average molecular mass (m/z) from MALDI-TOF MS spectra of pristine poly (MA-alt-1-octadecene) copolymer.

4.1.2. Chemical and Physical Structures of Copolymer (MA-*alt*-1-dodecene)-g-Silica Nanoparticles

The chemical and physical structures, and composition of prepared copolymer-g-APTS-$(SiO_2)_n$ NPs were examined by FTIR, ^{13}C and ^{29}Si solid state NMR spectroscopy methods. The obtained results are given in Figure 4.1. FTIR spectra in Figure 4.1A confirmed the presence of the following characteristic absorption bands from functional groups of copolymer: broad peaks at 2921 and 2858 cm^{-1} are related to C–H stretching from CH and CH_2 propylene group, dodecyl branched chain and backbone chain; the bands at 1842, 1763, 1710 and 1646 cm^{-1} are associated with C=O stretching in anhydride, free –COOH and amide groups; 1447 cm^{-1} band appears from CH_2 bending vibration; 1263 and 1215 cm^{-1} bands come from C-O-C and C-O groups. The absorption peaks at 1079, 1026 and 921 cm^{-1} can be attributed to Si-O and Si-O-Si vibrations from silica NPs; band at 710 cm^{-1} is related to rocking vibration from –$(CH_2-)_n$ segment.

Chemical structure of copolymer-g-SiO_2 NPs is also confirmed by solid state ^{13}C-NMR (Figure 4.1B) and ^{29}Si-NMR (Figure 4.1C) spectroscopy analyses. The degree of hydrolysis was proved by solid-state ^{13}C CP/MAS NMR (Figure 4.1B). The carbonyl group peak was observed at 173 ppm while the peaks for methyne, methylene, and methyl carbon at 67 ppm, 41 ppm, and 22 ppm were detected respectively in the hybrid prepared with 0.02 ml of the catalyst. The peak at 52 ppm is related to the carbon of the residual methoxy group of TMOS precursor.

Sol-gel bonding in the synthesized hybrid structure was also studied with solid-state ^{29}Si NMR. Figure 4.1C displays the solid-state ^{29}Si MAS NMR spectra of the poly (MA-alt-1-dodecene)/SiO_2 nanohybrid structure. ^{29}Si solid-state NMR gives further information on silica structure and the degree of Si-OH condensation reaction. The silicon atoms, generated by the condensed siloxane species originating from TEOS, through di- and tri- and tetra-substituted siloxane bonds were designated as Q^2, Q^3 and Q^4, respectively. Mono-substituted siloxane fragment is not seen in the spectra, and condensation reactions due to hydrolysis predominantly occur by the tri- and full-substitution with the formation of organo-silica nanoparticles covered with covalent bonding macromolecules of alternating copolymer. Q^4 indicated complete silicon condensation and the existence of Q^3 and Q^2 reflected the incomplete condensation of the TEOS. The chemical shifts and peak areas from the ^{29}Si NMR spectra of Q^2, Q^3, and Q^4 of poly (MA-alt-1-dodecene)/SiO_2 nanohybrid allow us to calculate the contents of silica NPs in $(SiO)_2Si(OH)_2$ (Q^2), $(SiO)_3SiOH$ (Q^3), and

$(SiO)_2(SiO)_2$ (Q^4) fragments using ^{29}Si MAS chemical shift assignments for silica. It has been found as $Q^2 = 13.5\%$, $Q3 = 51.0\%$ and $Q4 = 35.5\%$ (Figure 4.1C). Results were that Q^3 and Q^4 were the major parts of microstructures forming the copolymer network structure. Copolymer/silica NPs ratio was found as 0.316, i.e., 24 mass % of shell copolymer and 76 mass % of core silica NPs. The average molecular mass (9.060 m/z) was calculated from plot of intensity versus mass (m/z). Repeated monomer-comonomer unit (n x 7.087 = 1900 m/z, n = molecular mass of one unit) of alternating copolymer was evaluated from MALDI-TOF MS spectra (Figure 4.1E).

Thus, reactive alternating copolymer with measured molecular mass (9.060 m/z, Figure 4.1E) predominantly having an amorphous structure (softening point ~120 °C) and excellent hydrophilic (succinic anhydride unit) / hydrophobic (branched $C_{12}H_{21}$ alkyl unit) structural balance plays an important role in the synthesis of copolymer-g-APTS-silica hybrid and PP/EPDM based nanocomposites. It serves as a second reactive compatibilizer and a structural analogue of the first PP-g-MA compatibilizer used in the composition of blends of PP and EPDM based structures.

4.2. Investigation of Polypropylene Structures

4.2.1. Chemical and Physical Structures of Nanocomposites of Polypropylene Matrix

FTIR spectra of PP based NCs (see Figure 4.2) show the following characteristic absorption bands: broad peak at 3279 cm^{-1} belonging to OH groups from PLA (end group) and –COOH maleamide unit of poly (MA-*alt*-1-dodecene)-SiO$_2$, and PP-g-MA which is formed after amidation of MA unit with γ-aminopropyltrimethoxysilane and in situ amidation of anhydride units with octadecyl amine intercalant during the extrusion process; 2949 (s), 2917 (s) and 2877 (m) cm^{-1} from valence vibrations of C−H bands in CH$_2$, CH$_3$ and CH groups of PP chains and propylene unit of PP-*g*-MA; the C=O stretching bands of MA/maleamide units are detected at 1759 (m) cm^{-1} (in -COOH) and 1644 (w) cm^{-1} (in –NH-C=O), respectively; absorption bands at 1455 (s) and 1375 (s) cm^{-1} are associated with bending vibrations from CH$_2$ and CH$_3$ groups of propylene unit: these analytical bands are used to calculate the index of methylene group (IM) according to the following absorbance ratio: IM = A$_{1375}$/A$_{1455}$ = 0.69 (NC-1), 1.53 (NC-2) and 1.72 (NC-3). The observed order in the increase of IM values of NCs complies with the mass fractions of methylene groups (-CH$_2$-)$_n$ in the composition.

The absorption bands at 2838 (m) and 2722 (w) cm^{-1} are related to symmetric and asymmetric stretching from CH and CH_3 groups of PLA and their bending bands appear at 1420 (m) and 1359 (m) cm^{-1}, respectively; the C-O-C and C-O asymmetric and symmetric valence vibrations were found at 1255 (w) and 1217 (w) cm^{-1}; the absorption bands at 1167 (m), 1101 (m) and 1044 (w) cm^{-1} are associated with Si-O and Si-O-Si stretching from silica nanoparticles and silicate sheets; the isotacticity of the i-PP is confirmed by the two bands at 997 (m) and 972 (m) cm^{-1}; absorbance ratio of these bands is related to isotacticity index (ITI) of the PP chains in nanocomposites: ITI (A_{997}/A_{972}) values were found to be 1.22, 1.25 and 0.91 for the NC-1, NC-2, and NC-3, respectively. The bands at 840 and 809 cm^{-1} were attributed to shorter chain in helical conformation and to helical chains within crystals, respectively. These bands were also used to estimate the crystallinity of i-PP obtained from Raman FTIR spectroscopy [81].
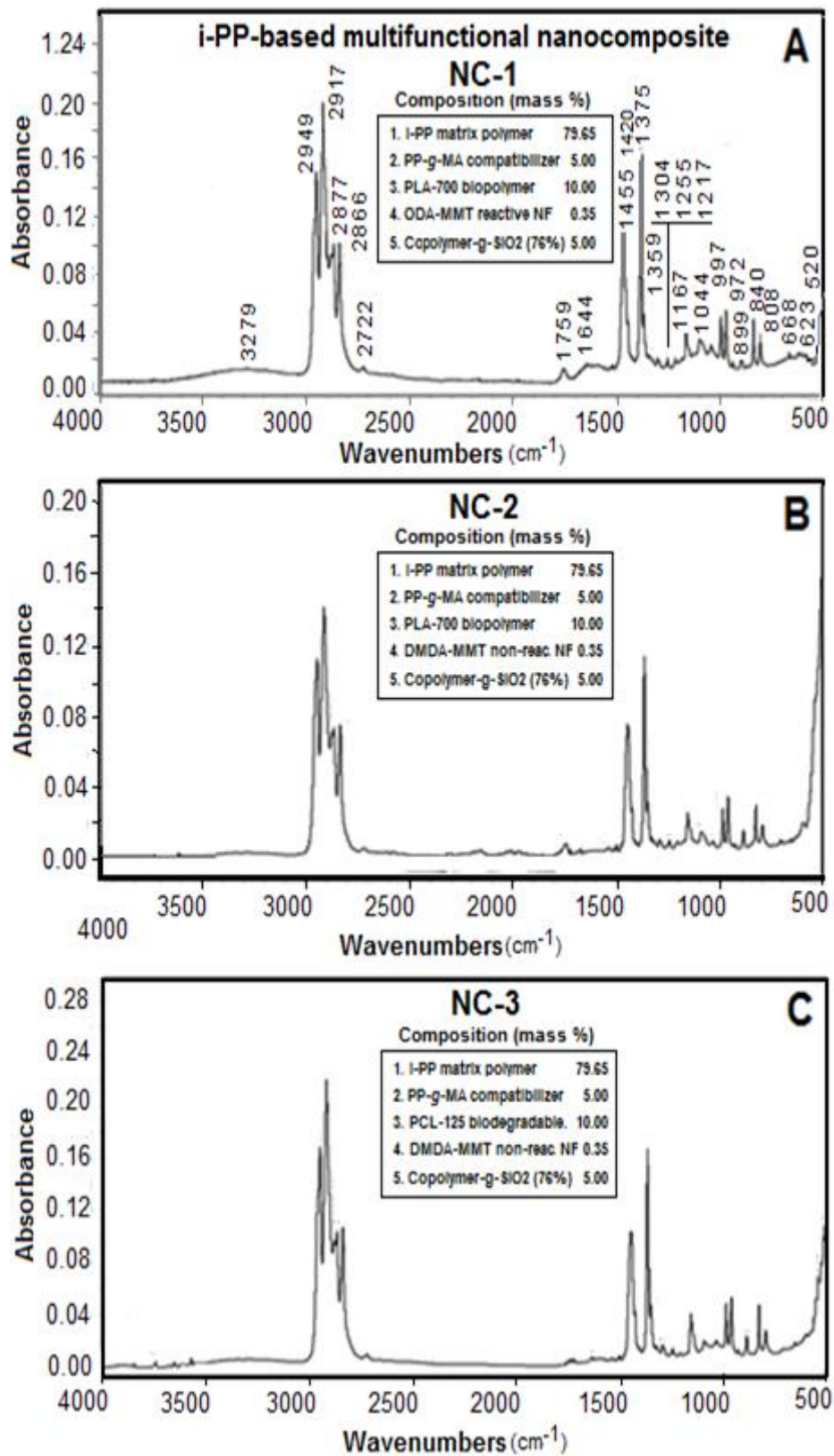
Figure 4.2. FTIR spectra graphs, NC-1 (A), NC -2 (B), NC-3 (C).

absorption bands were detected similarly in the graphs of the nanocomposites NC-2 and NC-3 (see Figure 4.2B and C). The compositions of biodegradable NC-2 (PLA-700) and NC-3 (biodegradable PCL-125) include DMDA/MMT non-reactive nanofiller, unlike the composition of NC-1. Appearance of strong absorbtion bands at 522 and 520 cm^{-1} in the spectra of NC-2 and NC-3 are associated with rocking vibrations of CH_2 in -$(CH_2)_n$- groups from dodecyl fragments of copolymer and DMDA-MMT organoclays, as well as from -$(CH_2)_5$- backbone chain of PCL.

4.2.2. XRD Results of NCs 1-3 and Comparison with Pristine Polymer

Physical structure and particle size of nanocomposites were investigated by XRD analysis method. The obtained XRD patterns and reflection parameters are given in Figure 4.3 and Figure 4.4. XRD patterns of pristine i-PP and its MA grafted derivative are given in Figure 4.3. Isotactic PP is expected to contain three crystalline structures like α-monoclinic, β-hexagonal, and γ-orthombic forms. The α-monoclinic is the most common and well established crystalline modification for i-PP [82]. XRD patterns for the reflections from the stable α-monoclinic crystals show the following characteristic crystal peaks at 14.08 (α-1), 16.84 (α-2) and 18.54 °2θ (α-3) with reflection index (110), (040) and (130). The response due to the changes of thermal and structural factors at 21.80 (4-060) where 4 is peak and 060 is plane number, 25.44 (5-200) and 28.44 °2θ (6-220) come from metastable smectic phase. Similar reflections to form functionalized PP-*g*-MA oligomeric graft copolymer (Figure 4.3B) were observed which also revealed the reason of lower peak intensity and areas, as well as higher number of crystals due to lower molecular weight (M_w = 9.100 Da) and the presence of hydophilic anhydride units (∼4.2 mass %).
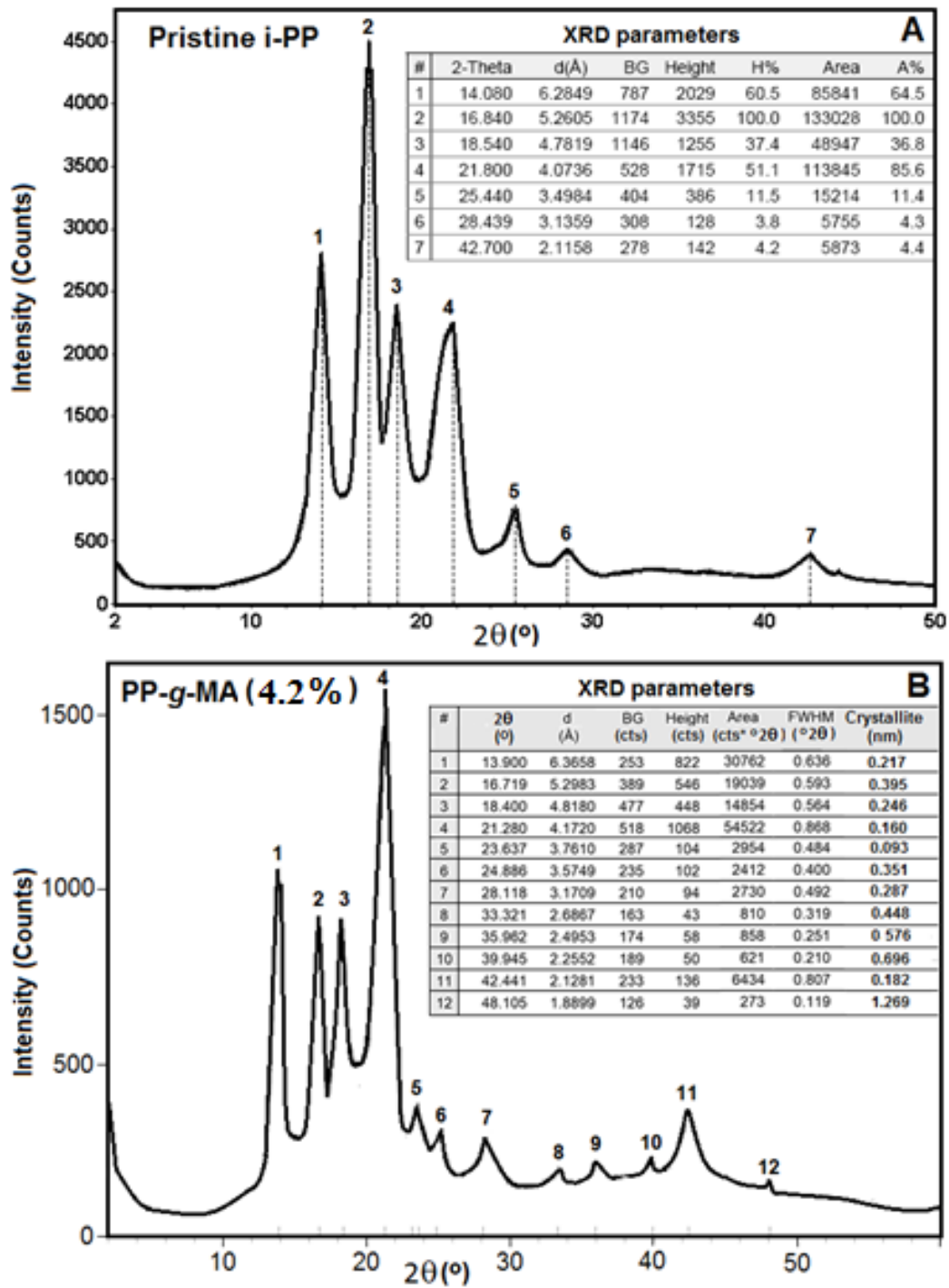
Figure 4.3. XRD patterns and reflection data of (A) i-PP and (b) PP-g-MA.

A — Pristine i-PP — XRD parameters

#	2-Theta	d(Å)	BG	Height	H%	Area	A%
1	14.080	6.2849	787	2029	60.5	85841	64.5
2	16.840	5.2605	1174	3355	100.0	133028	100.0
3	18.540	4.7819	1146	1255	37.4	48947	36.8
4	21.800	4.0736	528	1715	51.1	113845	85.6
5	25.440	3.4984	404	386	11.5	15214	11.4
6	28.439	3.1359	308	128	3.8	5755	4.3
7	42.700	2.1158	278	142	4.2	5873	4.4

B — PP-g-MA (4.2%) — XRD parameters

#	2θ (º)	d (Å)	BG (cts)	Height (cts)	Area (cts* º2θ)	FWHM (º2θ)	Crystallite (nm)
1	13.900	6.3658	253	822	30762	0.636	0.217
2	16.719	5.2983	389	546	19039	0.593	0.395
3	18.400	4.8180	477	448	14854	0.564	0.246
4	21.280	4.1720	518	1068	54522	0.868	0.160
5	23.637	3.7610	287	104	2954	0.484	0.093
6	24.886	3.5749	235	102	2412	0.400	0.351
7	28.118	3.1709	210	94	2730	0.492	0.287
8	33.321	2.6867	163	43	810	0.319	0.448
9	35.962	2.4953	174	58	858	0.251	0 576
10	39.945	2.2552	189	50	621	0.210	0.696
11	42.441	2.1281	233	136	6434	0.807	0.182
12	48.105	1.8899	126	39	273	0.119	1.269

The reflections from i-PP chain crystals of nanocomposite (Figure 4.4 NC-1) were detected at 14.39, 17.08, 25.52 and 29.30º 2θ with 110 (α), 040 (α), 060 (α) and 220 (α) planes, respectively. A reflection at 18.81º 2θ is associated with PLA particle size (25.76 nm). PP-g-MA chain crystals is related to the reflection at 21.39º 2θ (46.91 nm). The observed higher area (204.67) and lower particle size (17.97 nm) of the reflection peak at 22.13º 2θ can be

attributed to the reflections from long octadecyl side-chain and two dodecyl groups from copolymer and organoclay, respectively. Agreeing with the reflection parameters of the layered silicate and silica regions at 2-10º 2θ contained broad amorphous area at 6.75º 2θ, which can be attributed to colloidal SiO_2 NPs, covalently encapsulated with poly (MA-*alt*-1-dodecene) copolymer via amidation of anhydride unit with γ-aminopropyl-SiO_2.

NC-1

ODA-MMT/copolymer-g-SiO$_2$ NPs incorporated PP/PP-g-MA/PLA-700

No.	2θ (°)	d (A)	Height (cts)	FWHM (°2θ)	particle size (nm)
1	14.39	6.15	492.9	0.409	22.33
2	17.08	5.19	792.9	0.154	65.09
3	18.81	4.72	287.5	0.358	25.76
4	21.39	4.15	302.4	0.205	46.91
5	22.13	4.02	405.5	0.512	17.97
6	25.52	3.49	64.5	0.154	65.81
7	29.30	3.05	43.2	0.614	15.16
8	43.05	2.10	40.2	0.409	23.80

NC-2

DMDA-MMT/copolymer-g-SiO$_2$ NPs incorporated PP/PP-g-MA/PLA-700

No.	2θ (°)	d (A)	Height (cts)	FWHM (°2θ)	particle size (nm)
1	2.11	41.86	4.5	0.102	116.23
2	14.38	6.16	520.5	0.102	82.03
3	17.10	5.18	1098.5	0.332	114.49
4	18.82	4.71	389.5	0.153	27.76
5	21.36	4.16	319.3	0.512	65.20
6	22.34	3.98	389.6	0.153	17.95
7	25.83	3.45	83.3	0.358	64.48
8	29.02	3.07	36.1	0.921	26.07
9	42.99	2.10	32.7	0.512	10.07
10	68.98	1.36	4.2	0,256	18.95

NC-3

DMDA-MMT/copolymer-g-SiO$_2$ NPs incorporated PP/PP-g-MA/PCL-125

No.	2θ (°)	d (A)	Height (cts)	FWHM (°2θ)	particle size (nm)
1	2,53	34.92	1.34	0.819	10.96
2	5.03	17.58	2.91	0.819	10.96
3	14.61	6.02	26.46	0.819	11.06
4	17.30	5.12	41.88	0.256	36.60
5	18.98	4.68	24.95	0.256	36.68
6	21.54	4.12	28.04	0.307	30.36
7	22.35	3.98	32.18	0.512	17.96
8	24.29	3.66	5.33	0.409	22.66
9	25.98	3.43	4.93	0.614	15.05
10	29.17	3.06	4.43	0.614	15.15
11	58.79	1.57	2.84	0.128	90.39
12	60.57	1.53	0.75	0.716	14.53

Figure 4.4. XRD patterns and reflection parameters of NC-1, NC-2, and NC-3.

63

The XRD patterns of NC-2 and NC-3 are given again in Figure 4.4. Particle sizes of all reflection peaks were calculated using a High Score Plus Program (PANanalytical, XRD device software). It was observed that both nanocomposites show similar reflections but with different particle sizes (higher for NC-2 and relative lower for NC-3) due to predominantly hydrogen bonding in situ interfacial interactions in these systems prepared with DMDA-MMT.

Moreover, XRD patterns of these nanocomposites additionally contain the characteristic reflections from organoclay being shifted to a lower region. The NC-3 (Figure 4.4 NC-3) also shows a new reflection peak at 24.29º 2θ with particle size of 22.66 nm from PCL chains. It was proposed that a combination of chemically and physically (predominantly hydrogen bonding) active sites from free –COOH, –C=O, amide/amine, ester and ether groups play an important factor during the formation of nanocomposites via controlling in situ interfacial interactions during extrusion processing.

4.2.3. SEM Surface and TEM Internal Morphologies of Propylene Nanocomposites (NC-1, NC-2, and NC-3)

SEM images of all nanocomposites are given in Figure 4.5.
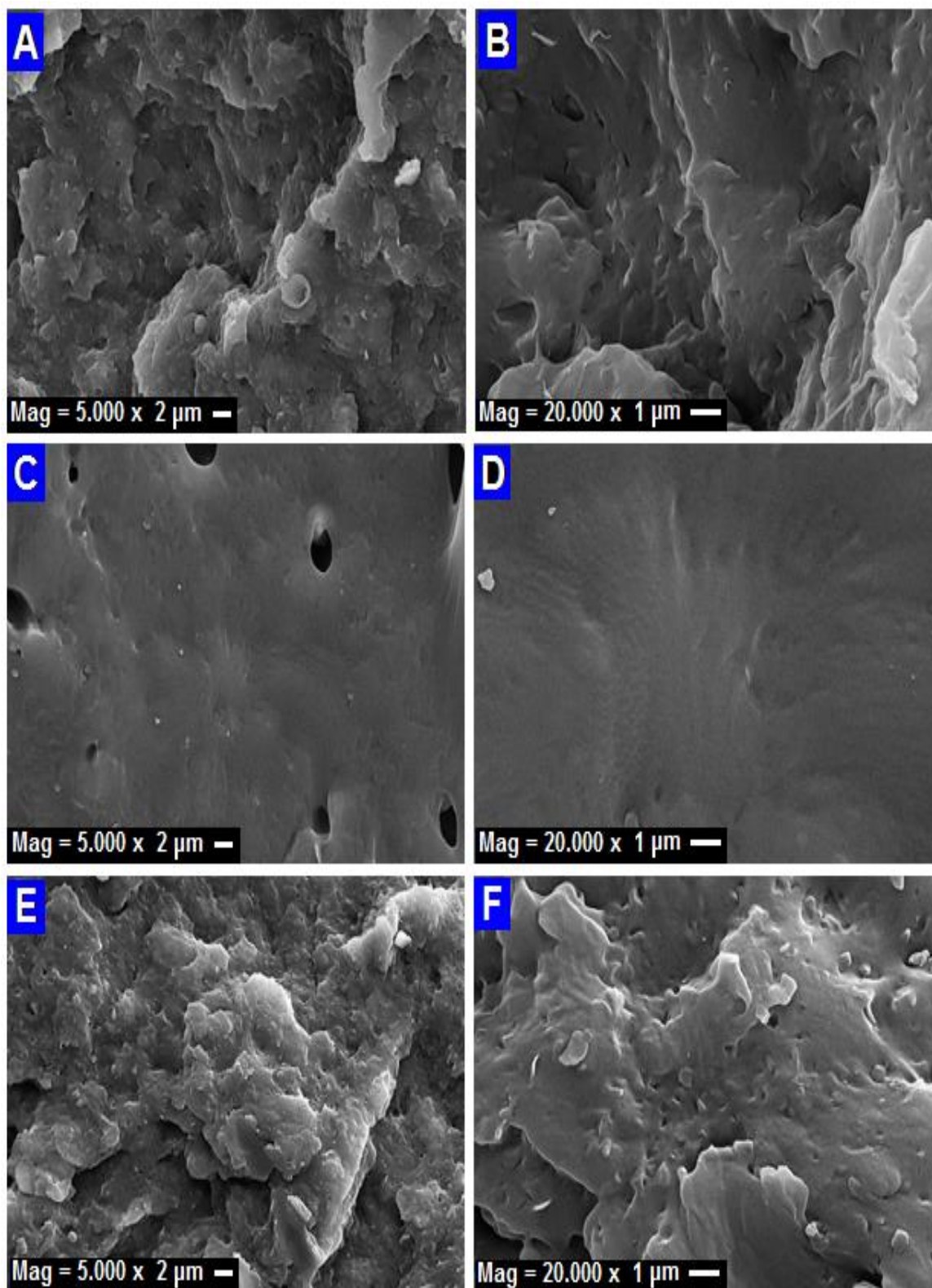
Figure 4.5. Surface SEM pictures of NC-1 (A, B), NC-2 (C, D) and NC-3 (E, F).

Agreeing with these images the surface morphology strongly depends on the origin of organoclay and selected polyester biopolymer (PLA, PCL). Nanocomposites NC-1 (Figure 4.5A and Figure 4.5B) and NC-3 (Figure 4.5E and Figure 4.5F) show better compatibilized blends and dispersed domains with fine surface distribution of silica micro- and nanoparticles (white points). However, NC-2 (Figure 4.5C and Figure 4.5D) exhibits smooth surface morphology without the formation of domains.
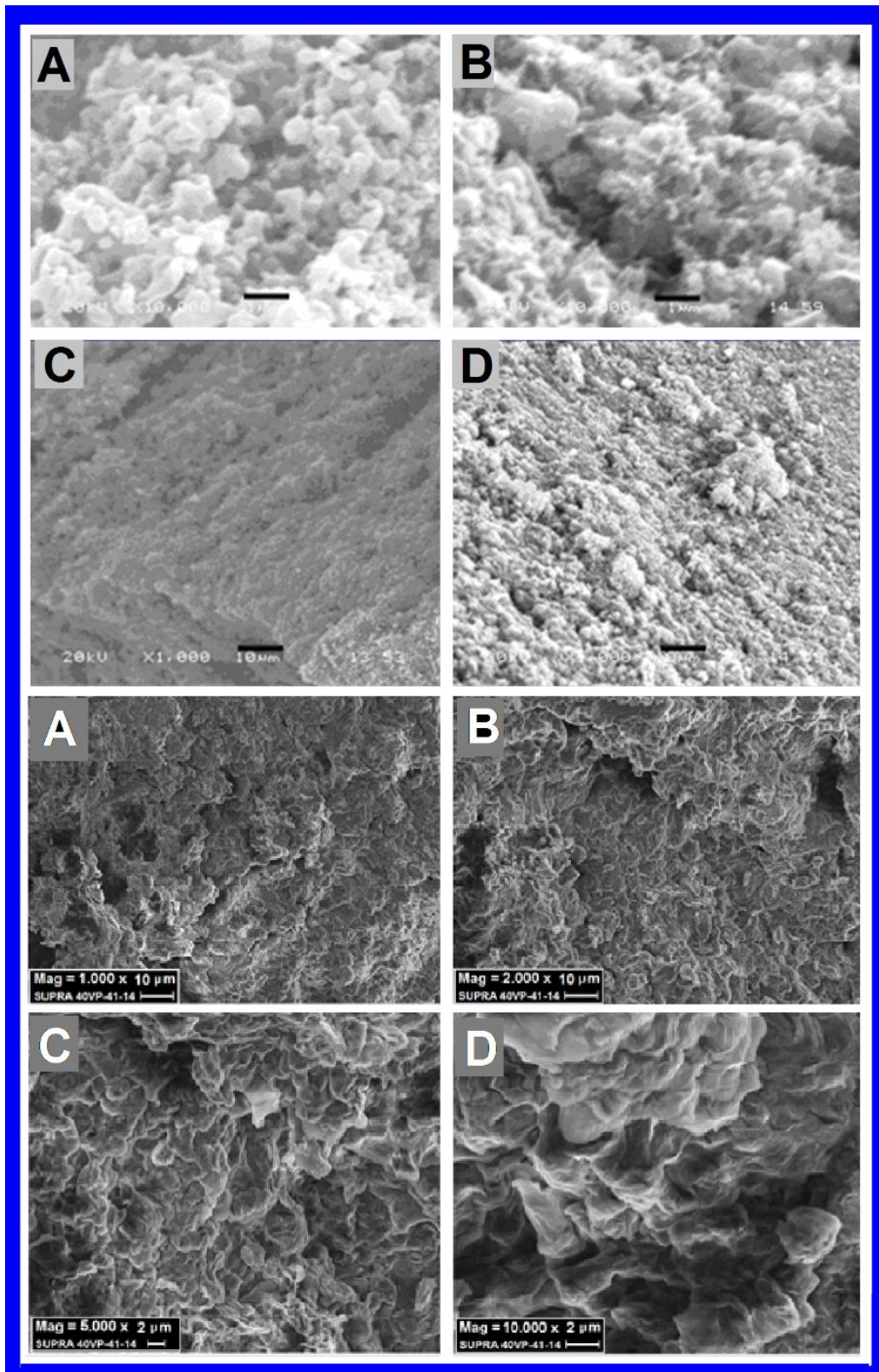
Figure 4.6. SEM images of two different masterbatches at different magnifications: PLA-700/DMDA-MMT (NC-13, 3.5 mass %) (upper A, B, C and D) and PLA-700/ODA-MMT (NC-15, 3.5 mass %) (bottom A, B, C and D) fabricated in melt by extrusion compounding.

Unlike NC-1 and NC-3, the nanocomposite NC-2 shows partially surface porous structures (pore size ~2.5 µm) due to visible hydrolysis of PLA polymer chains in the extruder conditions. On the other hand, masterbatch nanocomposites, namely, PLA-700/DMDA-MMT (NC-13, 3.5 mass %) and PLA-700/ODA-MMT (NC-15, 3.5 mass %) fabricated under the same extrusion conditions show homogeneously dispersed morphology (Figure 4.6) and unique X-ray reflection parameters (Figure 4.7). The reflection peaks related to ODA-MMT clay disappeared in XRD patterns of the nanocomposite (Figure 4.7) due to full intercalation/exfoliation processing during extrusion.
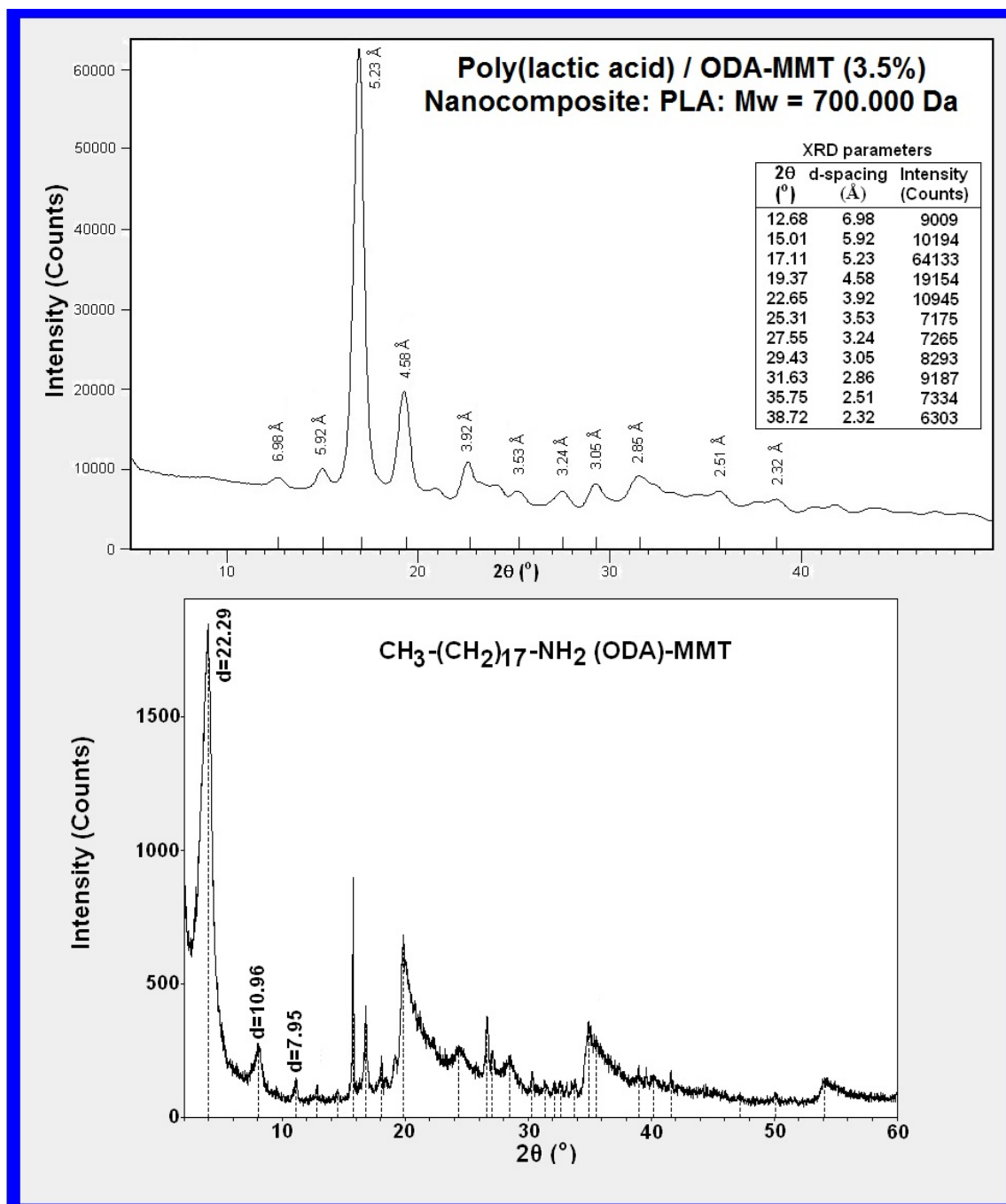
Figure 4.7. XRD patterns of PLA-700/ODA-MMT nanocomposite and pristine ODA-MMT clay.

TEM image of NC-3 shows well-oriented multi-layered structure of shells including various polymer chains from PP, PP-g-MA graft copolymer, and PCL on colloidal amphiphilic copolymer-g-SiO$_2$ NPs in spherical core phase (Figure 4.8). The dispersion of the other nanocomposites (NC-1 and NC-2) has not been investigated yet.
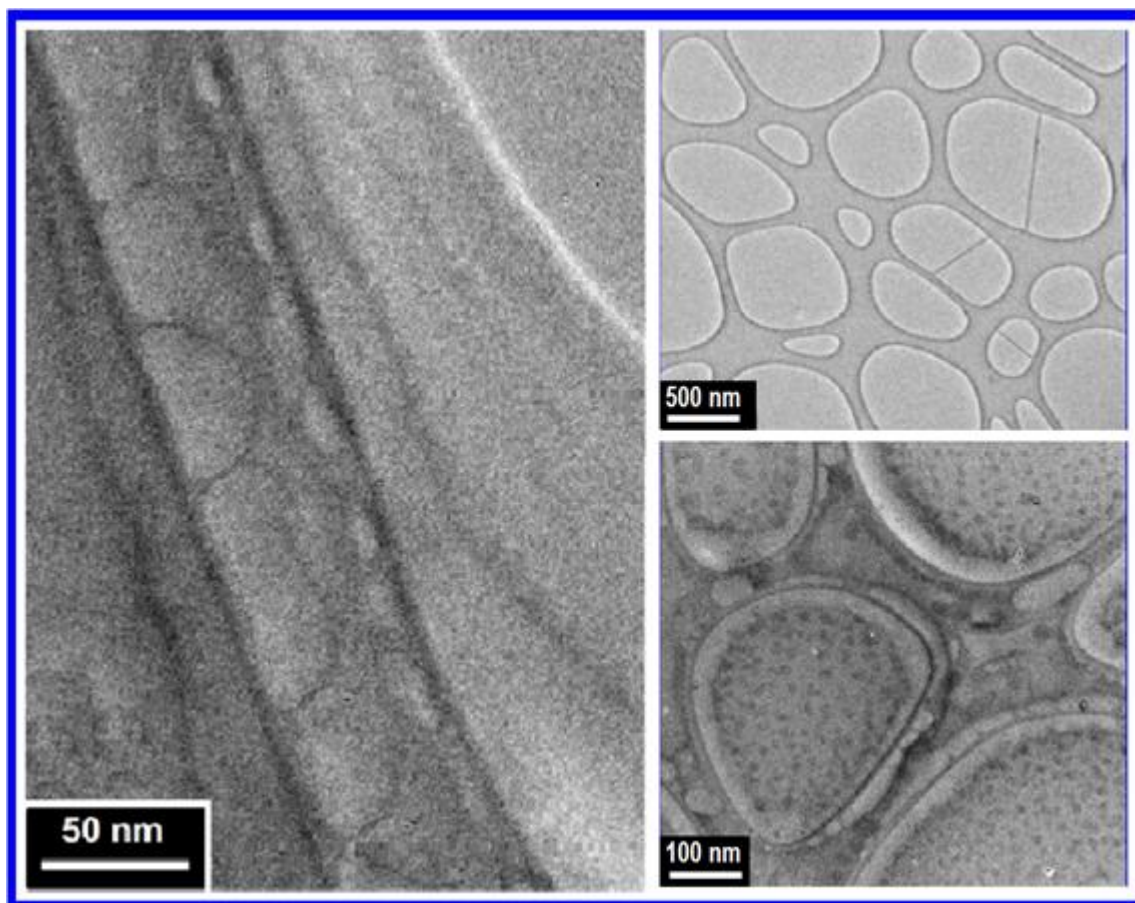
Figure 4.8. TEM images of internal morphology of NC-3 dispersed structures for the encapsulated copolymer-g-SiO$_2$ and polyester modified organoclay micro- and nanoparticles onto matrix PP, PP-g-MA, and PCL polymer chains.

It is expected that these nanocomposites will also exhibit approximately similar morphologies. TEM images clearly display that the core phases are composed of silica NPs. The diameters of the self-assembled core (copolymer)-shell (silica NPs) spherical micro- and NPs were approximately around 45-500 nm. The composed SiO$_2$ NPs in core phase show nano-scale sizes around 10-15 nm with unique distribution of NPs (Figure 4.8). It was demonstrated that the self-assemble of the multilayer polymers (i-PP, PP-g-MA and PCL) on colloidal copolymer-g-SiO$_2$ under provided melt reactive extrusion conditions leads to a successful synthetic pathway to fabricate core-shell multi-functional polymers/silica hybrids in the micro- and nano-scale size range.

4.2.4. Thermal Behaviors of Propylene Nanocomposites

The DTA, DSC and TGA-DTG comparative analysis results of nanocomposites generated (NC-1, NC-2 , and NC-3) and pristine i-PP are given in Figure 4.9 and Figure 4.10. DSC analyses were performed via measurement of the heat of fusion, area of the melting endopeaks and total energy absorbed in melting and recrystallizing regions of the nanocomposites under nitrogen flow with heating/cooling rate of 10 °C/minute.

In agreement with Figure 4.9 and Figure 4.10, the melting values for all composites (around 166.8-169.7 °C by DTA in Figure 4.9 and 168.1-166.7 °C by DSC in Figure 4.10) and recrystallization values (~123.5 °C for all NCs by DSC in Figure 4.10) exhibited approximately similar melting and crystallizing transitions but with different peak areas and enthalpy values. The crystallinity (χ_c) of pristine i-PP and nanocomposites were calculated employing the values of enthalpy of fusion (ΔH^{obs}) value at melt transition from the DSC curves. The literature value of enthalpy of fusion (ΔH^o) for 100 % crystalline i-PP is 165 J/g [83] and the following equation is employed to calculate the crystallinity of the pristine polymer (1):

$$\chi_c = (\Delta H^{obs}/\Delta H^o) \times 100 \qquad (1)$$

Xc (χ_c) has been evaluated as 48.02 % (Figure 4.9E). The NC-1, NC -2, and NC-3 nanocomposites exhibit the following crystallinities: 45.82, 50.91, and 45.73 %, respectively (Figure 4.10 A, B, C).

TGA-DTG analysis results (Figure 4.10) show that the nanocomposites NC-1 and NC-2 containing organoclay and hydrolytically degradable PLA chains exhibit two-step degradations with lower mass loss during the first step degradation, whereas, NC-3 containing PCL exhibits only one-step degradation. However, thermal stability of NCs ($T_{dmax} = 481.7$ °C/NC-1, 464.8 °C/NC-2 and 463.5 °C/NC-3) (Figure 4.10) is relatively higher than that of pristine i-PP for which, T_d (onset) = 357 °C and T_d (max) $_=$ 450 °C (Figure 4.9 E). The mass loss of the nanocomposites in the above mentioned critical degradation temperatures (T_{dmax}) essentially increases due to the presence of degradable polyesters, organic segments from the silicate and silica micro- and nanoparticles in the composition of

nanocomposites. Thermal analysis results indicate the formation of self-assembled homogeneous nanocomposites as the results of chemical and physical interfacial interactions of various reactive functional groups and fragments. All thermal data have been tabulated in Table 4.1 for comparison.
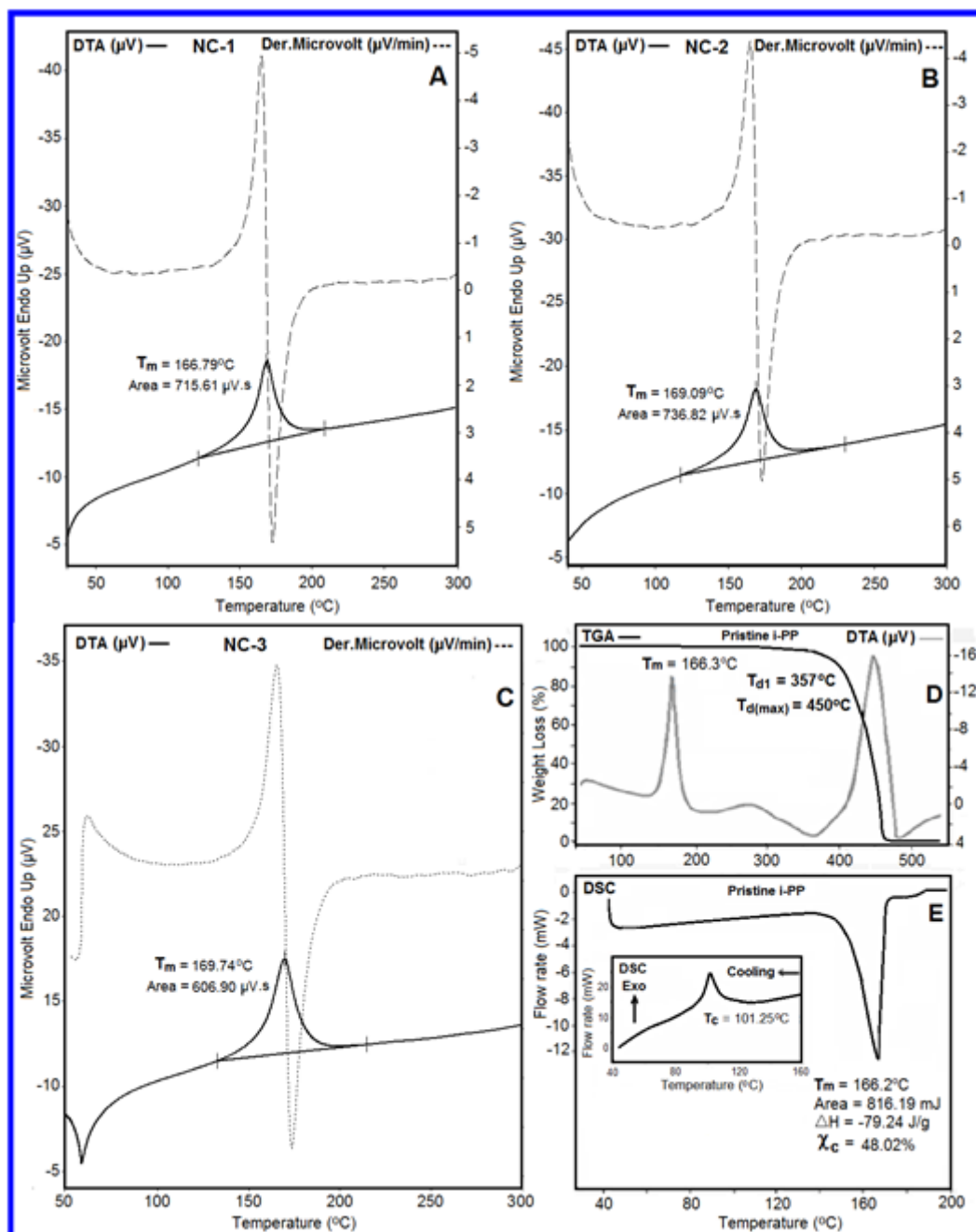
Figure 4.9. Thermal analysis results: DTA curves and melting values of NC-1 (A), NC-2 (B) and NC-3 (C); TGA-DTA curves (D) and DSC melting and recrystallization curves (E) for pristine i-PP. Heating/cooling rate of 10 °C/min under nitrogen flow.
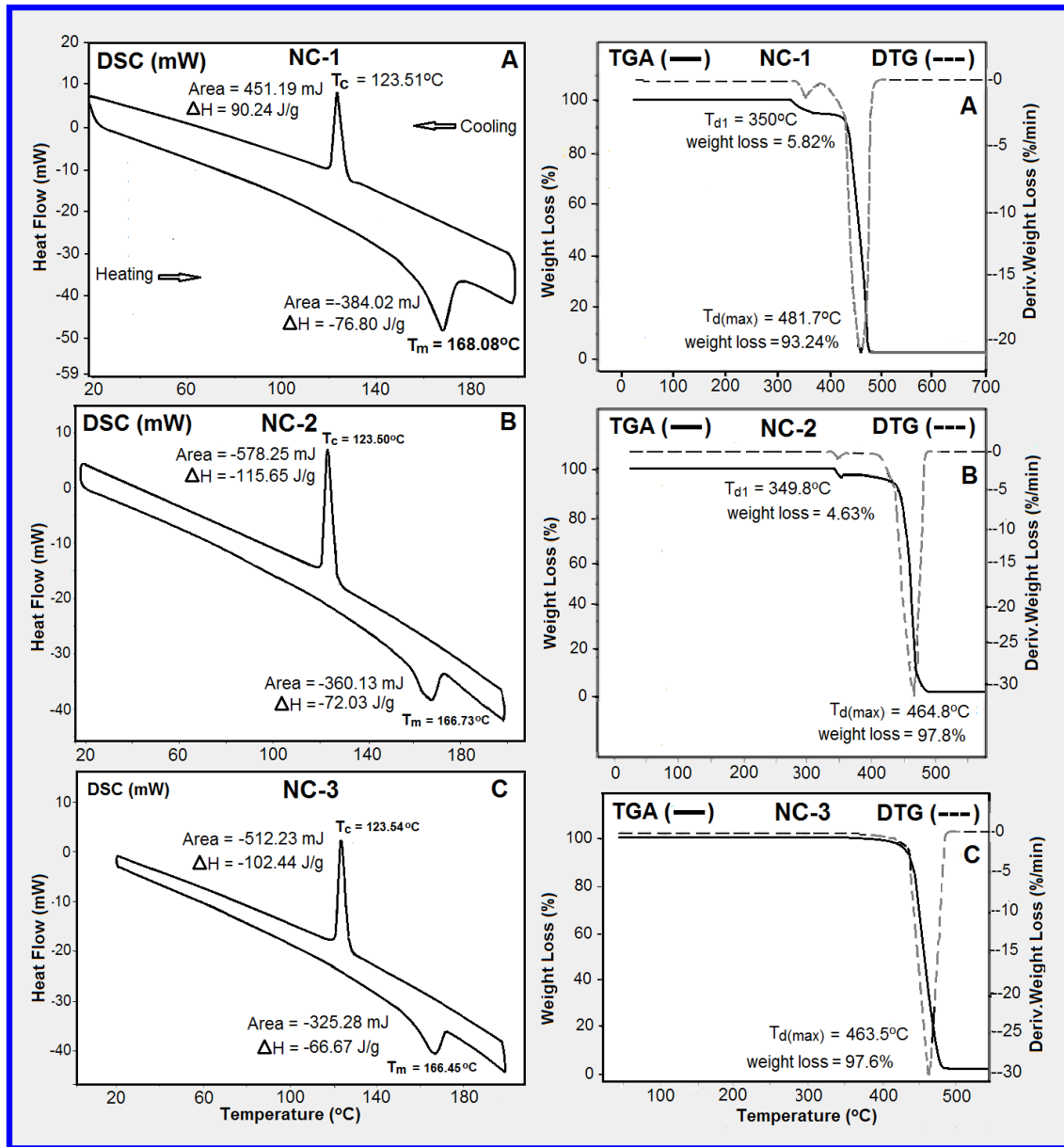
Figure 4.10. The DSC curves of melting (heating) and recrystallization (cooling) processing and TGA-DTG curves and thermal degradation parameters of NC-1 (A), NC-2 (B) and NC-3 (C) nanocomposites. Heating/cooling rate of 10 °C/min under nitrogen atmosphere.

Table 4.1. Thermal properties of i-PP and NC-1, NC-2, and NC-3.

	T_m (^{o}C)	T_c (^{o}C)	Crystallinity % (χ_c)	ΔH (J/g)	T_{dmax} (^{o}C)
i-PP	166.3	101.25	48.02	-79.24	450
NC-1	166.8	123.51	45.82	-76.80	481.7
NC-2	169.1	123.50	50.91	-72.03	464.8
NC-3	169.4	123.54	45.73	-66.67	463.5

4.2.5. Mechanical and Rheological Properties of Polypropylene Nanocomposites

Shear thinning non-Newtonian fluids of thermoplastics are the most common kind of non-Newtonian fluids and are characterized by a decreasing apparent viscosity in melt state with increasing shear rate [84-86]. This kind of non-Newtonian fluid with shear thinning Carreau model [87] is widely used in polymer fabricated industry, especially in polyolefin (PP, PE, various copolymers of α-olefins and elastomers and rubbers) production technology. The thermoplastic polymer composites including a PP/fiber composite, isotropic orientation state initially, shows a viscosity overshoot when sheared via a rheometer parallel plate in the melted phase [88]. Carreau et al. [89] have investigated the linear and nonlinear viscoelastic properties of immiscible polymer blends polypropylene/ethylene vinyl acetate–ethylene methyl acrylate [PP / (EVA–EMA)]. According to the authors, the transient shear flow experiments shows the morphology changes of the blends during the flow. They observed the dispersed phase is deformable during stress growth processing.

The shear stress/viscosity versus shear rate relationships of silicate layered and encapsulated copolymer-*g*-silica NPs incorporated with PP/polyester/biopolymer based nanocomposites were investigated by Dynamic Rotary Rheometer analysis method. The obtained results are given in Figure 4.11 and Figure 4.12.
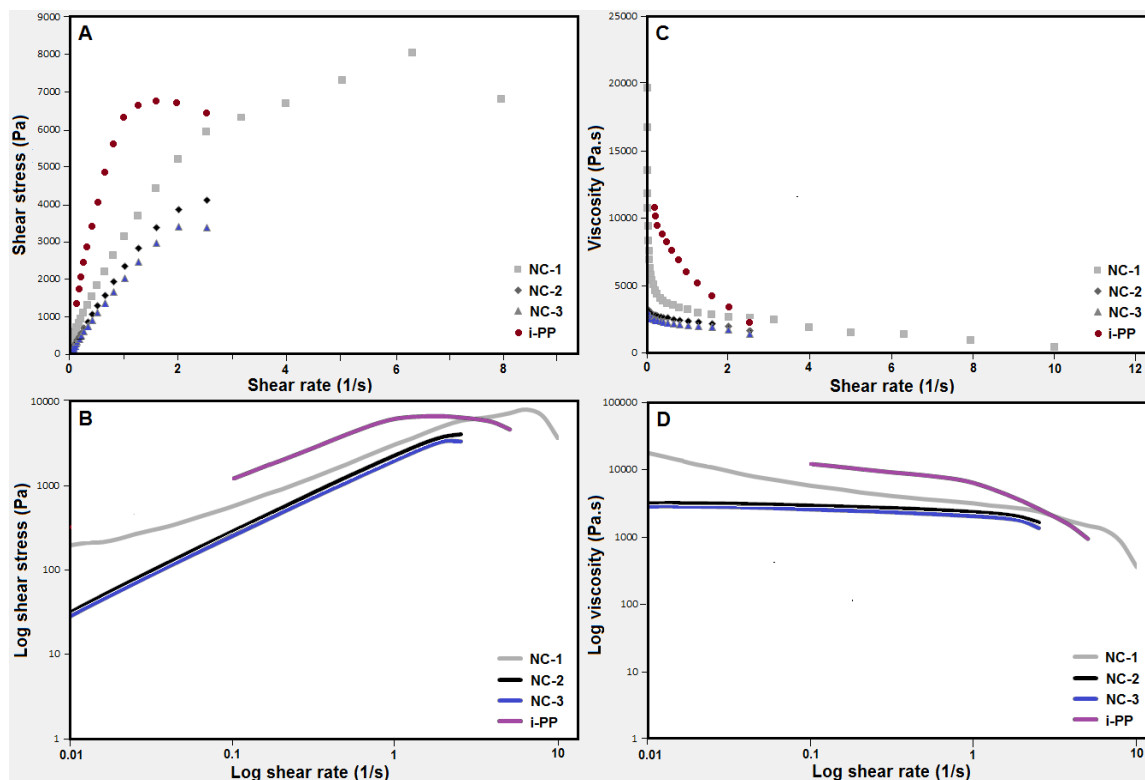
Figure 4.11. The flow curves for the correlation of shear stress /log shear stress vs shear/log shear rate (A and B) and viscosity/log viscosity vs shear/log shear rate curves (C and D) for NC-1, NC-2, and NC -3 nanocomposites, and pristine i-PP.

Figure 4.11 shows that the viscosity distribution is normal with respect to the applied forces in NC-3 containing PCL, amorphous colloidal copolymer-g-silica and DMDA-MMT non-reactive organoclay. A sharp decrease in viscosity has been estimated at a certain force (shear rate). This is due to slipping of layers or new material property due to the physical nanostructural changes during the extrusion process via formation of novel thermodynamically stable polymer nanostructures. These results are in reasonable agreement with SEM-TEM morphology and XRD reflection parameters (Figure 4.7 and Figure 4.8). Homogeneity of mixing of ingredients may not be good enough to show well distribution on shear stress and viscosity values of NC-2 containing PLA and reactive ODA-MMT (Figure 4.11 NC-1). A softening or sharp decrease in viscosity has been discovered at a certain shear rate due to lower fraction of octadecyl amine covalence bonding with maleic anhydride copolymer and/or PP-g-MA during reactive extrusion. The rheology of NC-2 composite containing PLA and DMDA gives a well distribution in values of shear stress and viscosity. The mechanical properties are in accordance with that of Carreau model [87]. The observed values of shear stress and shear viscosity significantly depend on the used

chemically and physically incorporated silicate layers and silica micro- and nanoparticles in the polymer matrix, as well as the functional copolymers as surfactant-compatibilizers, which essentially improved the rheological behavior of nanocomposites in the melt state. The shear stress values and the viscosity values of NCs are lower with regard to the values of pristine PP matrix polymer. This phenomenon is a consequence of the effect of nanomaterials on the mechanical properties of the polymers (for example: modified polyester fibers [89]). It was proposed that the silicate layers and silica micro- and nanoparticles can significantly decrease the viscosity, and consequently the molecular mobility of the shell macromolecules will also decrease since they cover these inorganic particles. For this reason, these polymer nanocomposites are less responsive to heating and sensitive to stress only at higher temperature. All NCs (NC-1, NC-2, and NC-3) were fabricated with copolymer-g-SiO$_2$ NPs. The viscosity of nanocomposites is defined as a fluid resistance to flow under an applied shear stress. Shear stress (τ) is tangential force (F) per unit area (A): $\tau = F/A$. The flow behavior is the correlation between shear-stress and shear-rate [87]. In general, the viscosity of a molten polymer composite increases with decreasing temperature and vice versa. At high temperature (165-170 ^{o}C) condition, the in situ interfacial interactions decrease due to decreasing mobility of macromolecular chains which are chemically and physically incorporated with micro- and nanoparticles. It is proposed that colloidal copolymer-g-SiO$_2$ NPs, as an effective compatibilizer and reactive reinforcement, essentially improve the mechanical and rheological parameters of the fabricated NCs.

To verify the effect of molecular weights (Mw) and origin of polyesters on the shear stress and viscosity properties, the same mass percentage of each component and process conditions were kept constant in all composites NCs (NC-4, 5, 6 and 7; i-PP 80 %, PP-g-MA 8.5 %, PLA (or PCL) 6.5 % and DMDA-MMT 5 %). Obtained results are given in Figure 4.12. The polymer nanocomposite blends contained bioengineering polyesters with different (Mw) s: PLA (Mw = 200 x 10^3, 360 x 10^3 and 700 x 10^3 Da for NC-4, NC-5 and NC-6, respectively) and PCL (Mw = 125 x 10^3 Da for NC-7).
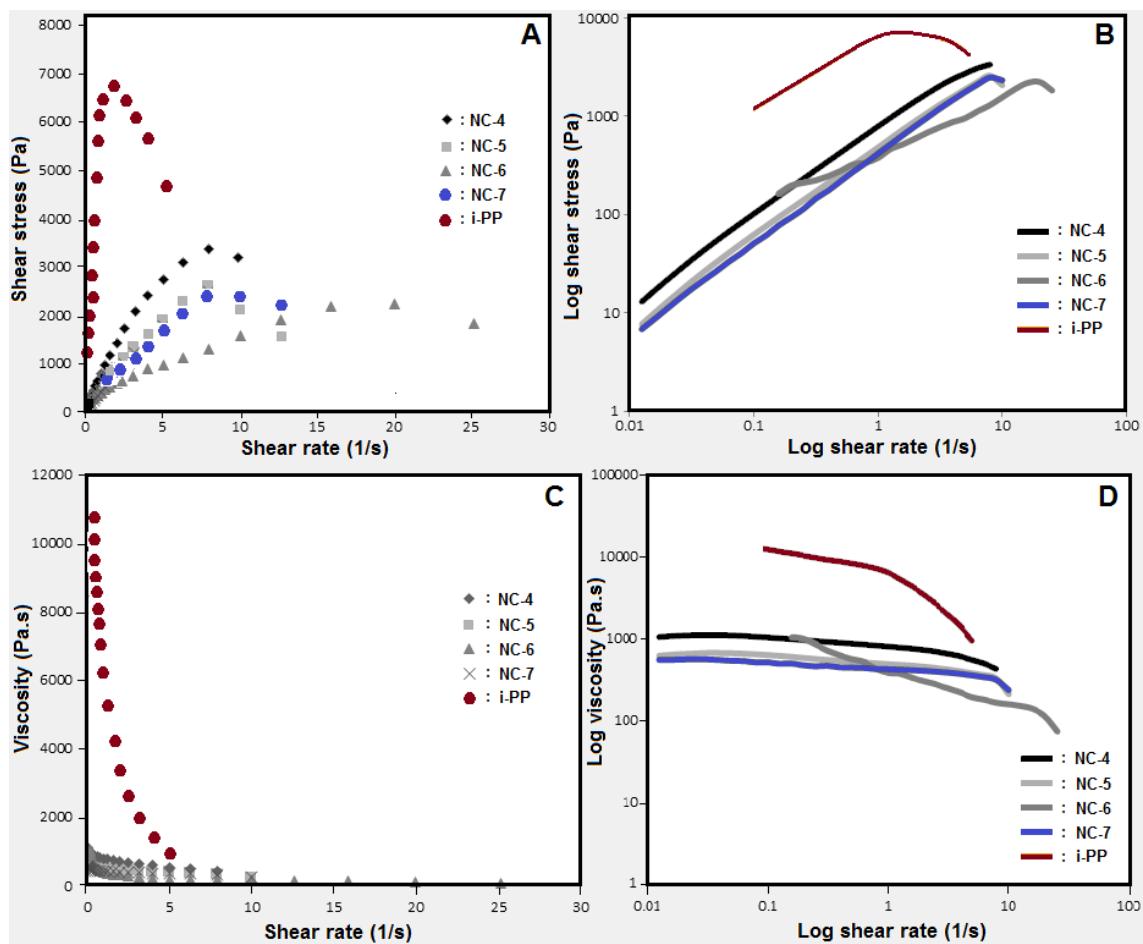
Figure 4.12. The shear stress and viscosity behaviors of pristine i-PP and its multifunctional nanocomposites. Effect of origin and molecular weight of polyesters (PLA-200 x10^3-NC-4, PLA-360 x10^3-NC-5, PLA-700 x10^3- NC-6 and PCL-125 x10^3-NC-7). Composition of NCs: i-PP-80, PP-g-MA-8.5, PLA (or PCL)-6.5 and DMDA-MMT-5.0 %.

NC-4 with PLA-200 (Mw = 200 x10^3 Da) shows good compatibility and shear rate and viscosity of the matrix structure which quite well fits the Carreau model. Matrix structure of NC-5 with PLA-360x10^3 Da seems to be in stable form, and mechanical and rheological testing results are in accordance with the expected model fitting. These results also indicated that structure of NC-5 has good compatibility due to occurrence of effective interactions between functional components. However, NC-6 structure with relatively higher Mw of PLA (700 x 10^3 Da) shows high viscosity in parallel plates during the experiment due to lower compatibility of polymer blends in this system. The curves from the plots of the shear rate versus viscosity/stress confirmed that NC-6 does not fit the above mentioned model. Unlike PLA contained NCs, nanocomposite with PCL-125 (NC-7) exhibits relatively low viscosity together with no familiar behavior. Both the shear stress and viscosity properties well fit the Carreau model.

Comparative analysis of the mechanical and rheological parameters of these NCs and pristine i-PP shows a significant decrease on shear and viscosity data of NCs compared with those of i-PP. The trends for shear stress and viscosity strongly depend on the molecular weight of PLA and essentially decrease with increasing Mw. It is well known that increasing in M_w of PLA decreases crystallinity [90], and therefore, increases the flexibility of polymer chains. It was proposed that in the multi-functional self-assembled nanocomposite systems, unlike the individual polymers, an increase in M_w and flexibility can accelerate interfacial interactions through chemical and physical incorporations between various reactive functional groups such as polymer-polymer and polymer-inorganic interfacial interactions. All of these structural factors strongly increase the fluid resistance of the nanocomposite to flow under an applied shear stress. Another PCL polyester with relatively lower M_w (125 x 10^3 Da) compared with PLA (M_w = 200/360 x 10^3 Da) shows the same effect (Figure 4.12 NC-7).

4.3. Investigation of EPDM Structures

4.3.1. Characterization of Raw Materials Used in Extrusion Processing of EPDM

Masterbatches have been prepared both to produce EPDM and polypropylene nanocomposites. Here, polyesters PLA/ODA&DMDA-MMT and PCL-DMDA-MMT have been produced to get better dispersion in main polymer/rubber matrix. In order to understand the interactions deeply, some characterization results of these masterbatches mentioned in polypropylene section, referring to XRD and SEM patterns of PLA-ODA-MMT in polypropylene have been compared to show scattering difference between ODA-MMT and PLA/ODA-MMT mixture and also reactive ODA-MMT and non-reactive, but physically active filler attractions DMDA-MMT with PLA in mixtures have been compared (Figure 4.13 and Figure 4.14). Here, the results of FTIR with estimation of characteristic bands, XRD patterns, X-ray reflection parameters, and SEM morphology analyses for only the PLA-700/ODA-MMT (3.5 %) nanocomposite masterbatch fabricated in melt by extrusion are given in Figure 4.13. Combined data (FTIR, XRD, and SEM) of masterbatch that will be used with EPDM will help to understand nanostructure interactions inside EPDM matrix.
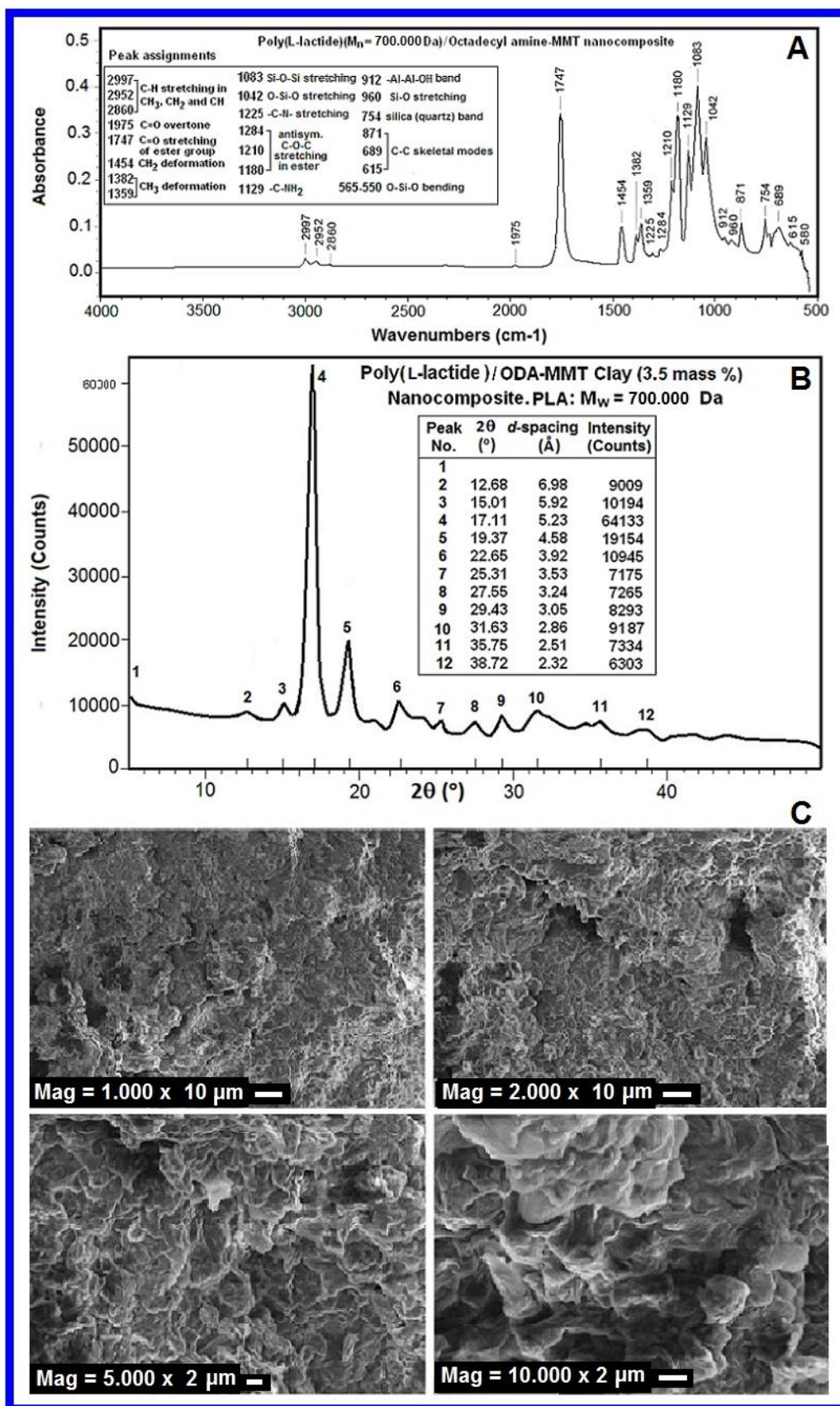
Figure 4.13. (A) FTIR spectra with estimation of absorption bands, (B) XRD patterns with X-ray reflection parameters, and (C) SEM images of PLA-700/ODA-MMT (NC-15, 3.5 mass %) nanocomposite masterbath fabricated in melt by extrusion.

The main absorption bands at around 2997-2860 cm^{-1} (C-H, CH$_2$ and CH$_3$ stretching) and their bending around 1454-1359 cm^{-1}, C=O at 1747 cm^{-1} and C-O-C ester groups at 1284 cm^{-1} as well as 1083 cm^{-1} (Si-O-Si) and 1012 cm^{-1} (Si-O) bands observed in FTIR spectra confirmed the chemical structure of PLA/ODA-MMT nanocomposite masterbatch (Figure 4.13A). Physical structure of this nanocomposite with good intercalated/exfoliated nanostructures (disappearance of characteristic X-ray reflections from reactive organoclays (ODA-MMT), at the region 5-10° 2θ was confirmed by XRD patterns and X-ray reflection parameters (Figure 4.13B) and finely dispersed surface morphology of nanocomposite by SEM at various magnifications (Figure 4.13 C).

X-ray reflection parameters

#	2θ (°)	d (A)	BG (cts)	Height (cts)	Area (cts.*°2θ)	FWHM (°2θ)	Crystallite (nm)
1	13.90	6.36	255	822	30762	0.636	0.217
2	16.71	5.29	389	546	19039	0.595	0.395
3	18.40	4.81	477	448	14454	0.564	0.246
4	21.28	4.17	518	1068	54522	0.448	0.160
5	23.63	3.76	287	104	2954	0.484	0.093
6	24.89	3.57	235	102	2412	0.400	0.351
7	28.11	3.17	210	94	2730	0.492	0.287
8	33.52	2.66	163	43	810	0.319	0.448
9	36.86	2.49	174	55	858	0.251	0.578
10	39.94	2.25	189	60	621	0.210	0.696
11	42.44	2.12	235	136	6434	0.807	0.182
12	48.10	1.89	126	39	273	0.119	1.209

d = 22.19 Å   ODA-MMT (1)
d = 32.11 Å   EPDM/ODA-MMT (2)
d = 32.78 Å   EPDM NC-8 (3)

Figure 4.14. (A) XRD patterns and reflection parameters of PP-g-MA, (B) XRD patterns from 1-ODA-MMT clay, 2-EPDM/ODA-MMT [61] and 3-nanocomposite NC-8 (Table 3.6).

The results of XRD analysis and X-ray reflection parameters of PP-*g*-MA compatibilizer, reactive organoclay (ODA-MMT) and EPDM/ODA-MMT nanocomposite (NC-8), as well

as the thermal behavior (TGA-DTG) of EPDM/ODA-MMT intercalated nanocomposite are given in Figure 4.14. Nanoparticle sizes from X-ray reflection crystal peaks of PP-g-MA graft copolymer were observed around 0.160-1.209 nm (Figure 4.14A) with 0.217 nm (1), 0.246 nm (3), 0.395 nm (2) for propylene units, and 0.160 nm (4) for grafted MA linkage. X-ray reflection peaks in the intercalated region of MMT, EPDM/ODA-MMT (Figure 4.14B-2), EPDM based NC-8 (Figure 4.14B-3) and ODA-MMT (Figure 4.14B-1) were exhibited at various 2θ angles with d-spacing 32.11 Å (EPDM/ODA-MMT), 32.78 Å (EPDM based NC-8). As seen from above comparative analyses, EPDM/ODA-MMT and EPDM based nanocomposites show relatively higher degree of intercalating/exfoliating nanostructures.

4.3.2. Chemical and Physical Structures of EPDM Based Nanocomposites, NC-8 and NC-9

FTIR spectra of EPDM elastomer based NC-8 and NC-9 (Figure 4.15 A and B) show the following characteristic absorption bands. There are weak peaks around 3735-3566 cm^{-1} associated with the stretching O-H group 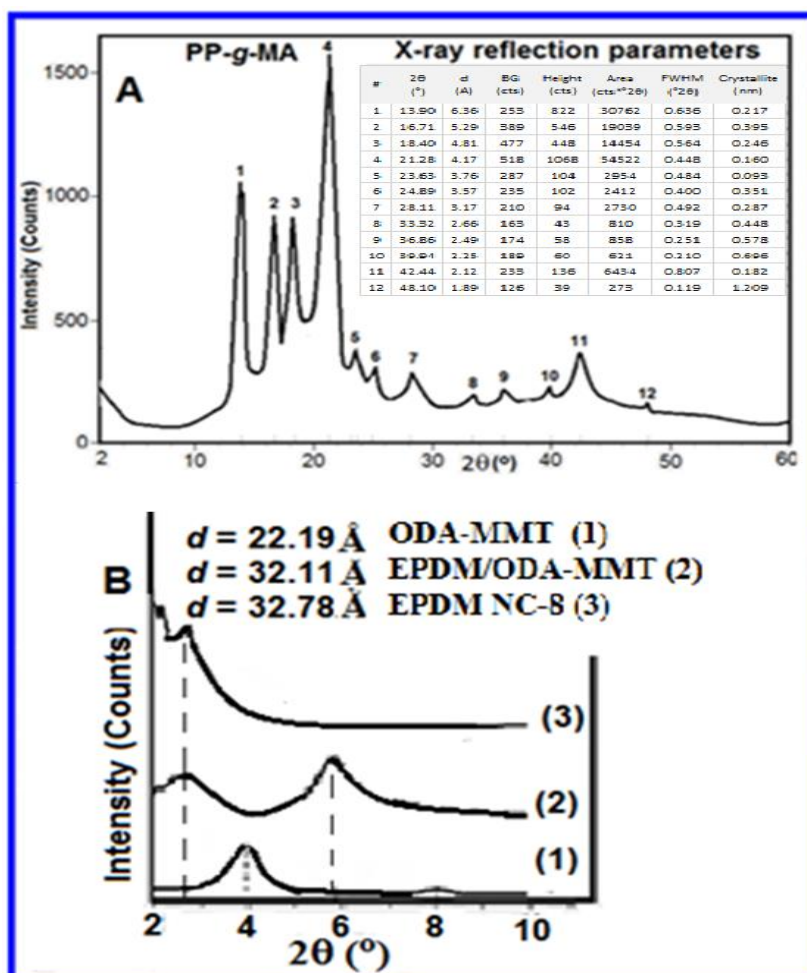from water in MMT and Si-OH of silica NPs. Peaks appear at 2918.44 (s), 2948.97 (s) and 2725.7 (w) cm^{-1} from valence vibrations of C–H bands in CH$_2$, CH$_3$ and CH groups of EPDM and PLA chains, and propylene unit of PP-*co*-MA graft oligomer. The C=O stretching bands come from ester group of PLA, -COOH. MA/maleamide units are detected at 1731.48 (w), 1681.18 (w), and 1646.43 cm^{-1}, respectively. Absorption bands at 1454.92 (s) and 1375.29 (s) cm^{-1} are associated with bending vibrations from CH$_2$ and CH$_3$ groups of EPDM chain. CH and CH$_3$ bending bands from PLA chain appear at 1507.35 (w) and 1296.22 (w) cm^{-1}, respectively. The C-O-C valence vibrations were found at 1087.78 cm^{-1}. The weak C-N-C band at 1167 cm^{-1} can be related to imidized maleamide unit from copolymer-g-silica during reactive extrusion process. Similar reaction of poly (MA-co-styrene) copolymer with ammonia in reactive extrusion conditions, which is confirmed by FTIR analysis was also reported by Vermeech et al. [68]. The absorption bands at 1100.95 (m) and 1044.61 (w) cm^{-1} are associated with Si-O and Si-O-Si stretching from silica nanoparticles and silicate sheets from copolymer-g-SiO$_2$ and organoclay. The propylene unit from EPDM chain is confirmed by a band at 972.96 (m) cm^{-1}. Absorption bands at 718.63 (s) and 520.18 (s) cm^{-1} can be attributed to (-CH2-)$_n$ bending and rocking vibrations from ethylene units of EPDM, dodecyl group of copolymer and octadecyl group of ODA-MMT clay.

Similar absorption bands were also seen in the nanocomposites NC-9 spectra (Figure 4.15 B). The composition of NC-9 includes DMDA/MMT non-reactive nanofiller and biodegradable PCL unlike the composition of NC-8. Appearance of strong absorption peaks at 718.85 and 520.23 cm^{-1} in the spectra of NC-9 are associated with rocking vibration of CH$_2$ in -(CH2)$_n$- groups from octadecyl and dodecyl fragments of copolymer and DMDA-MMT or nanoclays, as well as from -(CH$_2$)$_5$- backbone chain of PCL.
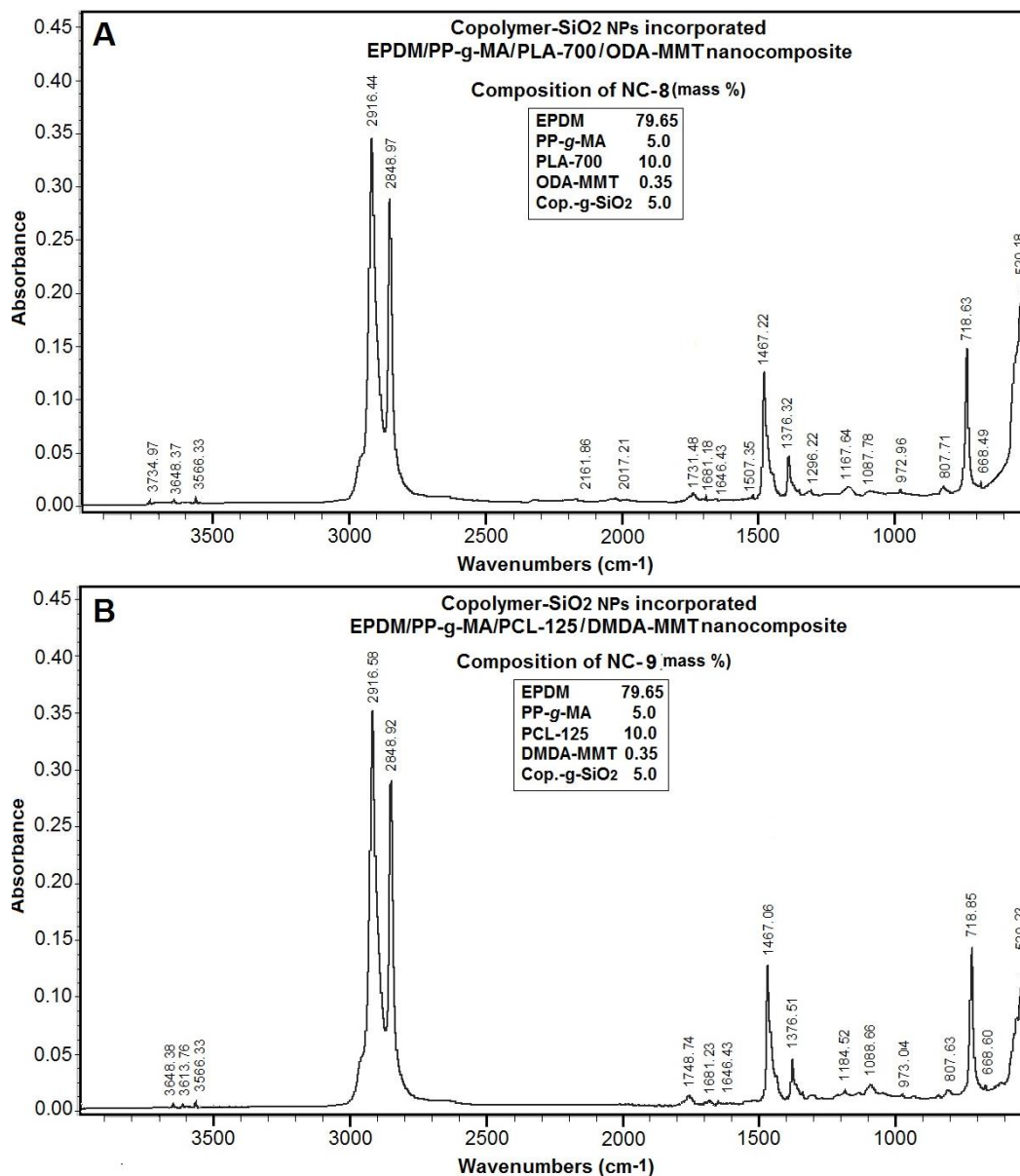
Figure 4.15. FTIR spectra of NC-8 (A) and NC-9 (B).

4.3.3. XRD results of EPDM Nanocomposites, NC-8 and NC-9

Physical structure and crystallite size of nanocomposites were investigated by XRD analysis. The obtained XRD patterns and X-ray reflection parameters are given in Figure 4.16. The particle sizes of crystals from reflected peaks were calculated using a High Score Plus Program (PANanalytical, XRD device software). EPDM that contain PP content is expected to contain also three different crystalline structures such as α-monoclinic, β-hexagonal, and γ-orthombic forms. The α-monoclinic is the most common structure to be seen and well-established crystalline morphology for i-PP and PE [69]. Here, the same reflections were detected from polyolefin fraction of nanocomposite (Figure 4.16 A). The nanoparticle sizes were observed at 14.67, 16.68, and 23.72 $^\circ$ 2θ with 110 (α), 040 (α), and 060 (α) planes, respectively.
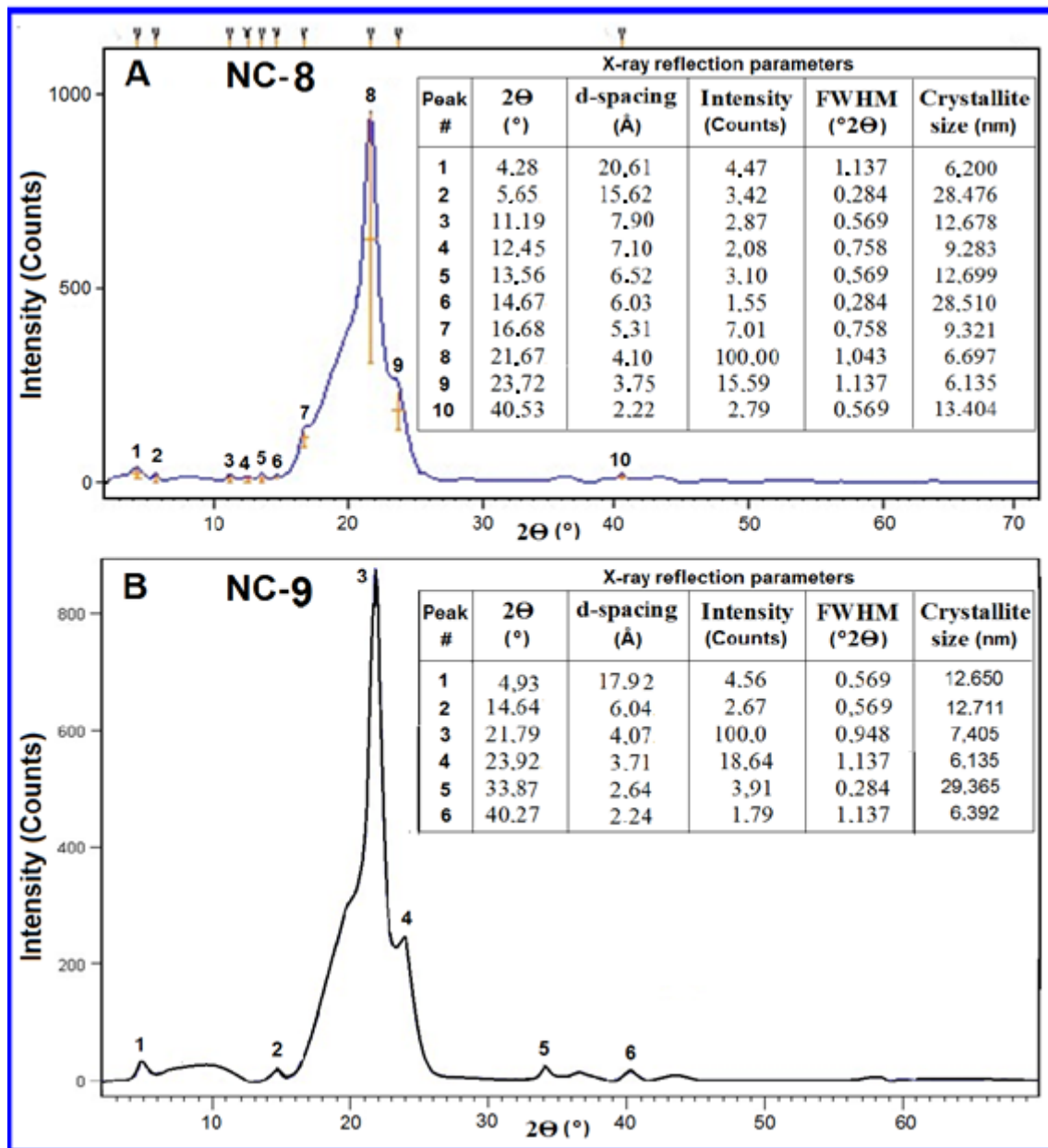
Figure 4.16. XRD patterns and reflection data of (A) NC-8 and (B) NC-9.

X-ray diffraction pattern of polyethylene (PE) linkage with Bragg angle (2θ) function is shown in Figure 4.16. The pure polyethylene shows three diffraction peaks at 2θ values of 21.67 (d = 4.10 Å for NC-8), 21.79 (4.07 Å), and 36.5 (2.46 Å for NC-9) corresponding to the (110) and (200) α plane reflections, respectively. The typical orthorhombic structure of the PE crystal reflection (NC-8) at 16.68.° 2θ is associated with PLA crystallinity (9.32.nm). Agreeing with the reflection parameters of the layered silicate and silica regions at 2-10° 2θ, NC-8 contained broad amorphous area at 9.6° 2θ, which can be attributed to colloidal SiO_2

NPs covalently encapsulated with poly (MA-*alt*-1-dodecene) copolymer via amidation of anhydride unit with γ-aminopropyl-SiO$_2$.

The XRD patterns of NC-9 are given in Figure 4.16 B. It was observed that both nanocomposites show similar reflections, however NC-9 has only different crystallite sizes due to predominantly hydrogen bonding in situ interfacial interactions in these systems prepared with DMDA-MMT. It was proposed that a combination of chemically and physically (predominantly hydrogen bonding) active sites from free –COOH, C=O, amide/amine, ester and ether groups play a significant role during forming of nanocomposites via controlled in situ interfacial interactions during extrusion process.

4.3.4. SEM-TEM Morphology of EPDM Structures

Comparative analysis of SEM morphology of PCL-125/DMDA, NC-14 with 3.5 mass % (Figure 4.17 A and B) and PLA-700/DMDA, NC-13, 3.5 mass % (Figure 4.17 C and D) masterbatch nanocomposites showed better dispersed morphological structures of nanocomposites consisting non-reactive organoclays (DMDA-MMT) and PLA-700 as a matrix polymer compared with PCL-125/DMDA. This can be attributed to excellent compatibility of high molecular mass of PLA matrix polymer via formation of complexing structure of PLA**...**DMDA-MMT clay (–C=O / C−O ester**...**N−MMT) in the melt extrusion conditions.
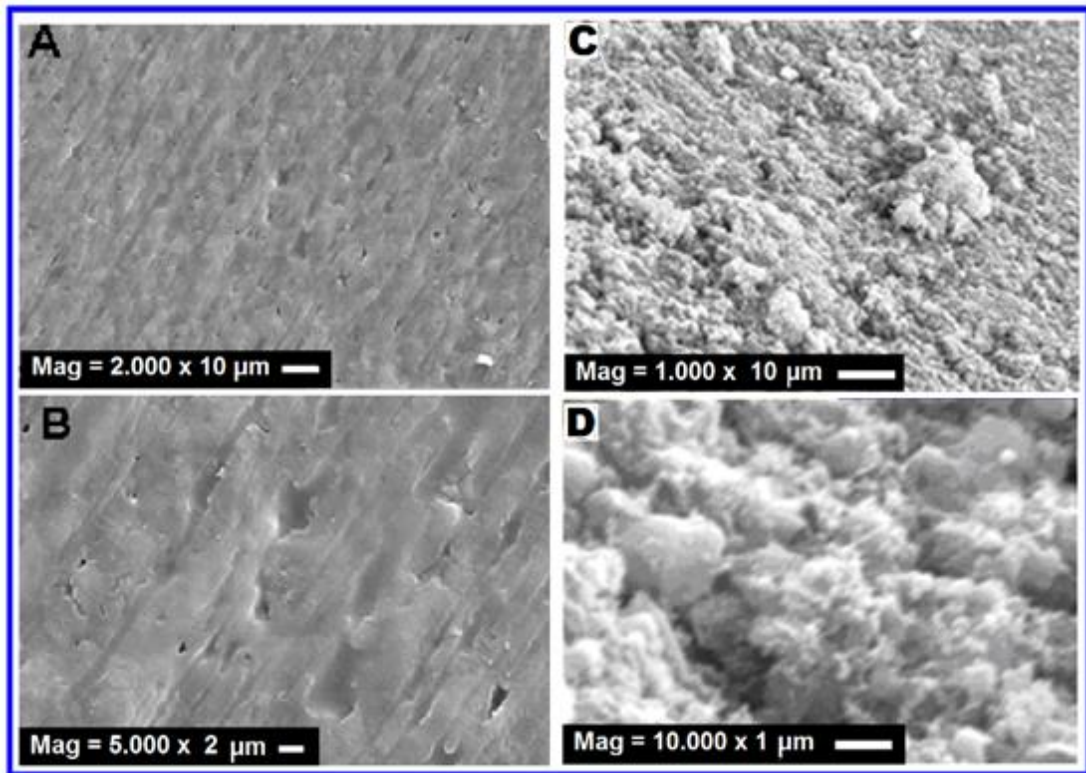
Figure 4.17. SEM images of masterbatches of NC-14 PCL-125 x 10^3 Da/DMDA (3.5 mass % ; A, B) and NC-13 PLA-700 x 10^3 Da/DMDA (3.5 mass % ; C, D).

Figure 4.18 shows fine dispersing surface morphology of EPDM based nanocomposite consisting masterbatch PLA-700/Clay (3.5 mass %) (Figure 4.18A and B) nanocomposite on different magnifications with dominantly hydrophilic complexable structure of PLA (-C=O and ester groups) chains compared with (Figure 4.18C) PCL-125/Clay (3.5 mass %) consisting hydrophobic - $(CH_2)_5$- linkage of PCL chains.
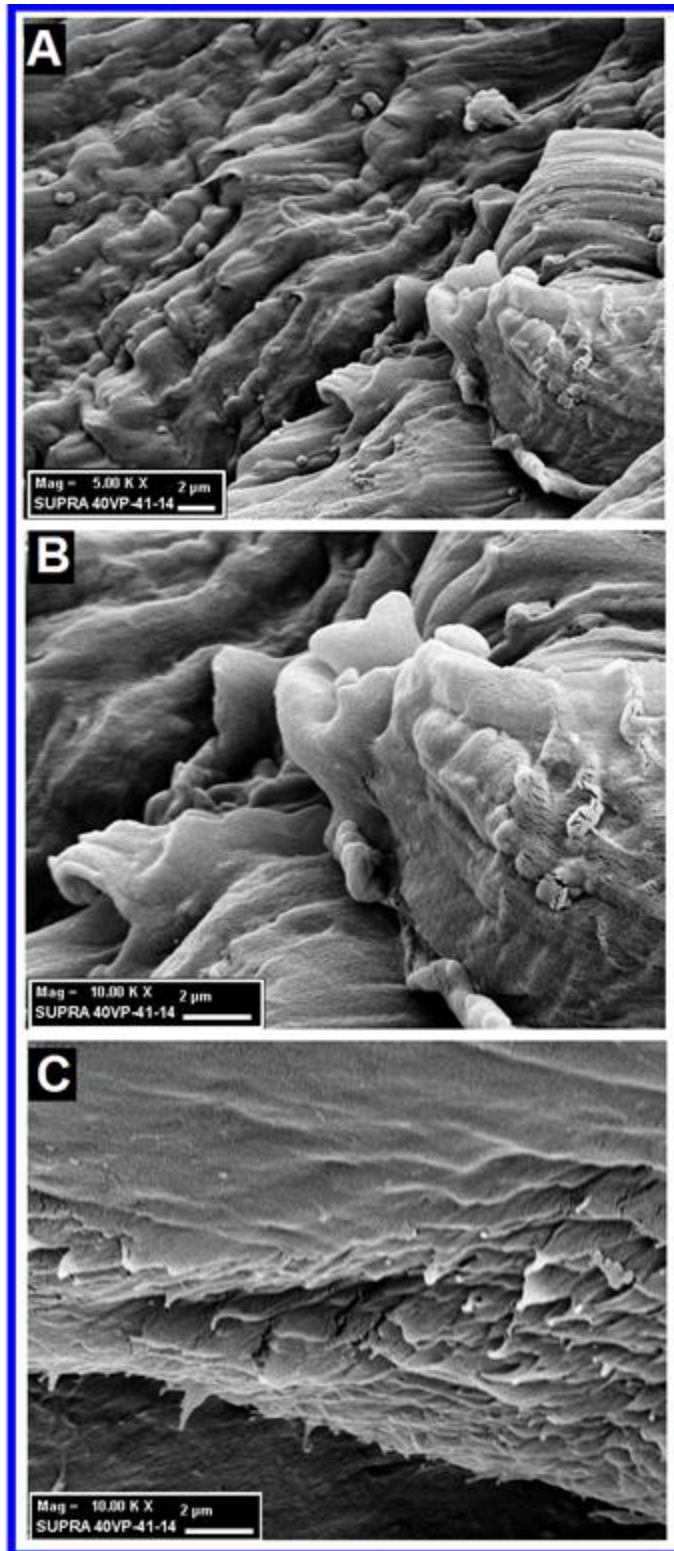
Figure 4.18. SEM images of EPDM nanocomposites with Masterbatches: PLA-700/Clay (3.5 mass %) (A, B) and with PCL-125/Clay (3.5 mass %) (C).

TEM internal morphologies of nanocomposite NC-9 are given in Figure 4.19 at different magnifications for both intercalating/ exfoliating structures and for partially agglomerated MMT layered structures. The morphology images of EPDM based nanocomposites at 10 and 20 nm magnifications show finely dispersed layered silicate with d-spacing around 30-40 nm, and a better distribution (at 5 nm magnification) of silica nanoparticles (Figure 4.19 A images). The result obtained is reasonable agreeing with nanoparticle sizes determined by previous XRD results. Partially agglomerating layered silicate structures with SiO_2 NPs and predominantly fine dispersing silica NPs onto matrix polyolefin linkages of EPDM chains were also observed (Figure 4.19 B images).

(A)   (B)
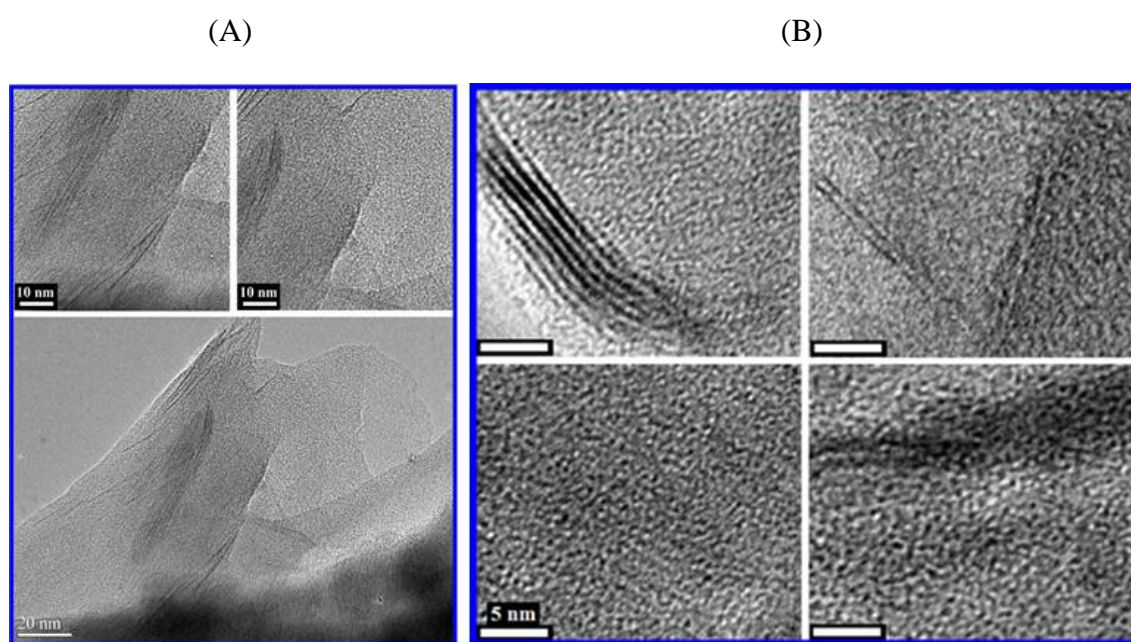
Figure 4.19. TEM images of EPDM rubber (79.65 %) / PP-g-MA (5.0 %) / PCL-125(10 %) /DMDA-MMT (0.35 %) /poly (MA-alt-1-octadecene)-g-ɤ-aminopropyltriethoxysilane-TEOS (hydrolyzed 76 % of SiO_2) (5.0 %) nanocomposite NC-9 at various magnifications. (A) intercalating/ exfoliating structures and (B) partially agglomerated MMT layered structures with SiO_2 NPs and predominantly fine dispersing silica NPs.

4.3.5. Thermal Behaviors of EPDM Based Nanostructures, NC-8 to NC-12

EPDM rubber and its compounds show excellent aging and high solvent resistance (polar chemicals and ozone) compared with PP compounds; a low temperature flexibility compared with that of natural rubber (polyisoprene) compounds; excellent electrical insulation properties; better heat resistance compared to other rubber types. In this work, it was observed that organoclay addition on EPDM rubber resulted in significantly improved

mechanical properties, thermal stability, and morphology of EPDM nanocomposites (Figure 4.20). The melt intercalating by extrusion technique provides an effective compounding of the EPDM/organoclay blends in the melt phase under shear. Under these conditions, the molten mass of EPDM chains intercalate between silicate galleries to form nanostructural composites. DSC and TGA-DTG curves of pristine EPDM, NC-8 and NC-9 are given in Figure 4.20 and Figure 4.21.
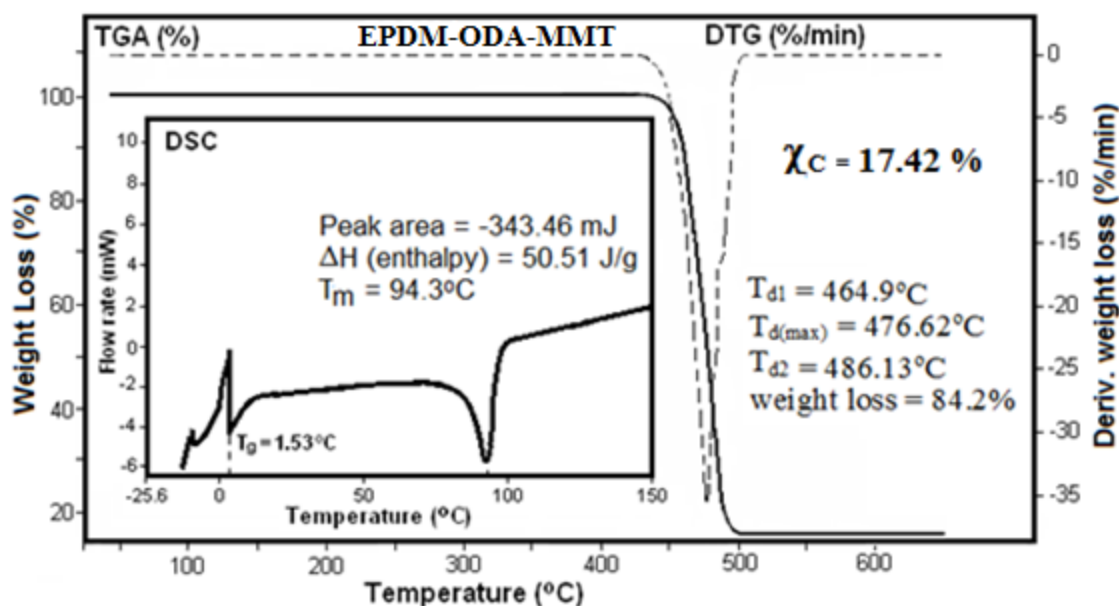
Figure 4.20. DSC and TGA-DTG curves of pristine EPDM/ODA-MMT rubber. Heating rate 10 $^{\circ}$C/min under nitrogen flow.

Agreeing with these results, intercalating structure of nanocomposite provides transfer of rubber structure to semi-crystalline form with shifted $T_g = 1.53$ $^{\circ}$C, and $T_m = 94.3$ $^{\circ}$C with enthalpy $\Delta H = -50.51$ J/g and crystallinity 17.42 %. Higher thermal stability ($T_{d\ max} = 476.62$ $^{\circ}$C) of nanocomposite can be estimated by transfer of matrix EPDM rubber macromolecules to thermoplastic structures during extrusion in-situ processing in the presence of reactive organoclay. Mousa [61] reported his work on EPDM/organoclay composite with good dispersion of organoclay. Here, similar effect was observed for the EPDM rubber/reactive organoclay NC (Figure 4.20). The result obtained shows that EPDM rubber/reactive organoclay NC exhibits semi-crystallinity ($T_g = 1.53$ $^{\circ}$C, $T_m = 94.3$ $^{\circ}$C and crystallinity = 17.42 %) and higher thermal stability ($T_{d\ max} = 476.62$ $^{\circ}$C).
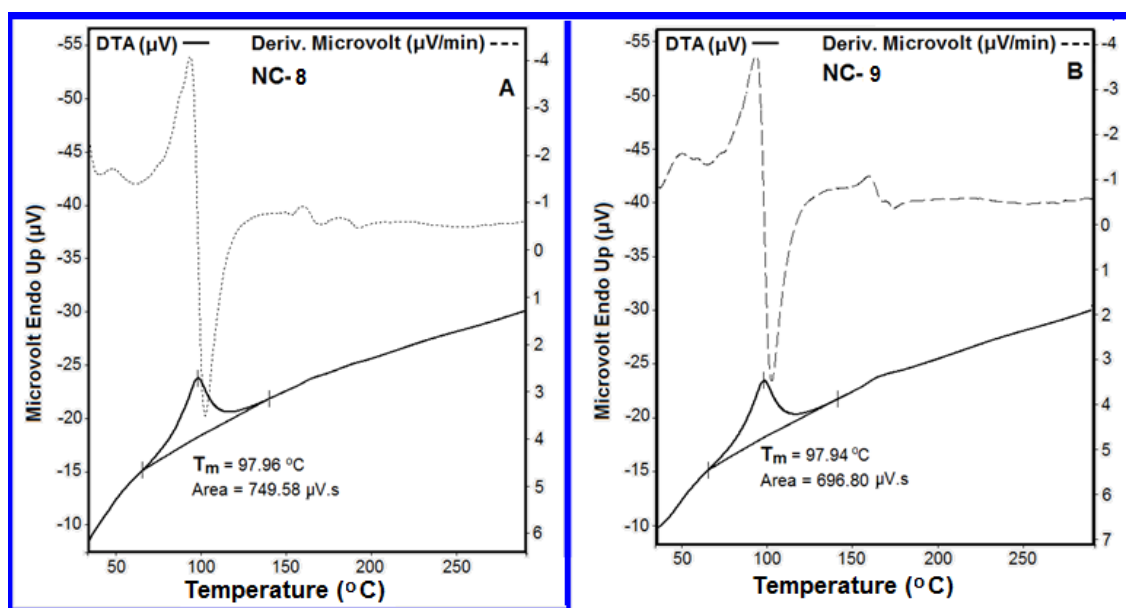
Figure 4.21. DTA curves and peak parameters of (A) NC-8 and (B) NC-9. Heating rate 10 °C/min under nitrogen flow.

The results of DTA thermal analysis of EPDM based multifunctional complexing nanocomposites consisting reactive/nonreactive but physically active organoclay (ODA/DMDA-MMT with complexable alkyl ammonium surfactant), copolymer-g-γ-aminopropyl trimethoxysilane-silica nanoparticles (NPs) used as reactive compatibilizer-nanofiller, and biodegradable polyesters such as PLA (in NC-8) and PCL (in NC-9) are given in Figure 4.21. Composition of these nanocomposites are also given in Figure 4.15. In agreement with these results, both NCs exhibited higher melt-transition values (T_m) at 97.96 °C and 97.94 °C compared with EPDM/ODA-MMT nanocomposite (Figure 4.20). Moreover, NC-8 consisting PLA shows a highly visible area (749.58 µV.s) compared to that of NC-9 consisting PCL (696.80 µV.s) due to higher complexing sites and crystallinity of PLA chains in NC-8.
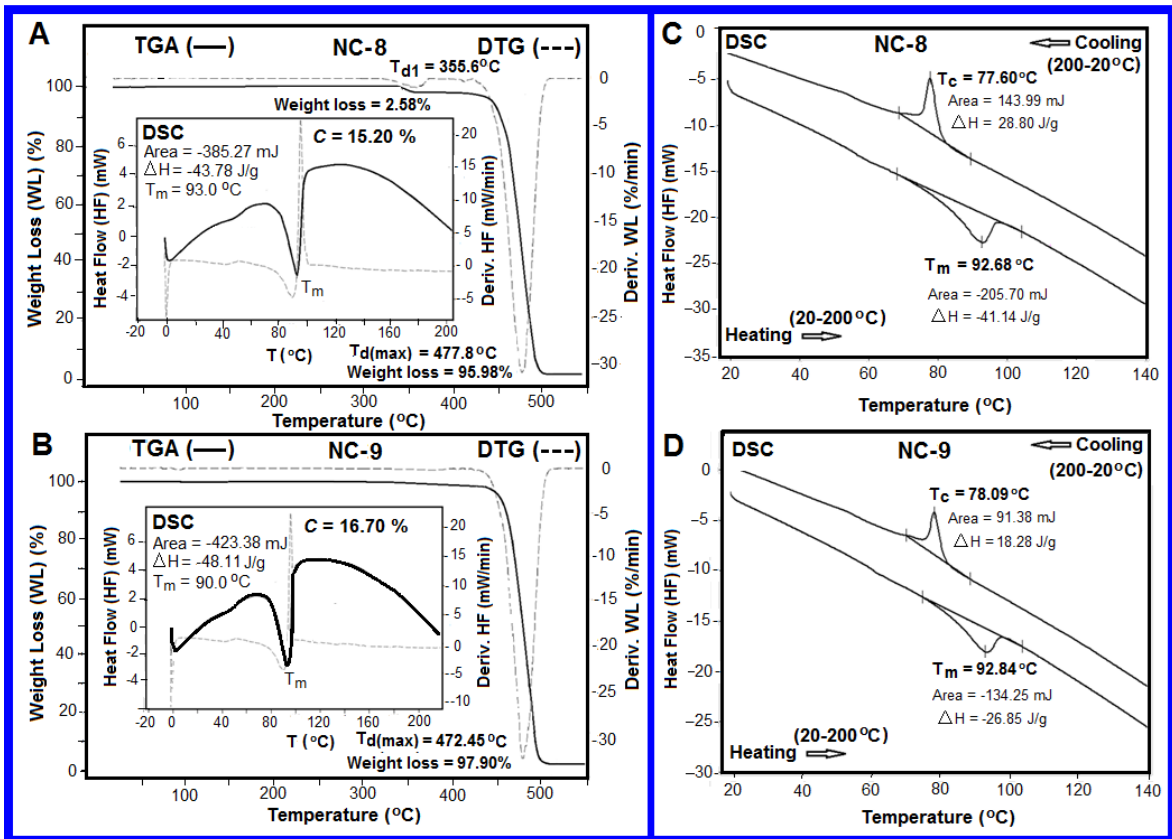
Figure 4.22. TGA-DTG (A, B) and DSC (C, D) curves of EPDM/PP-g-MA/copolymer-g-SiO$_2$ blend incorporated with PLA/ODA-MMT and PCL/DMDA-MMT nanocomposites in melt by one step extrusion.

Table 4.2. EPDM, NC-8, and NC-9 thermal properties.

	T_m (°C)	T_c (°C)	T_g (°C)	Crystallinity % (χ_c)	ΔH (J/g)	T_{dmax} (°C)
EPDM/ODA-MMT	94.3	-	1.53	17.42	-50.51	476.62
NC-8	97.96	77.60	-	15.20	-43.78	477.8
NC-9	97.94	78.09	-	16.70	-48.11	472.45

The results of thermal behaviors, crystallinity (by DSC analysis) and thermal stability of EPDM based NCs are given in Figure 4.20, 21, 22, and Figure 4.23. The melting temperature (T_m) and crystallization temperature (T_c) were determined from DSC data with heating/cooling conditions, respectively. The heat of fusion (ΔH_f) and crystallization enthalpy (ΔH_c) were calculated from the melting area under the melting and crystallization

peaks. Crystallinity of all NCs were evaluated by DSC methods using the following the well-known equation (2) through ΔH^o for 100 % crystallinity of PE copolymers. In this work, the heat of fusion of 100 % PE crystal is 288 J/g [77] used for the estimation of the fraction crystallinity in EPDM based nanocomposites.

$$\%\text{Crystallinity } (\chi_c) = \left[(\Delta H_m^{obs} - \Delta H_c^{obs}) / \Delta H_c^o \right] \times 100 \qquad (2)$$
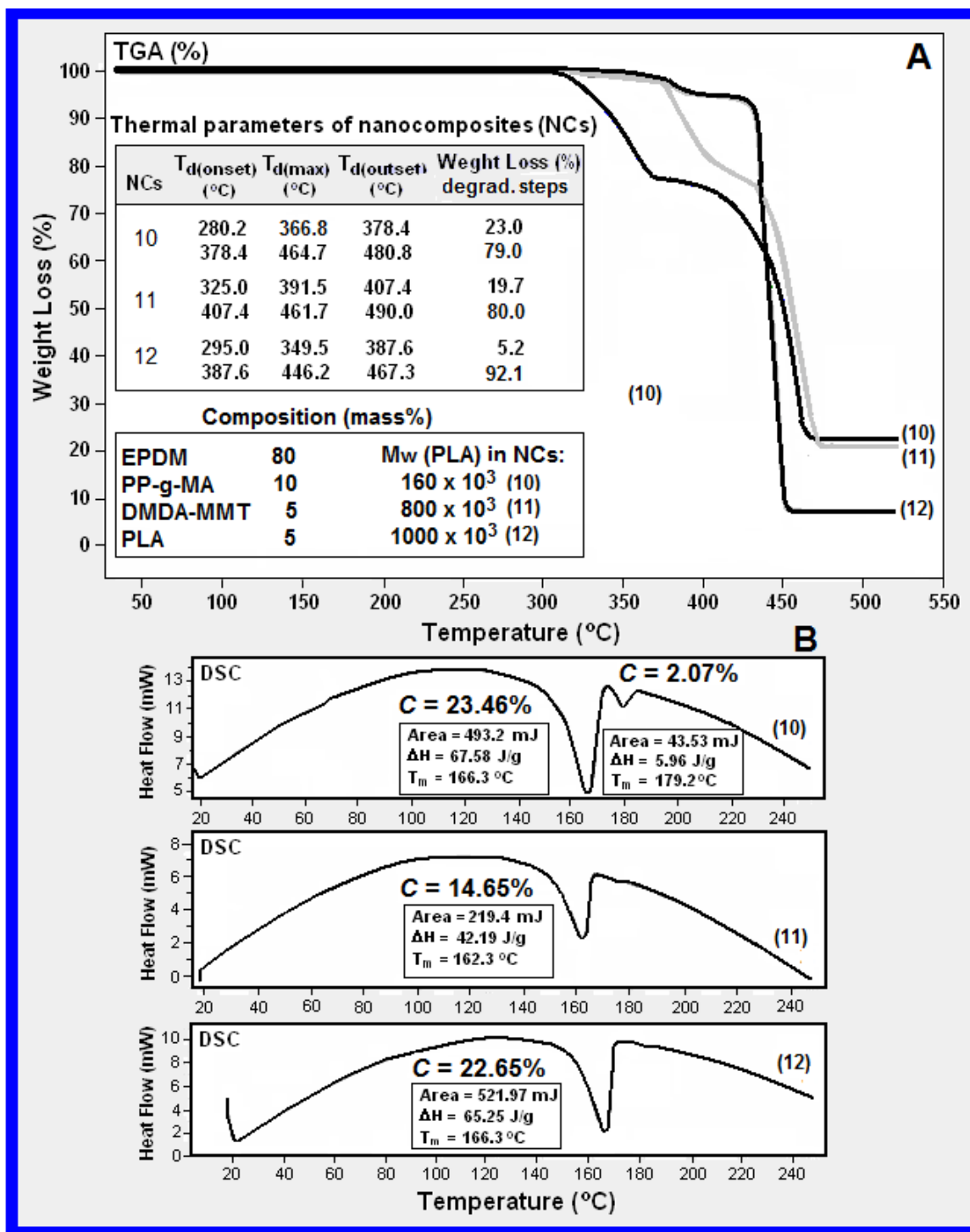
Figure 4.23. (A) TGA and (B) DSC curves of EPDM/PP-g-MA blend incorporated with PLA/DMDA (5 %) nanocomposite contained PLA with different Mw. Effect of PLA molecular mass on the thermal behaviors of NCs.

Table 4.3. Thermal properties of NC-10, NC-11, and NC-12.

	T_m (°C)	Crystallinity % (χ_c)	Area (mJ)	ΔH (J/g)	T_{dmax} (°C)
NC-10	166.3	25.53	493.2	67.58	464.7
NC-11	162.3	14.65	219.4	42.19	461.7
NC-12	166.3	22.66	521.9	65.25	446.2

We also searched the effect of molecular weights (M_w) of PLA on the thermal properties of NCs (10, 11 and 12) consisting PLAs with 160×10^3 Da (NC-10), 800×10^3 Da (NC-11) and 1000×10^3 Da (NC-12) (Figure 4.23). It was observed that all nanocomposites degraded by two-step mechanism (Figure 4.23 A). Increase of M_w visibly decreased thermal stability ($T_{d\ max}$) from 464.7 °C (NC-10) to 461.7 °C (NC-11) and 446.2 °C (NC-12), respectively, and crystallinity shows deviations from 25.53 % (NC-10) to 14.65 % (NC-11) and 22.66 % (NC-12) (Figure 4.23 B) due to the fine dispersion at an optimum value Mw around 700×10^3 Da for PLA. All values are tabulated in Table 4.3. However, multifunctional nanocomposite consisting copolymer-g-APTS-silica NPs and PLA (NC-8) (Figure 4.22 A) exhibits a relatively higher thermal stability ($T_{d\ max}$ 477.80 °C) due to the effect of reactive organo-SiO_2 NPs.

4.3.6. Mechanical and Rheological Properties, NC-8, NC-9.

The rheological characterizations, especially the shear stress/shear rate and viscosity/shear rate relationships of thermoplastic polyolefin and EPDM rubber were estimated by using Carreau model [87] and its various modified and simplified versions were the subject of many other investigations [91-94]. Shear thinning in thermoplastics and synthetic or natural rubber is the most common behavior of polymeric non-Newtonian fluids and are characterized by a decreasing apparent viscosity in melt state with increasing shear rate. For these kinds of non-Newtonian fluid with shear thinning, Carreau model [87] is widely used in polymer fabricated industry, especially in polyolefin (PP, PE, various copolymers of α-olefins, elastomers, and rubbers) production technology. Yong and Park [91] developed a highly useful analytical method to quantify the shear thinning effect (the shear thinning exponent *n*) and allows to evaluate intercalating/exfoliating degree in the polymer–clay nanocomposites. This method also helps to estimate the details of nanocomposite properties. Khosrokhavar et al. [95] reported the rheological outputs of polypropylene, EPDM, and the

respective silicate layered NCs using a stress-controlled rheometer (MCR 3000). The experiments were studied within a 25 mm parallel-plate under nitrogen inert atmosphere. The temperature was set to 180 °C and equipment was within the frequency range of 0.01-80 Hz. Authors observed the elastic modulus and complex viscosity of PP and EPDM at low frequencies. PP exhibited a Newtonian behavior, while EPDM rubber exhibited a shear thinning behavior clearly over applied range of shear rates.

In this experiment, viscosity and shear stress variations with shear rate have been analyzed using a Rotary Rheometer (model AR2000). Viscosity plots have been obtained with famous Carreau model. Zero shear rate viscosity value was determined as 1.31×10^5 (Pa.s) and 26520 (Pa.s) for NC-8 and NC-9 nanocomposites, respectively. High viscosity of NC-8 with PLA-700 is due to the more hydrophilic polar fraction ($-$O-C$=$O$-$ ester in monomer unit and trace of end $-$OH and $-$COOH groups) in nanocomposite compared with NC-9 with PCL-125 which contains more hydrophobic fragment $-(CH_2)_5-$ in the caprolactone monomer unit. Increase of polarity of NC-8 provides higher degree of chemical and physical interfacial interactions, consequently increasing the interfacial force between polymer chains and organoclay/copolymer-g-silica micro- and nanoparticles. Moreover, viscosity of NCs also strongly depends on the origin of used organoclay nanofillers. Chemically reactive organoclay (ODA-MMT) and chemically non-reactive but strongly physically active organoclay (DMDA-MMT) were used in the NC-8 and NC-9 blend composites, respectively. The same effects of origin of the polyesters and organoclay were estimated from the plots of shear stress versus shear rate and their logarithmic graphs (Figure 4.24). To evaluate the effects of the type of polyester and organoclay on the shear stress and viscosity properties, the following similar mass percentages of each component were used in both nanocomposites (NC-8 and NC-9): (EPDM 79.65 %, PP-g-MA 5 %, PLA (or PCL) 10 % and organoclays (ODA-MMT and DMDA-MMT) 5 %. In accordance with the plots of shear rate and viscosity, NC-8 nanocomposite has high viscosity of the matrix structure as a result of dominant covalent interfacial interactions and insignificantly fits the Carreau model due to these interfacial interactions. However, matrix structure of NC-9 with low viscosity seems to be in more stable form, and mechanical and rheological testing results are well in accordance with the expected model fitting. These results also indicated that structure of NC-9 has good compatibility due to occurrence of effective physical interactions between functional components.
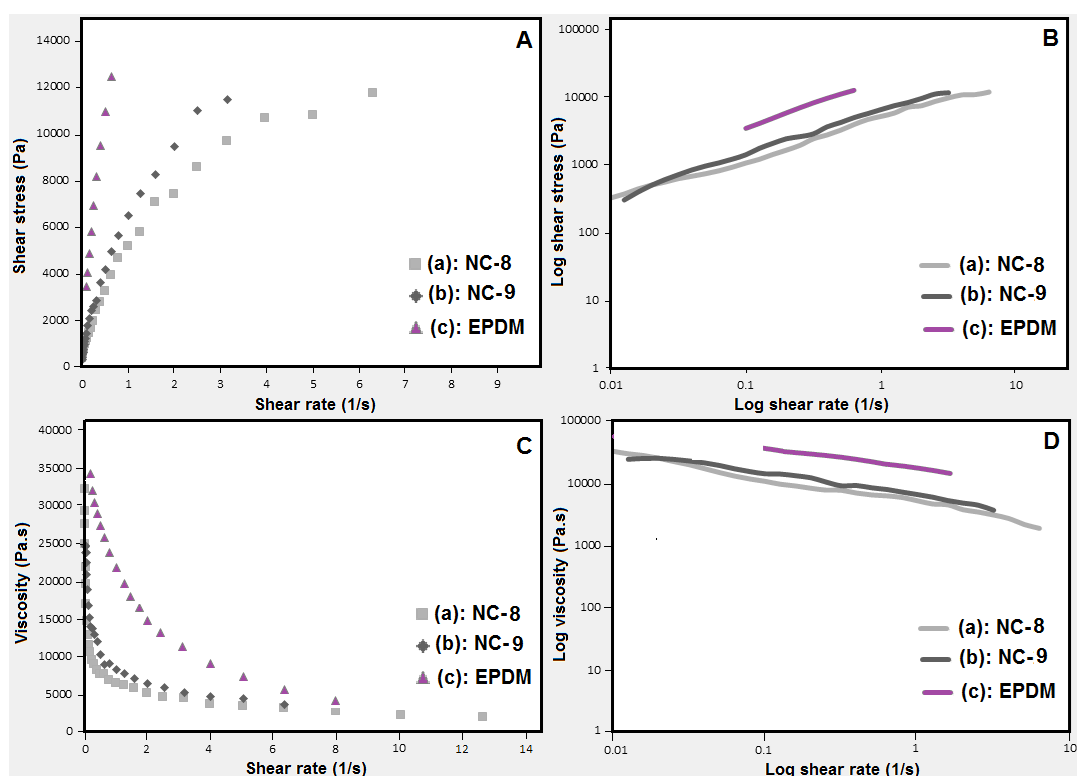
Figure 4.24. The plots of shear stress/ log shear stress vs shear/log shear rate and (A, B) and viscosity/log viscosity vs shear/log shear rate (C, D) for the nanocomposites NC-8 and NC-9, and pristine EPDM: NC-8 with PLA-700 and ODA-MMT and NC-9 with PCL-125 and DMDA-MMT.

Thus, unlike high molecular mass PLA-700 and chemically reactive ODA-MMT contained NC-8, which predominantly exhibits a Newtonian behavior, nanocomposite NC-9 with PCL-125 exhibits relatively low viscosity and non-Newtonian fluid behavior with shear thinning Carreau model. It may be concluded that the presence of highly reactive and polar components in the polymer blend composition can provide the successful transfer of elastomer matrix polymer structure (EPDM) to the same thermoplastic polyolefin nanostructures during the reactive extrusion processing. This proposal is also confirmed by estimated structural changes and important thermal transition parameters of NCs.

5. CONCLUSION

The important outputs of this dissertation can be summarized as following;

1- The chemistry for the synthetic pathway of the copolymer-*g*-silica NPs through sol-gel processing was proposed by a structural model where the following reactions and in situ interfacial interactions (i) amidation of amphiphilic poly(MA-*alt*-1-dodecene) (copolymer) with APTS, (ii) side-chain hydrolysis-condensation of copolymer-*g*-APTS with tetraethoxysilane (TEOS) precursor, and (iii) the formation of silica NPs encapsulated with copolymer chains via covalent incorporation occurred.

2- Agreeing with XRD patterns and peak reflection parameters, copolymer-g-SiO_2 nanohybrid predominantly exhibits amorphous structure due to colloidal structure of covalent encapsulated nanoparticles for which the average size is 0.34 nm and changes around 0.2-0.97 nm indicating a better distribution of covalence incorporated nanoparticles onto matrix copolymer chains.

3- The chemical and physical structures and composition of prepared copolymer-g-APTS-$(SiO_2)_n$ NPs were examined by FTIR, ^{13}C and ^{29}Si solid state NMR spectroscopy methods.

4- FTIR spectra confirmed the presence of the characteristic absorption bands from functional groups of the copolymer related to C–H stretching from CH and CH_2 propylene group; C=O stretching in anhydride, free –COOH and amide groups; and Si-O and Si-O-Si vibrations from silica NPs.

5- Chemical structure of copolymer-g-SiO_2 NPs was also proved by solid state ^{13}C-NMR (Figure 4.1B) and ^{29}Si-NMR (Figure 4.1C) spectroscopy techniques. The carbonyl group peak was observed at 173 ppm while the peak for methyne, methylene, and methyl carbon at 67 ppm, 41 ppm, and 22 ppm were observed respectively in the hybrid.

6- The degree of hydrolysis was proved by solid-state ^{13}C CP/MAS NMR. Copolymer/silica NPs ratio was found as 0.316, i.e., 24 mass % of shell copolymer and 76 mass % of core silica NPs. The average molecular mass (9.060 m/z) was calculated from plot of intensity versus mass (m/z). Repeated monomer-comonomer unit (n x 7.087 = 1900 m/z, n = molecular mass of one unit) of alternating copolymer was evaluated from MALDI-TOF MS spectra.

7- The reactive alternating copolymer plays a significant role in the synthesis of copolymer-g-APTS-silica hybrid and PP/EPDM based nanocomposites, and thus, serves as a second reactive compatibilizer and a structural analogue of the first PP-g-MA compatibilizer used in the composition of blends.

8- FTIR spectra of PP based NCs confirm the chemical structure of the prepared NCs and they have also been investigated by XRD. The reflected patterns confirm the isotactic PP and its MA grafted derivatives. PP is known to have three crystalline modifications such as α-monoclinic, β-hexagonal, and γ-orthombic forms and the most well known α-monoclinic crystal structure has been determined from the characteristic crystal peaks with lower peak intensity and area and high number of crystals. The reflection peak at 22.13° 2θ can be attributed to the reflections from long octadecyl side-chain and two dodecyl groups from copolymer and organoclay, respectively.

9- PP based NCs prepared with PLA (NC-2) and PCL (NC-3) biopolymers show similar reflection patterns with different particle sizes (higher for NC-2 and relatively lower for NC-3) due to predominantly hydrogen bonding in situ interfacial interactions in these systems prepared with DMDA-MMT.

10- Surface and internal morphology of these NCs have studied through SEM and TEM techniques. In agreement with SEM images, NC-1 and NC-3 show better compatibilized blends and dispersed domains with fine surface distribution of silica micro- and nanoparticles whereas, NC-2 exhibits smooth surface morphology without the formation of domains.

11- TEM image of NC-3 shows well-oriented multi-layered structure of shells including various polymer chains from PP, PP-g-MA graft copolymer, and PCL on colloidal amphiphilic copolymer-g-SiO$_2$ NPs in spherical core phase. TEM images clearly display that the core phases are composed of silica NPs. The dispersion of the other nanocomposites (NC-1 and NC-2) has not been investigated yet, however, It is expected that these nanocomposites will also exhibit approximately similar morphologies.

12- DTA, DSC and TGA-DTG methods were employed to investigate the thermal behavior of PP based NCs compared to i-PP and analysis results for NC-1, NC-2, NC-3 and pristine i-PP were found to exhibit approximately similar melting and crystallizing transitions but with different peak areas and enthalpy values. The

melting values were recorded for all composites around 166.8-169.7 °C by DTA; 168.1-166.7 °C by DSC; and recrystallization values ~123.5 °C for all NCs by DSC.

13- TGA-DTG analysis results show that the nanocomposites NC-1 and NC-2 containing organoclay and hydrolytically degradable PLA chains exhibit two-step degradations with lower mass loss during the first step degradation, whereas, NC-3 containing PCL exhibits only one-step degradation. Thermal stability of NCs is relatively higher than that of pristine i-PP. The mass loss of the nanocomposites at the critical degradation temperatures (T_{dmax}) essentially increases due to the presence of degradable polyesters, organic segments from the silicate and silica micro- and nanoparticles in the composition.

14- The shear stress/viscosity versus shear rate relationships of silicate layered and encapsulated copolymer-g-silica NPs incorporated with PP/polyester/biopolymer based NCs were investigated by Dynamic Rotary Rheometer analysis method. The viscosity distribution is normal under the applied forces in the NC, containing PCL, amorphous colloidal copolymer-g-silica and DMDA-MMT non-reactive organoclay. A sharp decrease in viscosity is observed at a certain shear rate due to the slipping of layers or new material property occurring by physical nanostructural changes during the extrusion process via formation of novel, thermodynamically stable polymer nanostructures which quite agree with SEM-TEM morphology and XRD reflection parameters.

15- The rheology of NC containing PLA and DMDA gives a well distribution in shear stress and viscosity. The mechanical properties are in accordance with that of Carreau model and it may be proposed that colloidal copolymer-g-SiO_2 NPs, as an effective compatibilizer and reactive reinforcement, essentially improve the mechanical and rheological parameters of the fabricated NCs.

16- EPDM-ODA-MMT based nanocomposites NC-8 and NC-9 were also investigated by FTIR, XRD, SEM and TEM techniques to confirm the chemical and physical structure of the prepared masterbatches. Weak peaks are associated with the stretching O-H group from water in MMT and Si-OH of silica NPs. Peaks appear from vibrations of C−H bands in CH_2, CH_3 and CH groups of EPDM and PLA chains, and propylene unit of PP-co-MA graft oligomer. The C=O stretching bands come from ester group of PLA, -COOH. CH and CH_3 bending bands from PLA chain are also observed. The weak C-N-C band can be related to imidized maleamide unit from copolymer-g-silica during reactive extrusion process. Similar absorption bands were

also observed in the spectrum of the nanocomposite NC-9 the composition of which includes DMDA/MMT non-reactive nanofiller and biodegradable PCL unlike the composition of NC-8. Appearance of strong absorption bands are associated with rocking vibration of CH_2 in -$(CH_2)_n$- groups from dodecyl fragments of copolymer and DMDA-MMT nanoclays, as well as from -$(CH_2)_5$- backbone chain of PCL.

17- Agreeing with the reflection parameters of the layered silicate and silica regions, NC-8 contained broad amorphous area which can be attributed to colloidal SiO_2 NPs covalently encapsulated with poly (MA-*alt*-1-dodecene) copolymer via amidation of anhydride unit with γ-aminopropyl-SiO_2.

The XRD patterns of NC-9 nanocomposite showed similar reflections, however NC-9 has only different crystallite sizes due to predominantly hydrogen bonding in situ interfacial interactions in these systems prepared with DMDA-MMT.

18- Comparative analysis of SEM morphology of PCL-125/DMDA, NC-14 with 3.5 mass % and PLA-700/DMDA, NC-13, 3.5 mass % masterbatch nanocomposites showed better dispersed morphological structures of nanocomposites consisting non-reactive organoclays (DMDA-MMT) and PLA-700 as a matrix polymer compared with PCL-125/DMDA. This can be attributed to excellent compatibility of high molecular mass of PLA matrix polymer via formation of complexing structure of PLA**...**DMDA-MMT clay ($-$C$=$O / C$-$O ester**...**N$-$MMT) in the melt extrusion conditions.

19- TEM internal morphology images of EPDM based nanocomposite NC-9 (PCL-125 and DMDA-MMT) at 10 and 20 nm magnifications show finely dispersed layered silicate with d-spacing around 30-40 nm, and a better distribution of silica nanoparticles, in agreement with nanoparticle sizes determined by previous XRD results. Partially agglomerating layered silicate structures with SiO_2 NPs and predominantly fine dispersing silica NPs onto matrix polyolefin linkages of EPDM chains were also observed.

20- DSC and TGA-DTG curves of pristine EPDM, NC-8 and NC-9 nanocomposites were obtained to investigate the thermal behavior and stability of those compounds. Intercalating structure of nanocomposite provides transfer of rubber structure to semi-crystalline form with shifted $T_g = 1.53$ ^{o}C, and $T_m = 94.3$ ^{o}C; enthalpy $\Delta H = -50.51$ J/g and crystallinity 17.42 %. Higher thermal stability at $T_{d\ max} = 476.62$ ^{o}C of nanocomposite (NC-8) can be estimated by transfer of matrix EPDM rubber

macromolecules to thermoplastic structures during extrusion in-situ processing in the presence of reactive organoclay. Both NCs exhibit higher melt-transition values (T_m) at 97.96 °C and 97.94 °C compared with EPDM/ODA-MMT nanocomposite. Moreover, NC-8 consisting PLA shows a highly visible area compared to that of NC-9 consisting PCL due to higher complexing sites and crystallinity of PLA chains in NC-8. It was observed that all nanocomposites degraded by two-step mechanism. Increase of M_w visibly decreased thermal and crystallinity and shows deviations due to the fine dispersion at an optimum value M_w around 700 x 10^3 Da for PLA.

21- Mechanical and rheological properties of EPDM based nanocomposites NC-8 and NC-9 were investigated by Dynamic Rotary Rheometer and the rheological characterizations, especially the shear stress-shear rate and viscosity-shear rate relationships of thermoplastic polyolefin and EPDM rubber were estimated by using Carreau model. The high viscosity of NC-8 with PLA-700 and chemically reactive ODA-MMT is due to the more hydrophilic polar fraction ($-O-C=O-$ ester in monomer unit and trace of end $-OH$ and $-COOH$ groups) resulting in dominant covalent interfacial interactions in the nanocomposite compared with NC-9 with PCL-125 and nonreactive DMDA-MMT which contains more hydrophobic fragment $-(CH_2)_5-$ in the caprolactone monomer unit being in more stable form. Consequently, fitting of NC-8 to the Carreau Model is insignificant whilst NC-9 fitting to the expected model is quite well. These results also indicate that structure of NC-9 has good compatibility due to the occurrence of effective physical interactions between functional components.

REFERENCES

[1]   Khalid, M., Ratnam, C. T., Ali Chuah, T. C., Choong S., Thomas S. Y., Comparative study of polypropylene composites reinforced with oil palm empty fruit bunch fiber and oil palm derived cellulose, *Materials & Design*, 29 (1), 173–178, **2008**.

[2]   Jayaraman, K., Manufacturing sisal–polypropylene composites with minimum fiber degradation, *Composites Science and Technology*, 63, 367–374, **2003**.

[3]   Rzayev, Z. M. O., *Advances in Polyolefin Nanocomposites (Ed. V. Mittal), Chapter 4. Polyolefin Nanocomposites by Reactive Extrusion,* CRC press, Taylor & Francis Group, 87-127, **2011**.

[4]   Yu, L., Katherine, D, Li, L., Polymer blends and composites from renewable resources, *Progress in Polymer Science*, 31(6), 576–602, **2006**.

[5]   Lee, S-H., Teramoto, Y., Endo, T., Cellulose nanofiber-reinforced polycaprolactone/ polypropylene hybrid nanocomposite, *Composites Part A: Applied Science and Manufacturing,* 42, 151–156, **2011**.

[6]   Rzayev, Z. M. O., Bryksina, L. V., Kyazimov, S. K., Sadikh-zade, S. I., Radical copolymerization of maleic anhydride, styrene and vinyltriethoxysilane, *Polymer Science USSR*, A14, 259-267, **1972**.

[7]   Rzayev, Z. M. O., Güner, A., Can, H. K., Aşici, A., Reactions of some anhydride-containing copolymers with γ-aminopropyltriethoxysilane, *Polymer*, 42, 5599-5606, **2001**.

[8]   Bozdoğan, D. D., Kibarer, G., Rzayev, Z. M. O., Morphological investigation of in situ generated silica nanoparticles encapsulated with poly (MA-*alt*-α-olefin) (C_{6-18}) copolymers, *Polymer Bulletin,* 70, 3185-3200, **2013**.

[9]   Das, A., Jurk, R., Stockelhuber, K. W., Silica-ethylene propylene diene monomer rubber networking by in situ sol-gel method, *Journal of Macromolecular Science Part A-Pure Applied Chemistry*, 45, 101-106, **2008**.

[10]   PAGEV, World & Turkey Plastics Industry Follow up Report, www.pagev.org (August, **2016**).

[11]   PAGEV, World & Turkey Polypropylene Report, www.pagev.org (August, **2016**).

[12]   EPDM global market forecasts report, Sealing Technology, 6-8, 2014 http://www.sciencedirect.com/science/article/pii/S1350478914702223, (October, **2017**).

[13]   Biodegradable Plastics, http://www.marketsandmarkets.com/PressReleases/ biodegradable-plastics.asp (August, **2017**).

[14] Carrasco, F., Cailloux, J., Sánchez-Jiménez, P., Maspoch, M. L., Improvement of the thermal stability of branched poly (lactic acid) obtained by reactive extrusion, *Polymer Degradation and Stability*, 40, 104, **2014**.

[15] Datta, R., Henry, M., Lactic acid: recent advances in products, processes and technologies—a review, *Journal of Chemical Technology and Biotechnology*, 81, 1119, **2006**.

[16] Rajeev, M., Vineet, K., Haripada, B., Upadhyay, S. N., Synthesis of Poly (Lactic Acid): A Review, *Journal of Macromolecular Science, Part C*, 45(4), 325-349, **2005.**

[17] Hartmann, M. H., High Molecular Weight Polylactic Acid Polymers. In: Kaplan D.L. Biopolymers from Renewable Resources, *Macromolecular Systems— Materials Approach*, 367-411, **1998**.

[18] Li, L., Tang, S., Wang, Q., Pan, Y.K., Wang T. L., Preparation of poly (lactic acid) by direct polycondensation in azeotropic solution, *Polymer*, 32, 672-675, **2006**.

[19] Hideto, T., Akira, M., Yoshito, I., Blends of aliphatic polyesters. III. Biodegradation of solution-cast blends from poly (L-lactide) and poly (ε-caprolactone), *Journal of Applied polymer Science,* 70, 2259–2268, **1998**.

[20] Fukushimaa, K., Abbate, C., Tabuan, D., Gennari, M., Camino, G., Biodegradation of poly (lactic acid) and its nanocomposites, *Polymer*, 94, 1646-1655, **2009**.

[21] Gupta, B., Revagade N., Hilborn J., Poly (lactic acid) fiber: An overview, *Progress in Polymear Science*, 32(4), 455-482, **2007**.

[22] Pitt, C. G., Chasalow, F. I., Hibionada, Y. M., Klimas, D. M. and Schindler, A., Aliphatic polyesters I. The degradation of poly (ε-caprolactone) *in vivo, Journal Applied Polymer Science*, 26, 3779–3787, **1981**.

[23] Labet, M., Thielemans, W., Synthesis of polycaprolactone: A review, *Chemical Society Reviews*, 38, 3484-3490, **2009**.

[24] Kun-Hong, L., Kim, H., Khil, M. S., Ra, Y. M., Lee, D. R., Characterization of Nano-Structured Poly (ε-Caprolactone) Nonwoven Mats via Electrospinning, *Polymer*, 44, 1287-1294, **2003**.

[25] Silicates, http://www.galleries.com/Silicates (September, **2017**).

[26] Hussain, F., Hojjati M., Okamoto, M., Gorga, R., Review article: Polymer-matrix Nanocomposites, Processing, Manufacturing, and Application: An Overview, *Journal of Composite Materials*, 40(17), 44-65, **2006.**

[27] Scott, M. A., Carrado, K. A., Dutta, P. K., *Handbook of zeolite science and technology*, Marcel Dekker, Inc., New York, **2003**.

[28] Alexandre, M., Dubois, P., Polymer-Layered Silicate Nanocomposites: Preparation, Properties and Uses of a New Class of Materials, *Materials Science and Engineering*, 28, 1-63, **2000**.

[29] Suprakas, S. R., Okamoto, M., Polymer/Layered Silicate Nanocomposites: A Review from Preparation to Processing, *Progress in Polymer Scien*ce, 28, 1539-1641, **2003**.

[30] Rzayev, Z., Söylemez, A. E., Davarcioğlu, B., Functional Copolymer/organo-MMT Nanoarchitectures. VII. Interlamellar Controlled/living Radical Copolymerization of Maleic Anhydride with Butyl Methacrylate via Preintercalated RAFT agent–Organoclay Complexes, *Polymers for Advanced Technologies*, 23, 278 – 289, **2012**.

[31] Rzayev, Z. M., *Polyolefin Nocomposites by Reactive Extrusion*, Advances in Polyolefin Nanocomposites, 87-127, **2011**.

[32] Altungöz, E., Rzayev, Z. M., Alper, E., Functional Copolymer/Organo-MMT Nanoarchitectures. XII. Polypropylene/Poly (MA-alt-1-octadecene)/Organoclay Based Biaxially Oriented Nanofilms through Reactive Extrusion, *International Review of Chemical Engineering-Rapid Communications,* 4, 91, **2012**.

[33] Tidjani, A., Polypropylene-Graft-Maleic Anhydride Nanocomposites: II-Fire Behaviour of Nanocomposites Produced under Nitrogen and _n Air, *Federal Institute for Research and Testing (BAM)*, 87, 12205, **2004**.

[34] Xu, W., Liang, R G., Wang, W., Tang, S., He, P., Pan, W.P., PP–PP-g-MAH–Org-MMT nanocomposites: I. Intercalation behavior and microstructure, *Journal of Applied Polymer Science*, 88, 3225–3231, **2013**

[35] Köksal, S., *Nanocomposite Materials*, M.Sc. Thesis, Yıldız Technical University, Chemical Engineering Department, Istanbul, **2007**.

[36] Altungoz, E., *Preparatıon of Polypropylene / Functıonal Copolymer / Organo-Montmorıllonite Clay Nanomaterıals by Reactıve Extrusıon*, M.Sc. Thesis, Hacettepe University, Fen Bilimleri Enstitüsü, Ankara, **2012**.

[37] Aranda, P., Ruiz-Hitzky E., Poly (ethylene oxide)/NH4+Smectite Nanocomposites, *Applied Clay Science*, 15, 119-135, **1999**.

[38] Tanoue, S., Utracki, L.A, Garcia-Rejon, J., Tatibouet, Kamal, M.R., Preparation of Polystyrene/Organoclay Nanocomposites by Melt Compounding Using a Twin Srew Extruder, *Journal of Applied Polymer Science*, 44, 1046–1060, **2004**.

[39] Blanton, T. N., Majumdar, D., Melpolder, S. M., Microstructure of Clay-polymer Composites, *Advance X-ray Analysis*, 42, 562–568, **2000**.

[40] Murthy, N. S., Recent Developments in Polymer Characterızatıon using X-ray Difraction, *The Rıgaku Journal*, 21, 15–24, **2004**.

[41] TEM analysis, http://www.mrs.org (September, **2017**).

[42] Shah, K. J., Shukla A. D., Shah, D. O., Imae, T., Effect of Organic Modifiers on Dispersion of Organoclay in Polymer Nanocomposites to Improve Mechanical Properties, *Polymer*, 97, 525-532, **2016**.

[43] Ozdemir, E., Hacaloglu, J., Thermal degradation of Polylactide/Poly(ethylene glycol) Fibers and Composite Fibers Involving Organoclay, *Journal of Analytical and Applied Pyrolysis*, in press, **2017**.

[44] Giovino, M., Pribyl, J., Benicewicz, B., Kumar, S., Schadler, L., Linear Rheology of Polymer Nanocomposites with Polymer-grafted Nanoparticles, *Polymer*, 131, 104-110, **2017**.

[45] Domenech, T., Peuvrel-Disdier, E., Vergnes, B., The Importance of Specific Mechanical Energy During Twin Screw Extrusion of Organoclay Based Polypropylene Nanocomposites, *Composites Science and Technology*, 75, 7–14, **2013**.

[46] Messori, M., *Recent Advances in Elastomeric Nanocomposites (V. Mittal et al., eds.), In Situ Synthesis of Rubber Nanocomposites*, Springer-Verlag Berlin Heidelberg, 57-85, **2011**.

[47] Karder-Kocsis, J., Wu, C. M., Thermoset Rubber/layered Silica nanocomposites: Status and Future Trends, *Polymer Engineering Science*, 44, 1083-1093, **2004**.

[48] Wu, T. M., Chu, M. S., Preparation and Characterization of Thermoplastic Vulcanizate/silica Nanocomposites, *Journal of Applied Polymer Science*, 98, 2058-2063, **2005**.

[49] Acharya, H., Pramanik, M., Srivastava, S., Bhowmick, A., Synthesis and Evaluation of High-Performance Ethylene-Propylene-DieneTerpolymer/Organoclay Nanoscale Composites, *Journal of Applied Polymer Science*, 93, 2429-2436, **2004**.

[50] Ahmadi, S., Huang, Y., Li, W., Fabrication and Physical Properties of EPDM/Organoclay Nanocomposites, *Composites Science and Technology*, 65, 1069-1076, **2005**.

[51] Wu, Y., Ma, Y., Wang, Y., Zhang, L., Effects of Characteristics of Rubber, Mixing and Vulcanization on the Structure and Properties of Rubber/Clay Nanocomposites by Melt Blending, *Macromolecular Materials and Engineering*, 289, 890-894, **2004**.

[52] Yang, H., Zhang, X., Qu, C., Li, B., Takeda, K., Lagely improved thoughness of PP/EPDM blends by adding nano-SiO_2 ternary composites, *Polymer*, 48, 860-869, **2007**.

[53] Yang, H., Zhang, X., Guo, M., Wang, C., Du, R. N., Fu, Q., Study of phase structures and toughening mechanism in PP/EPDM/SiO_2 ternary composites, *Polymer*, 47, 2106-2115, **2006**.

[54] Chang, Y. W., Yang, Y., Ryu, S., Nah, C., Preparation and properties of EPDM/organo-montmorillonite hybrid nanocomposites, *Polymer International*, 51, 319-324, **2002**.

[55] Naderi, G., Lafleur, P. G., Dubois, C., Microstructure-properties correlations in dynamically vulcanized nanocomposite thermoplastic elastomer based on PP/EPDM, *Polymer Engineering Science*, 47, 207-217, **2007**.

[56] Vijayalekshmi, V., Abdulmajeed, S. S. M., Mechanical, thermal and electrical properties of EPDM/silicone blend nanocomposites, *International Journal of Engineering Research and Application,* 3 (2), 1177-1180, **2013**.

[57] Kole, S., Roy S., Browmick, A. K., Interaction between silicone and Epdm rubbers through functionalization and its effect on properties of the blend, *Polymer*, 35, 3423-3426, **1994**.

[58] Uzuki, A., Tukigase, A, Kato, M., Preparation and properties of EPDM-clay hybrids, *Polymer*, 43, 2185-2189, **2000**.

[59] Wang, Z. H., Lu, Y. L., Liu, J., Dang, Z. M., Zhang, L. Q., Wang, W., Preparation of nanoalumina/EPDM composites with good performance in thermal conductivity and mechanical properties, *Polymer Advanced Technologies*, 22, 2302-2310, **2011**.

[60] Payne, A. R., Dynamic properties of heat-treated butyl vulcanizates, *Journal of Applied Polymer Science*, 7, 873-885, **1963**.

[61] Mousa, A., Cure characterizations and thermal properties of sulfur-cured EPDM-based composites by compounding with layered nano-organoclay, *Journal of Polymer-Plastic Technology and Engineering*, 45, 911-915, **2006**.

[62] Rajeev, R. S., De, S. K., Bhowmick, A. K., John, B., Studies on thermal degradation of short melamine fibre reinforced EPDM, maleated EPDM and nitrile rubber composites, *Polymer Degradation and Stability*, 79 (3), 449-463, **2003**.

[63] Mitra, S., Ghanbari-Siahkali, A., Kingshott, P., Rehmeier, H. K., Abildgaard, H., Almdal, K., Chemical degradation of crosslinked ethylene-propylene-diene rubber in an acidic environment. Part I. Effect on accelerated sulphur crosslinks, *Polymer Degradation and Stability*, 91 (1), 69-80, **2006.**

[64] Konar, J., Samanta, G., Avasthi, B. N., Sen, A. K., Oxidative degradation of EPDM rubber using phase transferred permanganate as oxidant, *Polymer Degradation and Stability*, 43 (2), 209-216, **1994**.

[65] Wang, Y., Liu, L., Luo, Y., Jia, D., Aging behavior and thermal degradation of fluoroelastomer reactive blends with poly-phenol hydroxy EPDM, *Polymer Degradation and Stability,* 94 (3), 443-449, **2009**.

[66] Tian, M., Zhang, X., Zhang, L., Yin, S., Nishi, T., Ning N., Interfacial enhancement of fibrillar silicates (FSs)/ EPDM nanocomposites by surface modification of FS in supercritical CO_2, *Composites Science and Technology*, 79, 21–27, **2013**.

[67] Stelescu, D. M., Airinei, A., Homocianu, M., Fifere, N., Timpu, D., Aflori, M., Structural characteristics of some high density polyethylene/EPDM blends, *Polymer Testing,* 32, 187-196, **2013**.

[68] Vermeech, I. M., Groeninckx, G., Coleman, M. M., Poly (styrene-co-N-maleimide copolymers by reactive extrusion, molecular characterization by FTIR, and use in blend, *Macromolecules*, 26, 6643-6649, **1993**.

[69] Mirabella, F. M., Bafna, A., Determination of the crystallinity of polyethylene/α-olefin copolymers by thermal analysis: Relationship of the heat of fusion of 100 % polyethylene crystal and the density, *Journal of Polymer Science, B: Polymer Physics*, 40, 1637-1643, **2002**.

[70] Albertsson, A. C., Varma, I.K., Recent developments in ring opening polymerization of lactones for biomedical applications, *Biomacromolecules*, 4, 1466–1486 **2003**.

[71] Krishnamachari, P., Zhang, J., Lou, J., Yan, J., Uitenham, L., Biodegradable poly (lactic acid)/clay nanocomposites by melt intercalation: A study of morphological, thermal, and mechanical properties, *International Journal of Polymer Analytic. Characterization*, 14, 336-350, **2009**.

[72] Ouyang, W. Z., Huang, Y., Luo, H. J., Wang, D. S., Preparation and properties of poly (lactic acid)/cellulolytic enzyme lignin/PGMA ternary blends, *Chinese Chemical Letter*, 23, 351-364, **2012**.

[73] Dilmani, M. A., Rzayev, Z. M. O., Alper, E., Functional Copolymer/Organo-MMT Nanoarchitectures. XIII. EPDM rubber/poly (MA-alt-1-octadecene)-g-PEO/organoclays nanocomposites through reactive extrusion, *International Review of Chemical Engineering, Rapid Communication*, 4 (1), 91-104, **2012.**

[74] Rzayev, Z. M. O., Graft Copolymers of Maleic Anhydride and Its Isostructural Analogues: High Performance Engineering Materials, *International Review of Chemical Engineering*, 3, 153-215, **2011**.

[75] Mittal, K. L., *Silane and Other Coupling Agents*, AH Zeist, the Netherlands: VSB BY, **1992**.

[76] Jain, S., Coossens, H., Picchioni, E., Magusin, P., Mezari, B., Van Duin, M., Synthetic aspects and characterization of polypropylene-silica nanocomposites prepared via solid-state modification and sol-gel reactions, *Polymer*, 46, 6666–6681, **2005**.

[77] Bikiaris, D. N., Vassiliou, A., Pavlidou, E., Karayannidis, G. P., Compatibilization effect of PP-g-MA copolymer on i-PP/SiO$_2$ nanocomposites prepared by melt mixing, *Polymer International*, 41, 1965–1978, **2005**.

[78] Wu, C.L., Zhang, M. Q., Rong, M. Z., Friedrich K. Silica nanoparticles filled polypropylene: Effect of particle surface treatment, matrix ductility and particle

species on mechanical performance of the composites, *Composites Science and Technology,* 65, 635–645, **2002**.

[79]   Chen, J. H., Rong, M. Z., Ruan, W. H., Zhang, M. Q., Interfacial enhancement of nano-SiO$_2$/polypropylene composites, *Composites Science and Technology*, 69, 252–259, **2009**.

[80]   Jenkins, R., Snyder, R. L., *Introduction to X-ray Powder Diffractometry*, John Wiley & Sons Inc., 89–91, **1996**.

[81]   Nelsen, A.S., Batchelder, D.N., Pyrz R., Estimation of crystallinity of isotactic polypropylene using Raman spectroscopy, *Polymer*, 43, 2671–2676, **2002**.

[82]   Karacan, I., Benli H., An X-ray difraction study for isotactic polypropylene fibers produced with take-up speeds of 2500-4250 m/min., *Textile and Confection*, 3, 201–209, **2011**.

[83]   Wunderlich, B., *Macromolecular Physics, Vol. 3, Crystal Melting*, Academic Press, New York, **1980**.

[84]   Maani, A., Blais, B., Heuzey, M. C., Carreau, P. J., Rheological and morphological properties of reactively compatibilized thermoplastic olefin (TPO) blends, *Journal of Rheology*, 56, 625–647, **2012**.

[85]   Maani, A., Heuzey, M. C., Carreau, P. J., Coalesence in Thermoplastic olefin (TPO) blends under shear flow, *Rheologica Acta*, 50, 881–895, **2011**.

[86]   Minale, M., Moldenaers, P., Mewis, J., Effect of shear history on the morphology of immisible polymer blends, *Macromolecules*, 30, 5470–5475, **1997**.

[87]   Carreau, P. J., Kee, D., Chabra, R. P., *Rheology of Polymeric Systems: Principles and Applications*, Hanser, Munich, **1997**.

[88]   Sepehr, M., Ausias, G., Carreau, P.J., Rheological properties of short fiber filled polypropylene in transient shear flow, *Journal of Non-Newtonian Fluid Mechanics*, 123, 19–32, **2004**.

[89]   Lacroix, C., Grmela, M., Carreau, P. J., Relationships between rheology and morphology for immiscible molten blends of polypropylene and ethylene copolymers under shear flow, *Journal of Rheology*, 42, 41, **1998**.

[90]   Xiao, W., Yu, H., Han, K., Yu, M., Study of PET fiber modified by nanomaterials: inprovement of dimensional thermal stability of PET fiber by forming PET/MMT nanocomposites, *Journal of Applied Science*, 96, 2247–2252, **2005**.

[91]   Yong, T. L., Park, O. O., Phase morphology and rheological behavior of polymer/layered silicate nanocomposites, *Rheologica Acta*, 40, 220-232, **2002**.

[92]   Wagener, R, Reisinger, T. J. G., A rheological method to compare the degree of exfoliation of nanocomposites, *Polymer*, 44, 7513-7518, **2003**.

[93] Krishnamoorti, R., Giannelis, E. P., Strain hardening in model polymer brushes under shear, *Langmuir*, 17, 1448-1452, **2001**.

[94] Mishra, J. K., Hwang, J. K., Ha, C. S., Preparation,mechanical and rheological properties of a thermoplastic polyolefin (TPO)/organoclay nanocomposite with reference to the effect of maleic anhydride modified polypropylene as a compatibilizer, *Polymer*, 46, 1995-2002, **2005**.

[95] Khosrokhavar, R., Naderi, G., Bakhshandeh, G. R., Ghoreishy M. H. R., Effect of processing parameters on PP/EPDM/Organoclay nanocomposites using Taguchi analysis method, *Iranial Polymer Journal*, 20 (1), 41-53, **2011**.

[96] Ray, S., Mosto, S. B., Biodegradable polymers and their layered silicate nanocomposites: In greening the 21st century materials world, *Progress in Materials Science*, 50 (8), 962–1079, **2005**.

[97] Muhammad, M. S., Lin, O. H., Akil H. Md., Preparation and Characterization of Palm Kernel Shell/Polypropylene Biocomposites and their Hybrid Composites with Nanosilica, *BioResources*, 8 (2), 1539–1550, **2013**.

[98] Abu-Sharkh, B. F., Hamid, H., Degradation study of date palm fiber/polypropylene composites in natural and artificial weathering: mechanical and thermal analysis, *Polymer Degradation and Stability*, 85, 967–973, **2004**.

[99] Arbelaiz, A., Fernández, B., Ramos, J. A., Retegi, A, Llano-Ponte R., I., Mondragon I. Mechanical properties of short flax fibre bundle/polypropylene composites: Influence of matrix/fibre modification, fibre content, water uptake and recycling, *Composites Science and Technology*, 65(10), 1582–1592, **2005**.

[100] Yang, H. S., Kim, H. J., Park, H.J., Lee, B. J., Hwang, T. S., Effect of compatibilizing agents on rice-husk flour reinforced polypropylene composites, *Composite Structures*, 77 (1), 45–55, **2007**.

[101] Fuqua, M. A., Huo, S., Ulven, C. A., Natural Fiber Reinforced Composites, *Polymer Reviews,* 52, 259–320, **2012**.

[102] Chung, T. C., Rhubright, D., Polypropylene-graft-polycaprolactone: synthesis and applicationd in polymer blends, *Macromolecules*, 27, 1313–1319, **1994**.

[103] Kaneko, H., Saito, J., Kawahara, N., Matsuo, S., Matsugi, T., Kashiwa, N., In Book: Polypropylene-graft-poly (methyl methacrylate) graft copolymers: Synthesis and compatibilization of polypropylene/polylactide, *ACS Symposium Series*, 1023 (24), 357–371, **2009**.

[104] Chung, M., Functional polyolefins for energy applications, *Macromolecules*, 46, 6671–6698, **2013**.

[105] Bret, D. U., Lakshmi, S. N., Cato, T. L., Biomedical Applications of Biodegradable Polymers, *Journal of Polymer Science B: Polymer Physics*, 49, 832–864, **2011**.

[106] Patlolla, A., Collins, G., Arinzeh, T. L., Solvent-dependent properties of electrospun nanofibrous scaffold, *Acta Biomaterialia*, 6, 90–101, **2010**.

[107] Gunatillake, P., Mayadunne, R., Adhikari, R., Recent developments in biodegradable synthetic polymers, *Biotechnology Annual Review*, 12, 301–347, **2006**.

[108] Garkhal, K., Verma, S., Tikoo, K., Kumar, N. J., Surface modified poly (L-lactide-co-ε-caprolactone) microspheres as scaffold for tissue engineering, *Biomedical Material Research A*, 82, 747–756, **2007**.

[109] Luciani, A., Coccoli, V., Orsi, S., Ambrosio, L., Netti, P. A., PCL microspheres based functional scaffolds by bottom-approach with predefined microstructural properties and release profiles, *Biomaterials*, 29, 4800–4807, **2008**.

[110] Chung, S., Ingle, N. P., Montero, G. A., Kim, S. H., King, M. W., Bioresorbable elastomeric vascular tissue engineering scaffolds via melt spinning and electrospinning, *Acta Biomaterialia*, 6, 1958–1967, **2010**.

[111] Plikk, P., Malberg, S., Albertsson, A. C., Design of resorbable porous copolyester scaffolds for use in nerve regeneration, *Biomacromolecules*, 10, 1259–1264, **2009**.

[112] Zuo, Y., Yang, F., Wolke, L. G. C., Li, Y., Jansen, J. A., Incorporation of biodegradable electrospun fibers into calcium phosphate cement for bone regeneration, *Acta Biomaterialia*, 6, 1238–1247, **2010**.

[113] Guarino, V., Ambrosio, L., The synergic effect of polylactide fiber and calcium phosphate particle reinforcement in poly ε-caprolactone composite scaffolds, *Acta Biomaterialica*, 4, 1778–1787, **2008**.

[114] Chen, H., Huang, J., Yu, J., Liu, S., Gu, P., Electrospun chitosan-graft-poly (ε-caprolactone) cationic nanofibrous mats as potential scaffolds for skin tissue engineering, *International Journal of Biomacromolecules*, 48, 13–19, **2011**.

[115] Wen, X., Zhang, K., Wang, Y., Han, L., Han, C., Zhang H., Study of the thermal stabilization mechanism of biodegradable poly (L-lactide)/silica nanocomposites, *Polymer International*, 60, 202–210, **2010**.

[116] Chrissafis, K., Pavlidou, E., Paraskevopoulos, K., Beslikas, T., Nanias, N., Bikaris, D., Enhancing mechanical and thermal properties of PLLA ligaments with fumed silica nanoparticles and montmorillonite, *Journal of Thermal Analysis Calorimetry*, 106, 313–323, **2011**.

[117] Maiti, P., Yamada, K., Okamoto, M, Ueda, K., Okamoto, K., New polylactide/layered silicate nanocomposites: Role of organoclay, *Chemical Materials*, 14, 4654–4661, **2002**.

[118] Song, X., Zhou, S., Wang, Y., Kang, W., Cheng, B., Mechanical properties and crystallization behavior of polypropylene non-woven fabrics reinforced with POSS and SiO_2 nanoparticles, *Fibers and Polymers*, 13, 1015–1022, **2012**.

[119] Barczewski, M., Chmielewska, D., Dobrzyriska, M. M., Dubziec, B., Sterzyriski, T., Thermal stability and flammability of polypropylene-slsesquioxane nanocomposites, *International Journal of Polymer Analysis and Characterization*, 19, 500–509, **2014**.

[120] Zhang, M. Q., Rong, M. Z., Zeng, H. M., Schmitt, S., Wetzel, B., Friedrich,, K., Atomic force microscopy study on structure and properties of irradiation grafted silica particles in polypropylene-based nanocomposites, Journal of Applied Polymer Science, 80, 2218–2227, **2001**.

[121] Zou, H., Wu, S., Shen, J., Polymer/silica nanocomposites: preparation, characterization, properties, and applications, *Chemical Reviews*, 108, 3893–3957, **2008**.

[122] Garcia, M., Van Vliet G., Jain, S., Schrauwen, A. G., Sarkissiv, A., Van Zyl W. E., Boukamp, B., Polypropylene/ SiO_2 nanocomposites with improved mechanical properties, *Review of Advance Material Science*, 6, 169–175, **2004**.

[123] Sun, D., Zhang, R., Jiu, Z., Huang, Y., Wang, Y., He, J., Han, B., Yang, G., Polypropylene/silica nanocomposites by in-situ sol-gel reaction with the aid of CO_2, *Macromolecules*, 36, 617–5624, **2005**.

[124] Bracho, D., Dougnac, V. N., Palza, H., Quijada, R., Functionalization of silica nanoparticles for polypropylene nanocomposite applications, *Journal of Nanomaterials,* 2012, 1-8, **2012**.

[125] Qian, J., Cheng, G., Zhang, H., Xu, Y., Preparation and characterization of polypropylene/silica nanocomposites by gamma irradiation via ultrafine blend, *Journal of Polymer Research*, 18, 409–417, **2011**.

[126] Rzayev, Z. M. O., Yilmazbayhan, A., Alper, E., A one step preparation of polypropylene-compatibilizer-clay nanocomposites by reactive extrusion, *Advance Polymer Technology*, 26, 41–56, **2007**.

[127] Güldoğan, Y., Eğri, S., Rzayev, Z. M. O., Pişkin, E., Comparison of MA grafting onto powder and granular polypropylene in the melt by reactive extrusion, *Journal of Applied Polymer Science*, 92, 3675–3684, **2004**.

[128] Devrim, Y., Rzayev, Z. M. O., Piskin, E., Functionalization of isotactic polypropylene with citraconic anhydride, *Polymer Bulletin*, 59, 447–456, **2007**.

[129] Sanchez, C., Julian, B., Belleville, P., Applications of hybrid organic-inorganic nanocomposites, *Journal of Material Chemistry*, 15, 3559-3592, **2005**.

[130] Novak, B. M., Hybrid nanocomposite materials-between inorganic glasses and organic polymers, *Advanced Materials*, 5, 422-433, **1993**.

[131] Mark, J. E., The sol-gel route to inorganic-organic composites, *Heterogeneous Chemical Review*, 3, 307-526, **1996**.

[132] Caravajal G. S., Leyden D. E., Quinting G. R., Maciel G. E., Structural Characterization of (3-Aminopropyl) Triethoxysilane-Modified Silicas by Silicon-29 And Carbon-13 Nuclear Magnetic Resonance, *Analytic Chemistry*, 60 (17), 1776–1786, **1988**.

[133] Zhang, K., Jiang, L., Luo, P., Jiang, J., Wu, G., Effect of melt flow on morphology and linear thermal expansion of injection-molded ethylene–propylene–diene terpolymer/ isotactic polypropylene blends, *Polymer International*, 64, 1225–1234, **2015**.

[134] Gomez, M., Bracho, D., Palza, H., Quijada, R., Effect of morphology on the permeability, mechanical and thermal properties of polypropylene/SiO$_2$ nanocomposites, *Polymer International*, 64, 1245–1251, **2015**.

[135] Sari, M. G., Stribeck, N., Moradian, S., Zeinolebadi, A., Bastani, S., Botta, S., Bakhshandeh, E., Dynamic mechanical behavior and nanostructure morphology of hyperbranched-modified polypropylene blends, *Polymer International*, 63, 195–205, **2014**.

[136] Costantino, A., Pettarin, V., Viana, J., Pontes, A., Pouzada, A., Frontin, P., Morphology- performance relationship of polypropylene-nanoclay composites processed by shear controlled injection moulding, *Polymer International*, 62, 1589–1599, **2013**.

[137] Campos-Requena, V. H., Rivas, B. L., Perez, M. A., Contreras, D., Munoz, E., Optimization of processing parameters for the synthesis of low-density polyethylene/ organically modified montmorillonite nanocomposites using X-ray diffraction with experimental design, *Polymer International*, 62, 548–553, **2013**.

CURRICULUM VITAE

Credentials

Name, Surname: Bayram Ali GÖÇMEN

Place of Birth: TARSUS

Marital Status: MARRIED, Two children

E-mail: gocmenbayram@yahoo.com

Address: Asagiyahyalar mah. Ayyıldız apt. 983. Sok no: 10 17 Yenimahalle/ANKARA

Education

High School: Tarsus Technical High School, 1999

B.Sc.: Bogazici University, Chemical Engineering&Chemistry, 2004

M.Sc.: Bogazici University, Chemical Engineering, 2006

Ph.D.: Hacettepe University, Nanotechnology and Nanomedicine, 2017

Foreign Languages

German: Intermediate

English: Fluent

Work Experience

- BOTAS
  OIL&GAS- UP&MIDSTREAM: ENGINEERING/PROCESS MANAGER
  ANKARA, JULY 2017- present
- GÜBRETAŞ, Gübre Fabrikaları T.A.Ş.
  OIL&GAS-FERTILIZERs: PLANT MANAGER,
  IZMIT, January 2016- March 2017
- SOCAR Türkiye
  OIL&GAS-REFINERY: TEAM LEADER/PROCESS, (LEAD PROCESS
  ENGINEER till 2014),
  ISTANBUL, August 2011- January 2016

- PETKIM Petrochemical Co.

  OIL&GAS-PETROCHEMICAL: COMMISSIONING&OPERATIONS

  SUPERVISOR (LDPE)

  İZMİR, August 2007- June 2011
- Turkish Armed Forces

  LIEUTENANT/LABORATORY SUPERVISOR/QUALITY CONTROL (TS EN

  ISO/IEC 17025),

  KONYA, September 2006- August 2007
- Bogazici University

  RESEARCH ASSISTANT

  ISTANBUL, January 2005- July 2006

Areas of Experiences

- Polymers, reactive extrusion,
- Nanoparticles Synthesis and Characterization,
- Rheology experiments of polymers,
- Morphology/Surface analysis of polymers and nanocomposites (TEM, SEM),
- Physical Properties of Polymers (Tensile Testing, Impact and Deformation Tests),
- Process controlling of small and industrial scale polymer production units,
- Polymer synthesis/forming by using Twin Screw Extruder,
- Injection Molding, Compression Molding and Blow molding for film production,
- Polymers Chemical Structure Analysis and thermal analysis, Morphology and Surface Analysis, MW of Polymers and Nanocomposites (FTIR, 1H-NMR, ^{13}C-NMR, solid state NMR & X-RAY, DSC, TGA, DTG, TEM, SEM, GC-MS),
- Rheology of Polymers (Dynamic rheometer, viscosity analyzer, film tests).

Projects and Budgets

- DPT-07K12630 project during master thesis research.
- TUBITAK-105M282 project during master thesis research.
- TUBITAK- project# TBAG-HD/249 during PhD thesis research.

Publications

- The Effect of Ni: Pt Ratio on Autothermal Reforming Performance of Pt-Ni/Al$_2$O$_3$ Catalyst, *Hydrogen Energy*, 2010.
- Multifunctional PP-based nanocomposites incorporated with organoclays, poly (MA-*alt*-1-dodecene)-*g*-SiO$_2$ nanoparticles and bioengineering polyesters in melt by reactive extrusion, *Polymer-Plastics Technology and Engineering*, 2016.
- EPDM elastomer and biothermoplastic polyesters based silicate layered multifunctional nanocomposites incorporated with poly (MA-alt-α-olefin) -g-APTS-SiO$_2$ NPs and PP-g-MA by reactive extrusion nanotechnology, *Polymer-Plastics Technology and Engineering*, 2017.

Oral and Poster Presentations

- IUPAC 44th Congress ORAL presentation, 2013
  Fabrication and Characterization of Polymer Layered Silicate Nanocomposites From EPDM / PP-g-MA / Polylactide / Organo-Mmt Blends In Melt By Reactive Extrusion.
- MACRO 2016 world polymer congress, POSTER presentation, 2016
  Multifunctional PP/PP-g-MA/Bioengineering Polyesters/Colloidal Poly (MA-alt-1-dodecene)-g-SiO$_2$ /Organoclays Nanocomposites by Reactive Extrusion.

HACETTEPE UNIVERSITY
GRADUATE SCHOOL OF SCIENCE AND ENGINEERING
THESIS/DISSERTATION ORIGINALITY REPORT

HACETTEPE UNIVERSITY
GRADUATE SCHOOL OF SCIENCE AND ENGINEERING
TO THE DEPARTMENT OF NANOTECHNOLOGY AND NANOMEDICINE

Date: 12./01./2018

Thesis Title / Topic: FABRICATION AND CHARACTERIZATION OF NOVEL POLYMER/ORGANO-MMT (ORGANO-SILICA)/ BIOPOLYMER NANOCOMPOSITE BLENDS BY REACTIVE EXTRUSION

According to the originality report obtained by ~~myself~~/my thesis advisor by using the *Turnitin* plagiarism detection software and by applying the filtering options stated below on 12./01./2018 for the total of ....113...... pages including the a) Title Page, b) Introduction, c) Main Chapters, d) Conclusion sections of my thesis entitled as above, the similarity index of my thesis is ..8.... %.

Filtering options applied:
1. Bibliography/Works Cited excluded
2. Quotes excluded / ~~included~~
3. Match size up to 5 words excluded

I declare that I have carefully read Hacettepe University Graduate School of Sciene and Engineering Guidelines for Obtaining and Using Thesis Originality Reports; that according to the maximum similarity index values specified in the Guidelines, my thesis does not include any form of plagiarism; that in any future detection of possible infringement of the regulations I accept all legal responsibility; and that all the information I have provided is correct to the best of my knowledge.

I respectfully submit this for approval.

		Date and Signature
Name Surname:	BAYRAM ALİ GÖÇMEN	17.01.2018
Student No:	N10248386	
Department:	NANOTECNOLOGY AND NANOMEDICINE	
Program:	DOCTORATE OF PHILOSOPHY	
Status:	☐ Masters ☒ Ph.D. ☐ Integrated Ph.D.	

ADVISOR APPROVAL

APPROVED.

PROF. DR. GÜNAY KİBARER

(Title, Name Surname, Signature)